# EVOLUTIONARY COMPUTATION BASED MULTI-OBJECTIVE DESIGN SEARCH AND OPTIMIZATION OF SPACECRAFT ELECTRICAL POWER SUBSYSTEMS

by

Samina Asif

A THESIS SUBMITTED IN FULFILLMENT OF THE
REQUIRMENTS FOR THE
DEGREE OF DOCTOR OF PHILOSOPHY

in the

Faculty of Engineering
Department of Electronics and Electrical Engineering

**UNIVERSITY OF GLASGOW**



September 2008

# Declaration of Authorship

The author hereby declares that this dissertation is a result of the work carried out in the Department of Electronics and Electrical Engineering at the University of Glasgow during the period between October 2004 to May 2008. This dissertation contains original contribution by the author unless otherwise indicated.

Samina Asif

September 2008

UNIVERSITY OF GLASGOW

# *Abstract*

Faculty of Engineering
Department of Electronics and Electrical Engineering

Doctor of Philosophy

by Samina Asif

Designing a spacecraft electrical power system (SEPS) is a complex and time-consuming engineering task that involves meeting several design objectives under constraints. A conceptual design of a spacecraft power system involves an optimal selection of available technologies for various components, such as solar cells, solar arrays, batteries, and bus voltages. Each technology has its own advantages and disadvantages that need to be taken into account in the search for an optimal design solution. This selection must meet certain criteria, the most important of which are cost-effectiveness, mass and performance. Traditionally, this task is a manual iterative process. At present, designs thus selected may not be realizable using the state-of-art design options available in the industry. However, advances in domain knowledge and in extra-numerical and multi-objective search techniques, such as evolutionary computation, offer a possibility of accelerating and improving this design cycle through a machine-automated design procedure.

This thesis addresses the key issue of intelligent design automation and optimization of spacecraft power systems implemented in realistic design processes. The SEPS design is multi-objective in nature, a situation where a designer searches for solutions that are feasible with respect to all conflicting objectives. To facilitate the intelligent search process, meta-heuristics techniques are exploited in this work to provide computationally inexpensive design optimization.

It extends the existing concept of computer-aided design to computer-automated design. To make the process of trade selection more efficient and reliable, a multi-objective design system for solving preliminary design problems for spacecraft electrical power subsystems is developed. It presents a system engineering framework that places design requirements at the core of the design activities. The thesis presents how simulation and optimization techniques can be used to automate and improve the design process of spacecraft power subsystems.

The automated design procedure involves the design parameterization and the tools for system sizing and analysis. For the SEPS analysis, an inexpensive method for estimating design behavior is presented. Truly multi-objective and globally optimal design solutions are then artificially evolved as a result of interfacing evolutionary computation techniques with system sizing and analysis tools under practical constraints. Compared with conventional optimization techniques, the multi-objective design approach provides system designers with a clearer understanding of the effect of their design selections on all design variables simultaneously.

In particular, the thesis extends a SEPS design problem from the basic technology selection to a detailed optimization based systematic design, which ensures the optimality and usability of designs from the beginning of the design process. Designs are made with implementation of solar cell modeling and parameter optimization using simulated annealing, which forms a very useful tool for simulating the behavior of solar arrays comprising of different types of solar cells. SEPS simulation is extended in MATLAB from existing work currently limited to Si solar cells and NiH2 batteries to a variety of solar cell and battery technologies. The thesis also develops a complete SEPS design and search framework, as a single tool and thus avoiding all compatibility issues involved. This feature makes this work very practical and efficient. It also keeps a way open for further improvements and modifications, both for optimization techniques and for the SEPS search space.

# *Acknowledgements*

All praise is due to Allah (SWT), the most Gracious, the most Merciful. I thank Almighty Allah (glory be to Him, the Exalted) for giving me the knowledge, strength and patience to complete this work. May His blessings continue to shower on Prophet Mohammad (peace be upon him).

I would like to express my profound gratitude and appreciation to my advisor Dr. Yun Li for his consistent help, guidance and attention that he devoted throughout the course of this work. Without his frequent encouragements and useful feedback, this work could not have been realized.

I also acknowledge the support and facilities provided by my department and the faculty at the University of Glasgow. I am especially thankful to Professor David Hutching, Professor John Arnold, and Pat Duncan who were always there to solve any issue during my stay at University of Glasgow. I would also like to thank Tom'O'Hara and Miss V. Romanes for their help and support.

Thanks are due to the Institute of Space Technology (IST), Pakistan, the Higher Education Commission (HEC) of Pakistan and the Faculty of Engineering at the University of Glasgow for their financial support during this study.

I am thankful to my friends and colleagues at the University of Glasgow for their moral support, good wishes and memorable days shared together. I would also like to thank my friends from the University of Engineering and Technology, Lahore for always being with me through their help, advices and prayers.

My heartfelt thanks are to my husband and my best friend Asif, for his continuous support and encouragement. I could always discuss my ideas with him and he has provided many useful scientific inputs to my research work.

Finally, I am indebted to my parents and my parents-in-law for their support, understanding and invaluable prayers.

# Contents

# List of Figures

# List of Tables

# Abbreviations

| | |
|---|---|
| $a$ | Semi-major axis |
| $A$ | Diode ideality factor |
| $Ah_{batt}$ | Battery Ampere-Hours |
| $A_{sa}$ | Solar array area |
| $A_{scell}$ | Solar cell area |
| $A_{sctotal}$ | Total solar cell area |
| $BCR$ | Battery charge regulator |
| $BDR$ | Battery discharge regulator |
| $C_{areal}$ | Solar array less solar cell cost |
| $C_{Ah}$ | Battery capacity in Ampere-Hour |
| $C_{batt}$ | Battery cost |
| $C_{eps}$ | Power system cost |
| $C_{eff-launch}$ | Effective launch cost |
| $C_{sa}$ | Solar array cost |
| $C_{sc}$ | Solar cell cost |
| $C_{rate}$ | Battery discharge rate |
| $d_{eS}$ | Earth to sun distance |
| $d_{se}$ | Satellite to earth distance |
| $d_{sS}$ | Satellite to sun distance |
| $d$ | Array-sun distance |
| $D$ | Angle between centers of sun and earth |
| $D_e$ | Semi-diameters of earth |
| $D_S$ | Semi-diameters of sun |
| $DOD$ | Battery depth of discharge |

| | |
|---|---|
| $D$ | Direct energy transfer |
| $FOM$ | Figure of merit |
| $G$ | Illumination intensity at operating condition |
| $G_0$ | Illumination intensity at standard conditions |
| $GEO$ | Geostationary earth orbit |
| $h$ | Satellite altitude |
| $i$ | Orbit inclination |
| $J$ | General coefficient of gravitational harmonics |
| $k$ | Boltzman constant |
| $L_d$ | Solar array performance degradation factor |
| $I_{disrate}$ | Battery current discharge rate |
| $I_{ph}$ | Photo-current |
| $I_{sa}$ | Solar array current |
| $I_{sat}$ | Diode saturation current |
| $I_{scell}$ | Solar cell current |
| $I_{sc}$ | Solar cell short circuit |
| $I_{sc\phi}$ | Temperature coefficient for solar cell short circuit current under radiation influence |
| $I_{mpp}$ | Solar cell current at maximum power point |
| $I_{mpp\phi}$ | Temperature coefficient for solar cell maximum power point current under radiation |
| $IPI$ | Inverse performance index |
| $K_{voc}$ | Solar cell open circuit voltage radiation degradation coefficient |
| $K_{vmpp}$ | Solar cell maximum power point voltage radiation degradation coefficient |
| $K_{Isc}$ | Solar cell short circuit current radiation degradation coefficient |
| $K_{Impp}$ | Solar cell maximum power point current radiation degradation coefficient |
| $LEO$ | Low earth orbit |
| $M_{areal}$ | Solar array areal mass |

| | |
|---|---|
| $M_{batt}$ | Battery mass |
| $M_{box}$ | Power control unit's box mass |
| $M_{cable}$ | Cables mass |
| $M_{eps}$ | Power system mass |
| $MEO$ | Medium earth orbit |
| $MOEA$ | Multi-objective evolutionary algorithm |
| $MOO$ | Multi-objective optimization |
| $MOOP$ | Multi-objective optimization problem |
| $M_{PCU}$ | Power control unit mass |
| $M_{sa}$ | Solar array mass |
| $M_{scell}$ | Solar cell mass |
| $N$ | Mission life |
| $N_{batt}$ | Number of battery in parallel |
| $N_{cell}$ | Number of cells in series in battery |
| $N_p$ | Number of cells in parallel in solar array |
| $P_{avg}$ | Average load power |
| $N_s$ | Number of series cells per string in solar array |
| $P_{sa}$ | Required solar array power |
| $P_{BOL}$ | Solar array beginning of life power |
| $P_{Coeff}$ | Solar cell power factor |
| $P_{dis}$ | Maximum steady state power required during eclipse |
| $P_e$ | Required power during eclipse |
| $PCU$ | Power control unit |
| $PMAD$ | Power management and distribution unit |
| $PPT$ | Peak power tracker |
| $PF$ | Solar array packing factor |
| $R_{batt}$ | Battery reliability factor |
| $R_e$ | Radius of earth |
| $R_{eps}$ | Power system reliability |
| $R_{launch}$ | Launch cost factor |
| $R_p$ | Solar cell parallel resistance |

| | |
|---|---|
| $R_S$ | Radius of sun |
| $R_s$ | Solar cell series resistance |
| $R_{sa}$ | Solar array reliability factor |
| $R_{scell}$ | Solar cell reliability factor |
| $S$ | Solar intensity at 1AU |
| $SEPS$ | Spacecraft electrical power subsystem |
| $SOC$ | Battery state of charge |
| $T$ | Solar cell temperature at operating condition |
| $T_0$ | Solar cell temperature at standard test condition |
| $T_d$ | Orbital daylight period |
| $T_{Coeff}$ | Solar cell power temperature coefficient |
| $T_e$ | Orbital eclipse time |
| $T_p$ | Orbital time period |
| $V_{avg}$ | Battery cell average voltage during discharge |
| $V_{BattMax}$ | Maximum battery voltage |
| $V_{bus}$ | Bus voltage |
| $V_d$ | Diode voltage |
| $V_{max}$ | Maximum allowable bus voltage |
| $V_{min}$ | Minimum allowable bus voltage |
| $V_{mpp}$ | Solar cell voltage at maximum power point |
| $V_{oc}$ | Solar cell open circuit voltage |
| $V_{oco}$ | Solar cell open circuit voltage at standard test conditions |
| $V_{oc\phi}$ | Temperature coefficient for solar cell open circuit voltage under radiation influence |
| $V_{mpp\phi}$ | Temperature coefficient for solar cell maximum power point voltage under radiation influence |
| $V_{ref}$ | Reference bus voltage |
| $V_{sa}$ | Solar array voltage |
| $V_{scell}$ | Solar cell voltage |
| $V_t$ | Solar cell thermal voltage |
| $X_d$ | Solar array system efficiency |

| | |
|---|---|
| $X_e$ | Battery round trip efficiency |
| $\beta$ | Sun-orbit-plane angle |
| $\mu$ | Product of the universal gravitational constant and mass of earth |
| $\Omega$ | Right ascension of the ascending node |
| $\Omega_0$ | Right ascension of the ascending node at epoch |
| $\Gamma$ | Angle of incidence |
| $\gamma$ | Sun central angle |
| $\gamma_0$ | Sun central angle at epoch |
| $\theta$ | Sun angle |
| $\rho_{cell}$ | Battery cell energy density |
| $\eta_{charge}$ | Battery cell efficiency during charging |
| $\eta_{discharge}$ | Battery cell efficiency during discharging |
| $\forall$ | For all values of |
| $\exists$ | Except for the values of |
| $w$ | Argument of perigee |
| $v$ | True anomaly |
| $\phi$ | Radiation flunece |

*Dedicated to my parents and beloved husband . . .*

# Chapter 1

# Introduction

The process of a space mission design starts with mission and objectives definitions. Depending upon these objectives, many possible mission concepts are identified. At this initial stage of design, there is a need to choose among different concepts available after going through an initial trade-off process. After the selection of mission concept, and going through a number of design cycles, this process enters the preliminary design phase. At this stage, the architecture of subsystem is of concern.

In addition to the payload, the spacecraft consists of many supporting subsystems like the power subsystem, propulsion subsystem, thermal subsystem, etc. Each subsystem is responsible for a particular function. A spacecraft electrical power subsystem (SEPS), also known as a spacecraft power system (SPS), generates power, regulates it, stores it for periods of peak demand or eclipse, and distributes to the entire spacecraft. Designing these subsystems to meet the mission objectives with the possible minimum cost and weight limits is one of the most important and challenging aspects of the design process.

Spacecraft power system design involves the selection of a system topology, which is governed by the requirements of load power, mission life and regulation. At the lower level, it is mainly concerned with the technology for the components such as solar array, battery, and regulators. Usually, the initial designs are made by repeated trade-off studies among different design concepts and technologies. The trade-off among different design parameters to achieve the desired goals is a lengthy and iterative process [1]. This stimulates the need of the development of

an *intelligent* frame-work that can help the design engineer with an automated optimal design of the spacecraft power system.

Competition in the spacecraft industry has forced system designers to choose the design for spacecraft systems in a way that results in the most cost-effective product. Thus, the aerospace design practice has moved from maximizing performance under technology constraints to minimizing cost under performance constraints [2]. However, in some mission scenarios it may not be the case, so there is always a trade-off between performance, mass, and cost, which varies from mission to mission. Automating the design of a spacecraft power system is a complex task. Optimization of the process of designing and sizing a spacecraft power system can provide the best possible trade-off among the conflicting objectives.

For the design optimization of a spacecraft power system, there is a need to develop various tools. A sizing tool is required, to calculate physical parameters like size, mass, volume or cost of the system. On the other hand, analysis of the design is typically performed using simulation in order to check that the desired behavior is met. There are already some analysis tools with limited availability. However the development of an analysis tool using most commonly available platform, efficient enough to perform analysis over a certain period of time and robust enough to be expendable to include all possible technologies and topologies, still remains relatively untouched.

Most of the spacecraft optimization work reported in the literature has been performed using specialized software packages or has been carried out in a classified manner. A brief review of the available analysis tools, and the problems associated with them, are discussed in section 2.1. In addition, the problem of spacecraft power systems has not been explored for generalized application of multi-objective optimization.

## 1.1 Problem statement

At present, there exist certain limitations in spacecraft power system optimization rules and dynamic simulation available in the public domain. Firstly, most of the optimization problems are designed for solar array and battery technology selection only. Other design parameters which affect overall system design configuration and performance such as the bus voltage, battery configuration, etc., have not been

taken into account. These considerations are real and very important prior to the early design search being carried out.

In a design problem, it is usually desirable to choose design variables from within the commercially available sizes and configurations. In existing optimization problems, no consideration is given to the requirement that only the design configurations that are available in the market should be chosen. The use of continuous variables in optimization procedure, though very straightforward, can lead to non-available sizes. Any attempt to substitute these values by the closest commercial designs or to ask for new products, can make the design non-optimal and, in certain cases, even infeasible.

Thirdly, the problem under consideration is of a multi-objective nature, where a designer needs to optimize the competing objectives such as mass, cost and performance simultaneously. The performance index takes into account the solar array figure-of-merit, operational constraints of battery and also the reliability of power system for selected technologies. So far it has not been solved as a pure multi-objective problem, rather as a single objective or constrained optimization problem.

In addition, no work has been done for the development of a complete framework based on a single platform, which incorporates system analysis, for design search and optimization of spacecraft power systems. Work has already been carried using different commercial tools. This impose limitations in extending the work either on the optimization side or in incorporating further design options, while at the same time, making it unsuitable for academic research.

## 1.2 Research Objectives and Approach

### 1.2.1 Objectives

The aim of this research is to develop a framework based on evolutionary computational techniques for computer-automated design and multi-objective optimization of spacecraft power subsystems. It aims at the design and development of a simple frame-work based on a common platform. The application of this framework for the optimal selection of components and configurations will give great help to

spacecraft power system (and other subsystem) designers. This will reduce the time of design of selection and will provide them with a better basis to make more detailed system architecture and design decisions with confidence. In addition to the application of evolutionary computations for SEPS design, their application in the modelling of spacecraft power system components will also be investigated.

Specifically, this work aims to develop a methodology and framework for intelligently solving SEPS design as an optimization problem. This enables an efficient search for the best families of design solutions within the system trade space. The developed methodology will incorporate modelling and simulations to predict the performance of candidate spacecraft power systems for intelligent design iterations. With a multi-objective problem formulation, finding sets of optimal designs that represent the trade-offs among conflicting objectives, such as mass, cost, and performance, can be very useful in making system design decision.

This research will also expand on previously established approaches in such a way that the resulting system provides flexibility and improvements under changing requirements. The work carried out in this thesis is in a similar area to that presented in [1] and [3], in that it involves an integrated modelling approach with evolutionary computation that trades design variables (discrete and integer) in an optimization environment to yield a best possible design concept.

The work here will include both sizing and performance analysis tools in formulating the problem. This is not limited to one specific kind of mission and can handle both low earth orbit (LEO) and geosynchronous earth orbit (GEO) missions. It will include not only technology selection but also a preliminary design selection. In the work reported [3], the design analysis has been based on a proprietary SEPS simulation tool, which is available only within NASA. In this thesis, a SEPS simulation tool is developed on the widely available Matlab/Simulink platform, and hence it offers broad applicability in spacecraft power system optimization problems. To the best of the author's knowledge, there exists no such complete, robust framework available in the public domain. Further, it can be extended to include detailed design capabilities. More importantly, this work will also include interfacing with and applications of evolutionary computation to the modelling and design of SEPS, which has not been implemented elsewhere.

The main objectives of this research are as follows:

- To develop a methodology for formulating the SEPS design problem as an optimization problem. This methodology will make use of global and structural optimization techniques to efficiently and effectively search the system trade space.
- To develop a low cost and widely applicable analysis tool, to predict the performance of the spacecraft power subsystem design for any given design parameters.
- To integrate the sizing, analysis and optimization tools in order to develop a complete framework for spacecraft power subsystem design and optimization.
- To utilize, further to weighted sum optimization, multi-objective techniques for design optimization to find better design solutions to those already reported upon in the literature.

### 1.2.2 Approach

There are several objectives in the spacecraft power system design, namely, mass, cost and performance. Using classical search and optimization methods, it is impossible to take into account all these objectives in an optimization process. Since this is a multi-objective problem, a set of non-dominated solutions are expected. Multi-objective solutions should prove useful to the designer in trying to understand trade-offs and should assist in the selection of the final design. However, this is impossible if classical methods are employed, where a pre-weighted single objective is used. Therefore, this work seeks to study and to solve the problem with multi-objective techniques.

To achieve this goal, a detailed study of spacecraft power system design concepts, approaches and requirements needs to be made first. Through this study, the spacecraft power system design methodology may be extracted. This is accomplished by a thorough survey of various technologies regarding the components and configurations. Based upon these two studies, the design problem for optimization can be formulated and the tools required for further implementation are identified.

In the next step, research can be carried out to develop the tools identified. Based upon these studies, new tools for sizing and simulation analysis of spacecraft can

then be developed. Following the development of the analysis tool, application of and interfacing with evolutionary algorithms can be explored for solar cell modelling and SEPS design. In the third step, the tools selected and developed can be integrated into one framework. Then this frame-work may be used for the analysis of conceptual design search and optimization of spacecraft power subsystem for two multi-objective optimization approaches: one, classical (based on single a weighted sum objective); and the other, truly multi-objective. Results of both will be compared.

In the last step, this approach is applied to the design and optimization of a commercial communication satellite. The system design achieved by the optimization and the one obtained otherwise will be compared.

## 1.3 Contributions

The major contributions made in this work are:

- Extension of the spacecraft power system design optimization problem from basic technology selection to a detailed systematic design. With existing research reported in the literature, the design selected may not be realizable using the state-of-the-art design options available in the industry. The approach developed in this thesis assures the optimality and usability of designs from the beginning of the design phase.
- Design and implementation of solar cell modelling and parameter optimization using simulated annealing. This results in a very useful tool for simulating the behavior of solar arrays comprising various types of solar cells.
- Extension of spacecraft power system simulation into MATLAB, including variety of solar cell and battery technologies. Most of the existing work reported in the literature in this area is limited to Si solar cell and $NiH_2$ battery.
- Development of a complete SEPS design and search framework, as a single tool, and thus avoiding all compatibility issues involved. This feature alone makes the work at hand very practical and efficient. It also keeps a way open for further improvements and modifications, both for optimization techniques and for the spacecraft power system design search space.

The contributions to the scientific literature have produced the following peer-reviewed publications:

- Samina Asif, Yun Li. *Application of meta-heuristics to spacecraft power subsystem design trades*, published in the Proceedings of $7^{th}$ Asia-Pacific Conference on Control and Measurement, Nyingchi, Tibet, China, 11-16 Aug 2006.
- Samina Asif, Yun Li. *Spacecraft Power Subsystem Technology Selection*, Published in the Proceedings of IEEE Vehicle Power and Propulsion (VPPC) Conference 2006, 6-8 September, 2006, Windsor, UK.
- Samina Asif, Yun Li. *Intelligent search and multi-criteria optimisation of spacecraft power subsystems*, published in the Proceedings of $12^{th}$ Chinese Automation and Computing Society Conf, Loughborough, UK,16 Sept 2006.
- Samina Asif, Yun Li. *Multi-objective Optimization of Spacecraft Power Subsystem Design/Sizing*, published in the Proceedings of SAE-Power Systems Conference, November 7-9, 2006, Chateau Sonesta Hotel, New Orleans, Louisiana, USA. (Published in SAE Technical Papers (Doc no. 2006-01-3059)).
- Samina Asif, Yun Li. *Solar Cell Modelling and Parameter Optimization Using Simulated Annealing*, published in the Proceedings $5^{th}$ International Energy Conversion Engineering Conference and Exhibit (IECEC),25 - 27 June 2007, St. Louis, Missouri.
- Samina Asif, Yun Li. *Solar Cell Modeling and Parameter Optimization Using Simulated Annealing*, accepted for publication in Journal of Propulsion and Power.

## 1.4 Thesis Organization

The organization of the rest of the thesis is as follows:

Chapter 2 presents an overview of those aspects of research that are relevant to spacecraft power system design. Since the work done in this thesis is multi-disciplinary in nature, this chapter has three main sections: i) reviewing the previous attempts on application of optimization techniques in the field of spacecraft

design, ii) spacecraft power system simulation tools, and iii) multi-objective design optimization.

Chapter 3 formulates the spacecraft conceptual design as an optimization problem. In the first section, the fundamentals of any engineering system design and optimization, and analogy between engineering and spacecraft power system design and optimization, are discussed. A detailed description of spacecraft power system design trades is also given. Then a brief overview of evolutionary computations is presented. This chapter concludes with problem formulation and identification of the implementation tool.

In chapter 4, tools encompassing all necessary design attributes defined in chapter 3 are developed. The tools include spacecraft power subsystem sizing, and modeling and simulation tools. Along with these tools, two different methodologies used for multi-objective optimization are also discussed.

Chapter 5 develops solar cell/array modeling and design techniques using simulated annealing. Following the solar cell modeling techniques, the chapter develops the model and application of simulated annealing for solar cell parameter extraction. Then the results of the model are compared with test data. Finally, algorithms for the analysis of solar arrays in varying environment are presented.

The remaining chapters of the thesis are dedicated to the application of the framework developed by integrating the tools discussed in chapter 4. In chapter 6, a power system for a mission to LEO with medium power requirements is optimized using classical multi-objective approach. This analysis is undertaken for two cases. First, the study is carried out using conventional weighted sum optimization approach, where no analysis tool is incorporated. In the second case, the study is made using a complete framework developed for this work.

In chapter 7, the optimization problem is solved using multi-objective techniques. Here the problem is evaluated as two and three objectives and results are analyzed. Finally, multi-objective optimization frame work is applied to the design of the power system of a commercial satellite. The results are discussed and compared with reference to the selected baseline design.

Chapters 8 summarizes the results, the contributions this work has made to the field of spacecraft system engineering and recommendations for future work.

# Chapter 2

# Literature Review

The research related to the problem under consideration involves three different topics including simulation of SEPS, spacecraft power system design optimization, and multi-objective optimization. Therefore, the literature review is carried out in three sections. The first section provides a brief overview about the research efforts in the field of spacecraft power system modelling and simulation. Section two discusses the search and optimization techniques applied to the aerospace systems design. In the third section, a brief review of multi-objective optimization techniques is presented.

## 2.1 Spacecraft Power System Simulation Tools

This section presents a brief history of the tools developed for spacecraft power system simulation. In 1982, Capel presented a power system simulation for LEO spacecraft [4]. Another work on Spacecraft power system modelling and simulation was presented in [5], where a simple modelling approach for DC spacecraft power system is presented. In this work, the development of individual component models was presented first and later they were integrated to simulate COBE spacecraft system using EASY5.

Colombo in [6], presented a Matlab based satellite power simulation. Here, a generalized model of SEPS for single specific type of solar cell and battery was presented. The recent work on SEPS modelling and simulation has been undertaken by a research group at the University of South Carolina. This group has

developed a software tool called Virtual Test Bed (VTB), having capability of simulating the SEPS. This software is still in its testing phase. Although many successful applications have been presented [7], there is still a large amount of work that needs to be done; as in its present format it cannot be integrated with an optimizer.

In the field of modelling and simulation of individual components of SEPS, there has been extensive research in the field of solar cells and batteries modelling, and a detailed review of them is out of context of this thesis. A brief review of some related research work will be discussed in section 4.2, where the modelling approaches used in this work will be discussed.

On the other hand, there exists some commercial software packages, the problem with such tool is the difficulty in getting access to them as well as the cost. One of these packages is MMPAT (Multi-Mission Power Analysis Tool), developed by Jet Propulsion Laboratory, NASA. MMPAT is a multi-platform software simulator written in C language, used to analyze the performance and resources of space vehicle electrical power subsystem. It has been applied to MER (Mars Explorer Rovers) and Deep Impact missions and same has been presented as part of optimization applications in [3, 8]. This software is available only within NASA and is not accessible in public domain.

There is another tool, PowerCap, developed by SAE Inc, Canada [9]. This is a dynamic performance simulation tool. Components of the power system are replaced by their equivalent mathematical modes. In [9], a long term simulation is realized using PowerCap and transient analysis is performed by an industrial software like PSpice, Saber or any equivalent software. This software does not allow changing its parameters through another application such as an optimizer.

## 2.2 Spacecraft Design Optimization

In spacecraft industry, one key aspect of design decisions is economy. Goals of high performance under constrained budgets can only be achieved through a well structured optimized design process.

Some attempts have been made in spacecraft, or its subsystem design optimization in its early design phase. In 1995, a design tool was presented by George and Peterson [10], which connects all spacecraft performance analysis tools on a network under the control of a master design program. The main idea of this research is to allow design groups to change their components or subsystems and analyze its effects on the system level. Riddle in [11, 12], explored the use of dynamic programming to provide an insight into the effects which individual technologies have on the performance and cost parameters of a satellite during the conceptual design phase. Riddle developed a software tool named ESSAM (Early Small Satellite Analysis Method), which employs a dynamic programming approach, and tested it on the design of a satellite power subsystem. ESSAM is used to find the optimal solution that minimizes the power subsystem mass. However, the illustrative case study here contains only two decision variables and four possible solutions. In realistic space system design, problems often contain many internally coupled decision variables, making the dynamic programming approach impractical for systems with higher design variables. This is because dynamic programming can only handle problems of relatively small dimension. Based on the work of George, Fukunaga presented the application of an adaptive evolutionary algorithm based optimization techniques to the spacecraft design [13]. Further improvements in this work were made by incorporating web based real time collaborative interactivity [14].

Pullen successfully presented the application of heuristic search methods in the reliability-based optimization of the Gravity Probe-B spacecraft bus design [15], using Simulated Annealing and Genetic Algorithm (GA) to optimize eighteen design variables representing the redundancy level of the bus components and subsystems. This work shows that such non-gradient optimization approach can lead to designs that offer higher reliability values than a baseline design.

Mosher surveyed several multidisciplinary optimization (MDO) techniques, including classical optimization, decomposition, the Taguchi method, and heuristics, for conceptual spacecraft design [1, 2]. Mosher eventually chose a heuristic approach, a genetic algorithm, to create a software tool named SCOUT (Spacecraft Concept Optimization and Utility Tool) for the conceptual design of scientific spacecraft, and benchmarked the tool against NASA's Near Earth Asteroid Rendezvous (NEAR) spacecraft. The optimization problem here is based on single objective;

minimum cost for the system. This work demonstrates the effectiveness of application of evolutionary optimization for spacecraft conceptual design.

Hassan presented the application of genetic algorithm to conceptual satellite design with uncertain reliabilities in [16]. The design combines satellite sizing and reliability modelling and applied a genetic algorithm using population based sampling. In this case, the problem involves both spacecraft payload and bus design. It has been shown that a GA is able to find good design solutions with only 0.075 of the computational cost required by the Monte Carlo approach at the same level of accuracy.

Recently, much research on automation of spacecraft systems design has been carried out at Jet Propulsion Laboratory (JPL) NASA. Their work includes both the application of evolutionary computation for spacecraft design automation and for optimization of spacecraft power system in a parallel processing environment. They have also shown successful application of GAs and SA to the automation of rover arm path planning, optimization of low thrust trajectories, automatic tuning of Micro gyroscope, and automatic design of power subsystems [3, 8, 17].

There have been other efforts that are focused on the advancement of spacecraft design, but have fairly different focus from research presented in this thesis. For example, optimization codes are commonly used today in the design of aircraft wing platform [18] and in structural engineering to design a truss that will safely meet all the loading requirements with possible minimum mass [19]. Another field of aerospace which incorporates optimization is orbital dynamics, such as spacecraft trajectory modelling and optimization [20]. Application of GAs to optimize the placement of eight actuators on 1507 possible locations to control the vibration of a large spacecraft is presented in [13]. The spacecraft trajectory modelling and optimization are presented in [20]. Jilla presented an application of multi-objective, multidisciplinary optimization methods for the design of distributed satellite systems, where optimization tool is developed to find the best architecture for conceptual design of distributed satellite systems [21].

## 2.3 Multi-objective Design Optimization

In any engineering system design, including spacecraft systems design, there are usually several design objectives reflecting the interest of various engineering aspects and stakeholders. If there were only one objective, the design concept that measures the best against this objective should clearly be a matter of choice. However, when there are several competing design objectives, there are usually several good designs that measure differently against the individual objectives, but equally well against one measure that includes all the objectives. From system engineer's point of view, it is highly desirable to obtain this set of design concepts, because they represent the trade-off between various design objectives. One of the major objectives of this research is to formulate the SEPS conceptual design as a multi-objective design optimization to obtain the trade-off between SEPS performance, mass and cost.

In a multi-objective design optimization problem, there is seldom one optimal solution as in a single objective and usually there are many optimum design points, which are called a Pareto-optimal set of solutions [22]. For each of these Pareto-optimal designs, there is no other feasible design that is better on all objectives, i.e., these designs are non-dominated to one another.

In classical methods, finding a Pareto optimal set has been used to reduce a multi-objective problem to single objective optimization problem [23]. The most common approach is the use of weighted sum where each objective is assigned a weight and added together into a single objective function. Another method is the e-constraint approach where one objective is selected for optimization and others are reformulated as constraints.

An attractive approach is to use multiple runs of optimization, each of which targets one objective only. In classical methods one optimization run finds one optimal solution on Pareto front, so multiple runs are needed to find all solutions on the optimal front. Evolutionary algorithms can exploit the population-based feature and converge in parallel to the Pareto front. While optimizing, various solutions in the population converge to various areas of the Pareto front, and thus an approximation of the Pareto front can be obtained in a single optimization run. Research interest has increased over the past two decades on the development and application of evolutionary algorithms for Pareto optimization. Some of the common multi-objective evolutionary algorithms (MOEAs) are multi-objective genetic

algorithm (MOGA), non-dominated sorting genetic algorithm (NSGA), NSGA-II, strength pareto evolutionary algorithm (SPEA), SPEA-II, multi-objective messy genetic algorithm (MOMGA) and MOMGA-II. An exhaustive list of references can be found on the web page of Coello [24]. The detailed comparison of different MOEAs can be found in [25]. In addition to multi-objective techniques based on genetic algorithms, there are also some alternative heuristic methods for multi-objective optimization, such as particle swarm optimization, ant colony algorithm, simulated annealing, tabu search and etc. Detail of these can be found in [25].

Multi-objective optimization in general has been an attractive area of the research recently and there is simply too much literature on this topic to discuss all here. Examples of previous research efforts that to implement a multi-objective approach with the GA for aerospace applications can be found in [18], [26], and [27]. There have also been a few research efforts that implemented a multi-objective optimization approach for the design of satellite constellations and distributed systems with the focus of orbital design [21].A survey of Evolutionary techniques for multi-objective optimization of engineering system design is presented in [23]. The focus of this thesis is the application of multi-objective optimization approach to the design of SEPS.

# Chapter 3

# Problem Formulation

## 3.1 Spacecraft Power System Conceptual Design

System engineering design can be divided into four stages:

- Conceptual design
- Preliminary design
- Embodiment design
- Detail design.

Sometimes the conceptual design term is used collectively for conceptual and preliminary design and this is what is assumed in this work.

The first phase of any engineering design process is to identify the system specifications based on costumer needs. The second step is concept generation, which usually uses functional decomposition methods. In the third step, evaluation of the generated concepts i.e., decision matrices are usually employed. After selecting one or more concepts the subsystem design enters the detailed design phase. After the subsystem design is complete, some system level design activities are carried out to ensure the feasibility of the system design in terms of compatibility and interoperability of all subsystems. Optimality at system-level is usually ignored as it is hard to achieve for reasons of system level integrated modelling. Hence, the optimization is usually performed on the subsystem levels.

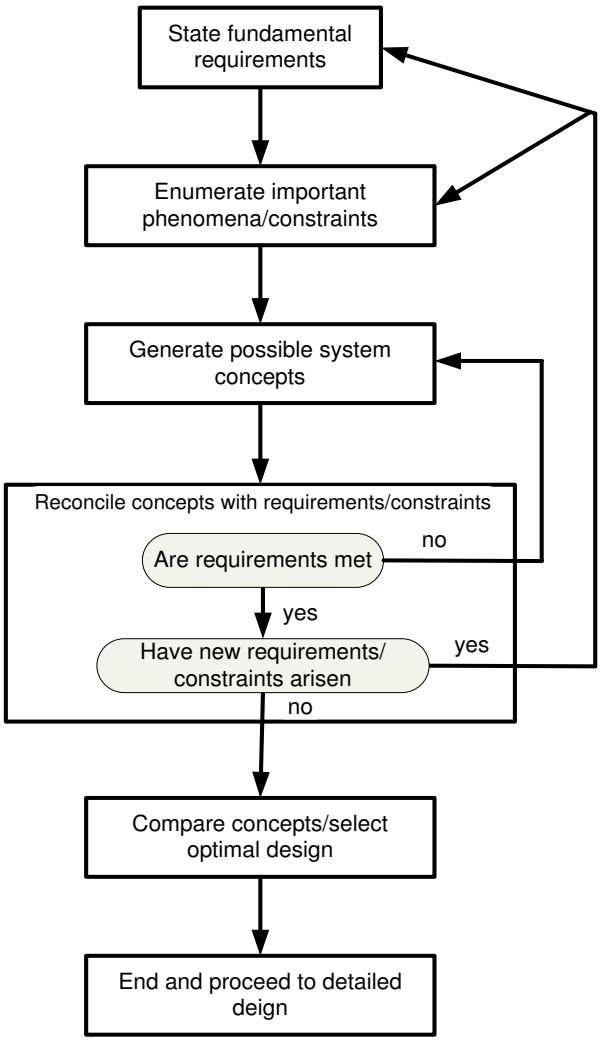


FIGURE 3.1: Conceptual engineering system design.

Within each phase a set of activities is performed. Ideally, the designer wishes to perform each phase once, but engineering design is very iterative. A large number of iterations are often required before the final design is achieved. An iterative model of a conceptual design is shown in Figure 3.1.

Like any engineering system design, the space system design process passes through a number of phases. Any aerospace system design process can be divided into following phases:

- Pre-phase A: Conceptual study
- Phase A: Preliminary analysis
- Phase B: Detailed definition

- Phase C: Development
- Phase D: Manufacture, integration, and test
- Phase E: Mission operation and data analysis.

During Pre-phase A, the mission ideas or requirements are translated into the mission concepts. This includes the development of preliminary requirements, determination of evaluation metrics, creation of alternative system architectures, preliminary analysis and trade of these architectures as well as initial cost estimation. Phase A work involves more detailed trade analysis and refining of cost estimation. Phase A results in the identification of best design architecture or design variables. Phase B is associated with detailed design and definition. It involves the definition of system and subsystem design in sufficient detail for phases C/D. Phase B completes the technical design including the final requirements document, lower level design specifications, interface control and the manufacturing plan. Phase C concludes the design. Phase C/D encompasses development, manufacture, integration and testing. It involves completion of design and analysis, preparation of manufacturing drawings, completion of development and qualification testing, and development of flight system and acceptance testing. Phase E is associated with launch, delivery of spacecraft in the orbit and support of in-orbit operation throughout the nominal mission life.

In the system engineering approach, special focus is given to top level design. If the decisions taken at conceptual/preliminary phase of design are made in a systematic way, given due consideration to trade studies and critical design objectives, the rest of design process should progress smoothly with minimal cost overhead at the design or manufacturing phases.

In the early design phase, the decisions are to be made in terms of technology choices and redundancy level. It usually ends up with large number of design variables that must be traded off. The next step in conceptual design is the analysis and evaluation of different design alternatives. The design alternatives are evaluated against the selected performance criteria based on the design requirements.

The process of conceptualizing design solutions that satisfy the design requirements is the core of the system engineering activities and is usually referred to as system architecturing. System architects are encouraged to apply a systems

engineering approach to synthesize alternative solutions based on functional requirements rather than starting with pre-built ideas. The implementation of the system engineering approach is particularly problematic in the early stages of the design process for a number of reasons. Firstly, the complex systems normally involve many interlaced design variables; therefore members of the design team must employ system sizing and performance evaluation tools. These tools must allow them to understand the effect of varying each design variable on the whole system. Early in the design process when most of the decisions are yet to be made regarding the system architecture in terms of technology choice and redundancy level, there are usually a large number of design variables that must all be traded off to yield architectures with optimal performance. For each top-level functional requirement, a system architect can list a few discrete design options, all of which can all satisfy this functional requirement. Combining all these options quickly turns this problem into a combinatorial one, where a large number of alternative architectures are possible.

In the next stage of conceptual design, the analysis and evaluation of alternative designs is performed to select a final design concept for a full design development. The generated design alternatives should be evaluated based on how well each of them measures against selected performance criteria that are related to the design requirements. Evaluating such a large number of design alternatives can be quite an impossible task to carry out for a small design team. To narrow down the design space, the designers usually add design constraints as well as rely on their experience.

### 3.1.1 Spacecraft Power System Design Trades

The most important system aboard any satellite is its electrical power system. In its simplest form, the spacecraft electrical power system consists of four major components as shown in Figure 3.2.

The prime power source provides the energy to the conversion unit for the conversion of a given energy into electricity. The electricity that is generated needs to be managed, regulated, monitored and conditioned to match the electrical needs of the spacecraft systems.

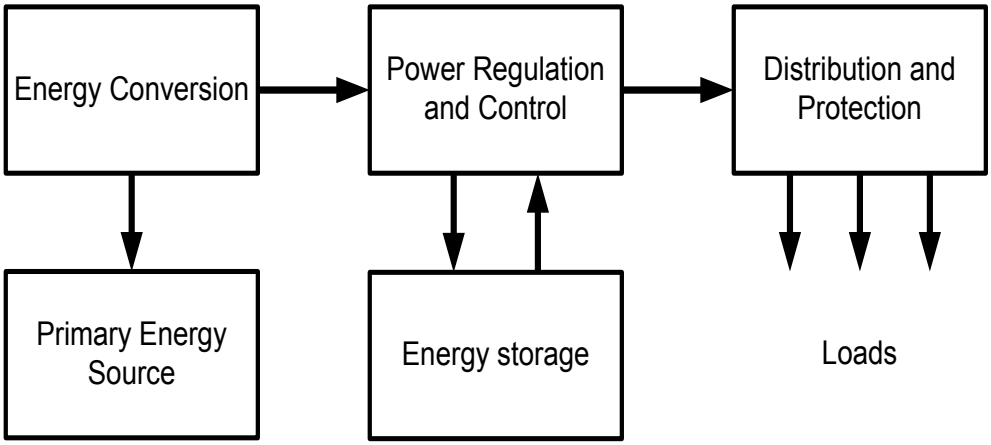


FIGURE 3.2: Basic elements of spacecraft power system (courtesy of [28])

The common choices available as the prime power generation source in space are limited to nuclear, chemical or solar. The key factor in the selection of a power generation source is the duration of the mission. For short duration missions or to supply power for activities that will be completed relatively quickly in longer missions, chemical systems such as primary batteries, fuel cells and chemical dynamic conversion may be the appropriate choice depending upon the total power requirement. For longer duration missions, the choice is restricted to a solar array in conjunction with secondary batteries or regenerative fuel cells, or a nuclear system. There are certainly other issues which affect the choice of power generation source such as the radiation profile of a given orbit. Compatibility with mission related sensors can also be a factor.

For earth orbiting satellites, power systems based on solar arrays as energy source with photovoltaic (PV) energy conversion and secondary batteries as power storage unit are most common. Such systems are commonly known as PV-battery power systems and are focus of this research. Spacecraft power systems are further characterized by their architecture,i.e., either direct energy transfer (DET) or peak power tracker (PPT). In direct energy transfer systems, the power is usually transferred directly from the solar array to the load without any power tracker in the path. In peak power tracker architectures, the solar array voltage is usually adjusted through a series of connected power trackers to get the maximum power from the solar array. DET architectures are further divided as: i) fully regulated, ii) sun regulated, and iii) hybrid systems. DET systems provide the lowest part count, high efficiency and lower cost in many cases. However, past experience

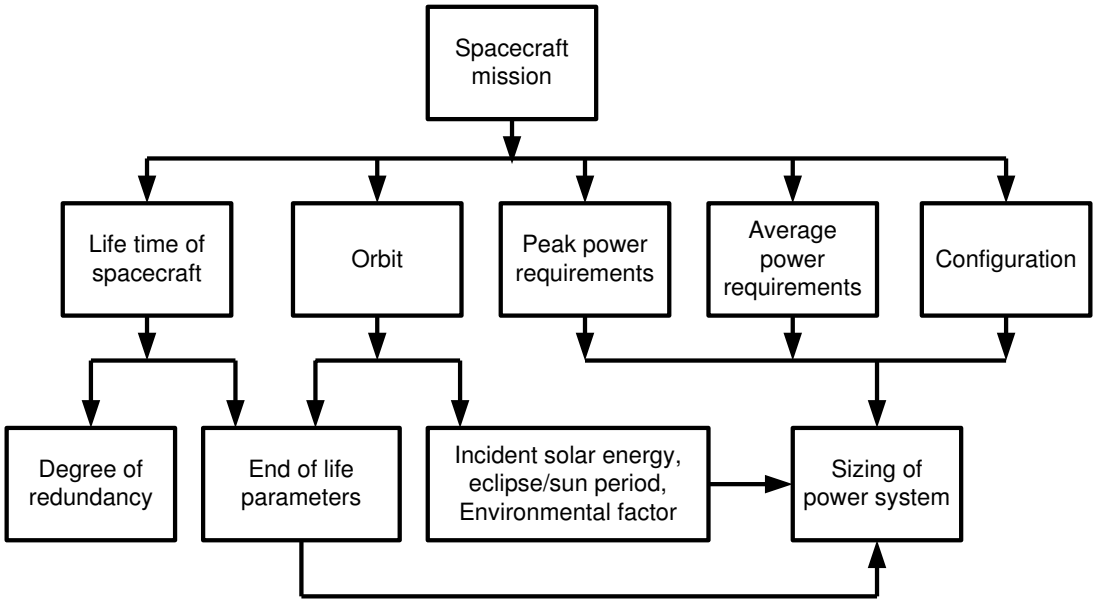


FIGURE 3.3: SEPS selection process

shows that PPT systems are advantageous for small satellites in low earth orbits with power requirements around 500W. For power level exceeding 1kW, DET architecture is generally considered advantageous.

An electrical power system is designed and configured to perform several key functions, the primary being a continuous and reliable source of peak and average electrical power for the life of the mission. Many factors contribute to the final design and the choice of technologies that must be integrated. The schematic of this selection process is shown in Figure 3.3.

In this study, we are dealing only with the PV-battery systems based on DET architecture. This system primarily consists of a solar array, a rechargeable battery and a power regulator which regulates power flow between various components to control the bus voltage. In the following sections, we will discuss the trades available within different modules of the SEPS.

### 3.1.2 Solar Power Generation

A space photovoltaic system consists of a number of elements, one of which is the solar array. Key design issues for the solar arrays include the spacecraft configuration, required power levels (peak and average), operating temperatures, shadowing, radiation environment, illumination or orientation, mission life, mass and area.

#### 3.1.2.1 Solar Cell Technology Trades

The solar cell technologies which are considered here are Silicon (Si), High efficiency Silicon (High-$\eta$ Si), Gallium Arsenide single junction (GaAs/Ge SJ), Gallium Arsenide dual junction (GaInP2/GaAs/Ge DJ), Gallium Arsenide triple junction (GaInP2/GaAs/Ge TJ) and ultra triple junction (UTJ). Si solar cells have a very long heritage in space applications. Although Si solar cells are still in use because of their low cost, they are increasingly replaced by multijunction solar cells in high power applications. High-$\eta$ Si are advanced solar cells with higher efficiency and lower mass density than conventional Si solar cells. In recent years, there has been very active research in improving the efficiency of solar cells. Further, in recent developments, hybrid solar arrays are also in use; so here two combinations of High-$\eta$ Si with GaAs/Ge SJ and Si with GaAs TJ are considered as design options.

When applied to the system level, it is clear that the desired attributes for low mass translate into high efficiency. The cell efficiency determines array area, which can then be used to determine the mass of the array. The mass of array can also be determined directly from efficiency. Solar cell characteristics, such as particle irradiation and temperature coefficients, determine their end of life (EOL) power. The output powers of solar arrays also get affected by radiation levels. The multijunction cells are more resistant to irradiations, hence they offer higher EOL power than Si. A comparison of beginning of life (BOL) efficiency, temperature coefficients, and radiation degradation factors (P/Po) at different radiation fluence levels for various technologies traded-off in this study, is given in Table 3.1. The size of all the single crystalline solar cells is kept constant.

#### 3.1.2.2 Solar Array Technology Trades

The main requirements for spacecraft solar array technologies are mass, size, cost and power growth capability. The solar array configuration can be either planar or concentrator, and either can be body or panel mounted. The most commonly used types of solar array technology, the *deployable* and *sun tracking solar array*, are considered here. Deployable solar arrays are typically wing type structures which are stowed with the spacecraft body during the launch and deployed from the spacecraft after final orbit acquisition. In this study, two solar array configurations:

| Solar Cell Technology | BOL Efficiency (28°C) | BOL Power ($W/m^2$) | Cost (K$/Kg) | Mass ($Kg/m^2$) | Power Temperature Coefficients (%/°C) | Radiation Degradation P/Po (Fluenece e/cm2 1 MeV Electrons) | | |
|---|---|---|---|---|---|---|---|---|
| | | | | | | $1 \times 10^{14}$ | $5 \times 10^{14}$ | $1 \times 10^{15}$ |
| Si | 13.7 | 185 | 20 | 0.55 | -0.045 | 0.92 | 0.82 | 0.77 |
| High-$\eta$ Si | 16 | 216 | 50 | 0.28 | -0.0415 | 0.92 | 0.83 | 0.79 |
| GaAs/Ge SJ | 19 | 253 | 140 | 0.83 | -0.022 | 0.90 | 0.85 | 0.75 |
| $GaInP^2$/ GaAs/Ge DJ | 22 | 297 | 140 | 0.85 | -0.030 | 0.96 | 0.89 | 0.83 |
| $GaInP^2$/ GaAs/Ge TJ | 25 | 337 | 150 | 0.85 | -0.06 | 0.96 | 0.92 | 0.83 |
| Ultra Triple Junction UTJ | 28.0 | 378 | 170 | 0.86 | -0.06 | 0.93 | 0.89 | 0.86 |

TABLE 3.1: Comparison of solar cell characteristics (courtesy of [29][30])

| Solar cell technology | Rigid Planar Array | | | | | Flexible Planar Array | | | | |
|---|---|---|---|---|---|---|---|---|---|---|
| | Solar panel mass ($Kg/m^2$) | Radiation fluence, 1 MeV/$cm^2$ | | Operating temperature | | Solar panel mass ($Kg/m^2$) | Radiation fluence, 1 MeV/$cm^2$ | | Operating temperature | |
| | | GEO | LEO | GEO | LEO | | GEO | LEO | GEO | LEO |
| Si | 2.52 | $9 \times 10^{14}$ | $2 \times 10^{14}$ | 50 | 60 | 1.72 | $1 \times 10^{15}$ | $4 \times 10^{14}$ | 55 | 65 |
| High-$\eta$ Si | 2.34 | $9.5 \times 10^{14}$ | $2 \times 10^{14}$ | 60 | 70 | 1.54 | $1.25 \times 10^{15}$ | $5 \times 10^{14}$ | 65 | 75 |
| GaAs SJ | 3.2 | $7 \times 10^{14}$ | $6.6 \times 10^{14}$ | 65 | 75 | 2.24 | $7.7 \times 10^{14}$ | $7.5 \times 10^{13}$ | 70 | 80 |
| DJ | 3.26 | $6 \times 10^{14}$ | $3 \times 10^{14}$ | 65 | 75 | 2.28 | $6.6 \times 10^{14}$ | $4 \times 10^{13}$ | 70 | 80 |
| TJ | 3.26 | $6 \times 10^{14}$ | $3 \times 10^{14}$ | 65 | 75 | 2.28 | $6.6 \times 10^{14}$ | $4 \times 10^{13}$ | 70 | 80 |

TABLE 3.2: Comparison of array characteristics (courtesy of [29])

rigid planar arrays and flexible planar arrays are considered. A comparison of these two types is given in Table 3.2. Equivalent radiation fluence is dependent upon the orbit and mission duration and cover glass thickness. Here the values are assumed for GEO with mission life of 15 years and LEO with mission life of 5 years. The selection of cover glass thickness also depends upon radiation environment of the mission. Here, the thickness of cover glass is assumed to be 100 micrometer for both LEO and GEO cases.

### 3.1.3 Power Storage System

The energy storage subsystem in a photo-voltaic system is based on electrochemical battery cells. It is designed to deliver electrical power during an eclipse. A battery consists of a number of cells connected in series or parallel arrangement. The

| Battery Technology | Cell Nominal Voltage (V) | Cell Average Discharge Voltage (V) | Cell-Specific Energy (W-hr/Kg) | Cell-Specific Power (W/Kg) | Operating Temperature °C |
|---|---|---|---|---|---|
| NiCd | 1.45 | 1.25 | 40 - 50 | 150 - 200 | -20 - 50 |
| NiH2 | 1.55 | 1.25 | 45 - 65 | 150 - 200 | -10 - 50 |
| Li-ion | 4.1 | 3.5 | 90-150 | 200-220 | 10-45 |

TABLE 3.3: Typical battery cell characteristics comparison (courtesy of [28])

prime requirement for a battery is to be capable of providing the required power and energy at a desired voltage and over a required period of time. Among the overriding requirements are those of minimum size, volume and cost to meet the spacecraft requirements.

#### 3.1.3.1 Battery/Cell Technology Trades

The most widely used type of batteries that are used in space are rechargeable Nickel Cadmium (NiCd) and Nickel Hydrogen ($NiH_2$). More recently the Lithium-ion batteries are also in use and are being flown on various space missions. During last two years, most of the research in the battery area has been focused on Li-ion and lately it has been proposed as the most desirable type of battery in European missions [31].

Batteries have many characteristics which influence the system design. The electrical characteristics include nominal voltage, capacity, operating temperature and energy density. Table 3.3 provides a comparison of these characteristics.

The comparison in the table gives the range of values for specific energy and specific power covering all cell capacities. In our calculations, the values of specific energy and specific power are calculated for individual cells of given capacity as found in data sheets or provided by manufacturer.

#### 3.1.3.2 Battery Configuration Trade

In addition to battery selection, there is a trade between selecting the configurations of battery. The configuration of the battery includes the number of batteries in parallel and number of cells in series per battery. There is no defined principle in selecting number of batteries for a given mission.

| Bus Voltage (V) | Number of Cells per Battery | | |
|---|---|---|---|
| | NiCd | $NiH_2$ | Li-ion |
| 28 | 20-22 | 20-22 | 6-7 |
| 50 | 26-30 | 26-30 | 10-12 |
| 100 | 52-60 | 52-60 | 20-24 |

TABLE 3.4: Number of cells as a factor of bus voltage.

The key factor in determining the number of cells per battery is bus voltage. The number of cells per battery is selected so that the battery capacity available for given mission is closest to the one available in the market. This will result in the battery mass and cost saving.

As far as redundancy in battery design is considered, in most of the cases battery level redundancy is not considered as it can have significant effect on the battery mass and cost. However redundancy in the cells per battery is usually considered to counter the open circuit faults in the cell. In this work, we have assumed one cell redundancy in each battery.

#### 3.1.3.3 Bus Voltage Level

The power requirements for the satellites, especially for communication satellites, have increased during last decade. At high power levels, low voltage power systems become impractical. With the size of a typical fixed satellite service (FSS) communication satellite bus approaching the size of small room, distribution of 10-15 kilowatts of power at low bus voltages would incur high ohmic losses. Also, high voltages allow better utilization of energy density from the secondary batteries. Still for low power LEO missions the 28V bus can be the most economical in context of highly developed heritage. In this study, three options: 28V (traditional low bus voltage level), 50V and 100V are compared.

The bus voltage also affects the configuration of the battery. For certain given voltages, there are some ready-made configurations available from vendors. These configurations may vary from vendor to vendor. The configurations which have been considered in this work are given in Table 3.4.

## 3.2 Optimization in Engineering Design

It has been stated before that the engineering design is very iterative, and a large number of iterations are often required before the final design is achieved. Usually the number of design alternatives is very large. An automated search process could be more efficient than manual techniques in finding optimal designs in such cases. In other words, formulating the design of a complex system in the conceptual design phase as an optimization problem can help the designer to discover new combinations of available components and subsystem options. This can lead to an optimal solution which might not had been a clear choice if system design was to be carried out manually.

The engineering system design process which employs modelling, simulation and optimization is shown in Figure 3.4. After selecting one or two concepts, the detailed design activities start. At this point, modelling and simulation are employed in order to evaluate the properties of particular system solutions. Each solution is evaluated for some already defined set of objectives. The solution which is most feasible is selected as an approved design and is put forward for detailed design.

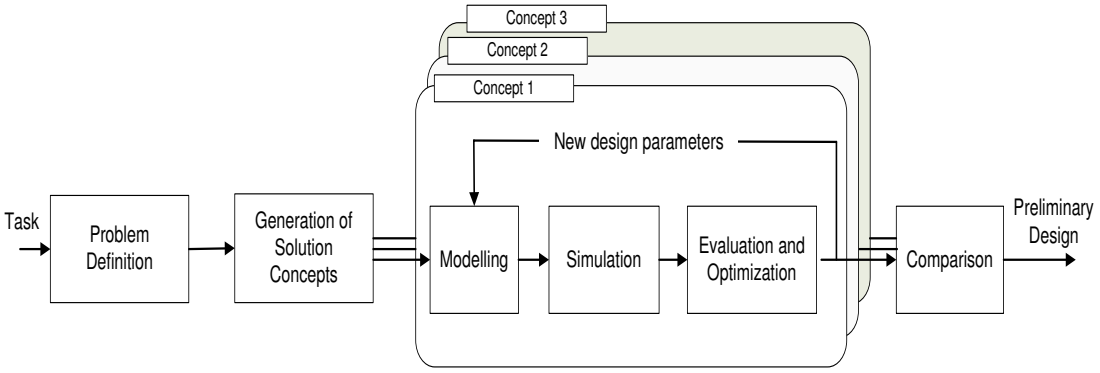


FIGURE 3.4: The System Design Process [32]

The optimization procedure makes use of modelling and simulation as a tool to evaluate the performance of each of the system solutions and to generate new system proposals. This process continues until the optimization process has converged and an optimal system is found. In some cases, the objectives are all related to the performance evaluation, such as the design optimization of a circuit or a motor design. In our case, performance analysis is just one of the objectives along with others such as mass and cost. In such cases, a sizing tool is also required along with modelling and simulation.

### 3.2.1 Components of an Optimization Problem

An optimization problem is basically formed from three basic components:

- Design variables: These are the parameters that are changed during the optimization procedure.
- Objective function: These are one or more function values which we want to minimize or maximize. For example in the SEPS design problem, we wish to minimize the cost and maximize the performance.
- Constraints: These are the conditions that allow the design variable to take certain values but exclude others. As with the SEPS problem, we have only certain battery capacities available. Other capacities will be excluded by the constraints.

### 3.2.2 Single Objective Vs Multi-Objective Optimization

A single objective optimization problem is a problem in which one seeks the best (lowest or highest) value of a well defined objective [33]. Equation 3.1 presents a constrained single objective problem for the minimization of a scalar function $f(\vec{x})$ (the objective function).

$$\begin{array}{ll} \min\ f(\vec{x}) & \vec{x} \in S \\ \text{subject to} & \\ g_i(\vec{x}) \leq 0 & i = 1, ..., J \\ h_i(\vec{x}) = 0 & i = 1, ..., K \end{array} \tag{3.1}$$

where $\vec{x} = (x_1, ..., x_n)$ is a vector of $n$ design variables such that $\vec{x} \in S \subseteq R^n$. Here the search space $S$ is defined as an $n$-dimensional rectangle. $g_i(\vec{x})$ and $h_i(\vec{x})$ are constraint functions, J is the index set of inequality constraints and K is the index set of equality constraints, where both sets $J$ and $K$ are finite.

If the problem is convex for a minimization objective function or concave for a maximization objective function, there will exist only one optimal solution to the problem. If the problem is non convex or non concave, there may exist more than one globally optimal solutions. But each globally optimal solution will have the

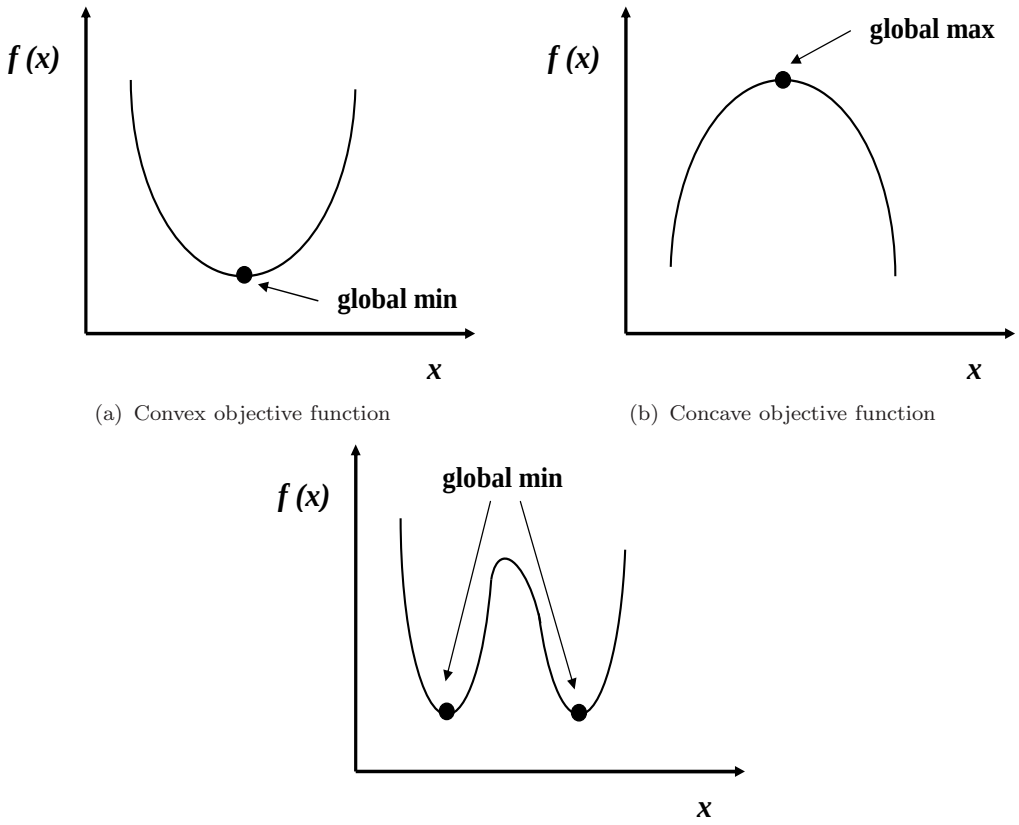


(a) Convex objective function

(b) Concave objective function

(c) Objective function with more than one global optimal solutions

FIGURE 3.5: Illustration of different types of objective functions

same objective function value. The illustration of these different cases is given in Figure 3.5.

While single objective optimization provides a powerful tool to explore the trade space of a given optimization problem, most problems in nature have several (possibly conflicting) objectives to be satisfied. These problems are classified as multi-objective or multi-criteria problems. Such problems are common in engineering design where one has to balance multiple requirements while trying to achieve multiple goals simultaneously. The multi-objective problem may be presented as:

$$\min F(\vec{x}) = \left[f_1(\vec{x}), f_2(\vec{x}), ..., f_k(\vec{x})\right] \quad \text{while } \vec{x} \in S \subseteq R^n \tag{3.2}$$

where $f_1(\vec{x})$, $f_2(\vec{x})$, ..., $f_k(\vec{x})$ are the $k$ objectives. The search space $S$ is usually defined as $n$-dimensional rectangle as in the case of single objective problem. The problem now is to search for solutions which minimize all the objectives $f_i(\vec{x})$.

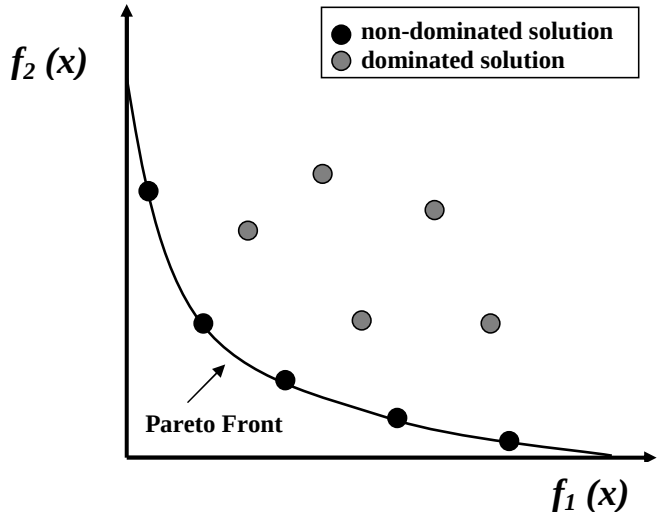


FIGURE 3.6: The concept of Parrto-front and non-dominated solutions for two conflicting objectives $f_1$ and $f_2$.

In multi-objective problems (MOPs), there may exist no single optimum solution. Rather, in such cases we are really trying to find good compromises (trade-offs) among the conflicting objectives. Hence in a certain class of MOPs, there always exist a number of solutions which can all be termed as optimal. A set of such optimal solutions is commonly known as Pareto-optimal solutions or a Pareto front. These solutions are optimal in the sense that there is no other solution in the search space superior than them when all the objectives are taken into consideration. In other words the Pareto optimal solutions are non-dominated solutions. Preference information of the decision maker is needed to perform a further selection.

Considering a minimization problem, a design with solution vectors $a$ is said to dominate a design with a vector of objectives $b$ if:

$$\forall i \in 1, 2, ...k : f_i(\vec{a}) \leq f_i(\vec{b}) \; and \; \exists j \in 1, 2, .., k : f_j(\vec{a}) < f_j(\vec{b})$$

It says that a solution $\vec{a}$ dominates another solution $\vec{b}$ if it is better in at least one objective and not worse in the other objectives. The illustration of Pareto front and non-dominated solutions is given in Figure 3.6.

Different design problems can have different shapes for the Pareto front. It can be convex, concave, non-convex or non-continuous. The shape of the Pareto front

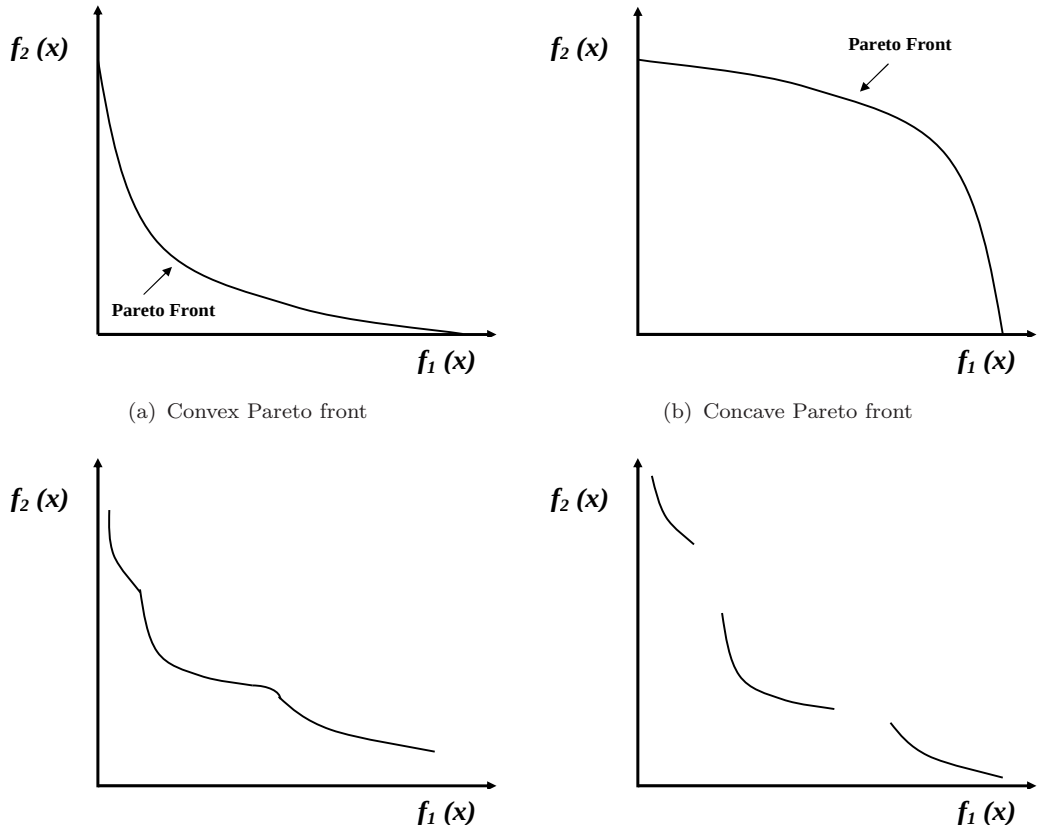


(a) Convex Pareto front

(b) Concave Pareto front

(c) Non-convex Pareto front

(d) Non-continuous Pareto front

FIGURE 3.7: Illustration of different shapes of Pareto front.

gives information about the behaviour of trade-off among the conflicting objectives. Figure 3.7 illustrates different shapes of the Pareto front.

## 3.3 Optimization methods

Optimization algorithms can be classified into three main classes; gradient-based, enumerative and guided random algorithms [33]. Gradient-based methods use gradient or higher order derivative information about the function to be optimized ($f(\vec{x})$). Indirect Gradient-based methods compute the position of the minima by differentiating the objective function and setting the obtained gradient equations to zero:

$$\frac{\partial f}{\partial x_i} = 0 \qquad i \in 1, 2...., n \tag{3.3}$$

such that

$$\frac{\partial^2 f}{\partial x_i \partial x_j} = 0 \qquad i, j \in 1, 2...., n \tag{3.4}$$

This method thus requires the mathematical equations of the objective functions which is difficult in real-world optimization problems.

Direct gradient-based methods converge iteratively to the optimum. For a given starting point ($x_0$), the derivative is computed and used as direction for successive search points. These methods rely on derivative information of all objectives and all constraints for determining the search direction of the optimization. The simplest approach for obtaining derivatives is the finite differencing with forward differences:

$$g_i = \frac{(f(x_0) + \Delta e_i) - f(x_0)}{\Delta} \tag{3.5}$$

where $g_i$ is the partial derivative of $f$ in the space direction $i$, $\Delta$ is the length of the finite step and $e_i$ is a unit vector in space direction $i$. This method does not require the mathematical equations of the objective function, as gradient is calculated by finite differences.

Enumerative methods evaluate the function to optimize at every point in the search space. Full enumeration is the most expensive technique in terms of number of function evaluations. It is only applicable to search spaces with a limited number of feasible points.

Guided random methods use random processes to find the optimum. The progress in optimization process is based on some predefined rules. They are also referred to as semi-stochastic algorithms. In past decade the stochastic methods have become more and more important in engineering design optimization problems. Well-known representatives of these stochastic methods are Evolutionary Algorithms and Simulated Annealing.

## 3.4 Evolutionary Algorithms

Evolutionary algorithms (EAs) are a class of global search algorithms inspired by natural evolution. Several different types of EAs exist. Genetic Algorithms (GAs), Evolution Strategies (ES), Evolutionary Programming (EP) and Genetic Programming (GP) are some of the best known. EAs are termed as non-gradient methods. In this work, most of the optimization work is done using GAs. In next section a short description of GA and multi-objective GAs is given.

### 3.4.1 Genetic Algorithm

The GA is derived from Darwin's theory of Natural Selection. A GA mimics the reproduction behaviour observed in biological populations and employs the principal of "survival of the fittest" in its search process. The idea is that an individual (design solution) is more likely to survive if it is adapted to its environment (design objectives and constraints). Therefore, over a number of generations, desirable traits will evolve and remain in genome composition of the population over traits with weaker characteristics.

A GA differs from conventional optimization in many ways. It allows coding for a combination of both discrete and continuous design variables. A GA is population-based search, which results in multiple solutions in one run, rather than only one solution. Thirdly a GA needs objective function values and not its derivatives (as required in gradient based methods) which may not exist in many real world applications. Keeping in view these advantages, and knowing that in the SEPS optimization problems come up with mixed type of variables, we can say that a GA will be advantageous in this case.

#### 3.4.1.1 Mechanics of evolution

A GA employs iterative selection process based on fitness, recombination and mutation. Selection is a process in which design candidates are selected based on the fitness value. It may include alteration of generation and selection for mating partners. The new candidates are then generated by recombination and mutation. Figure 3.8 illustrates the flow chart of a GA.

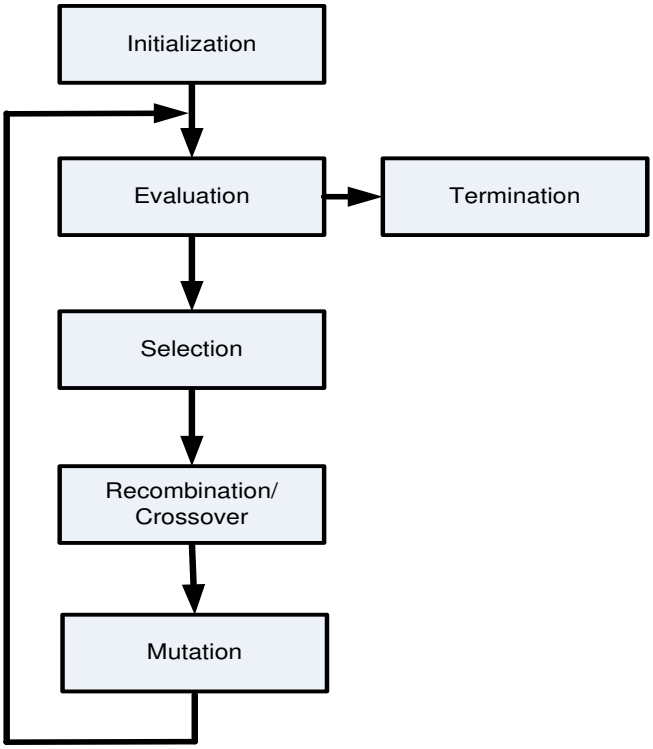


FIGURE 3.8: The flow chart presentation of a GA.

During initialization, an initial population of design candidates is generated. This is often accomplished by random sampling of a design space. Evaluation is the step where the fitness of all the individual candidates is evaluated by objective function values. When modelling and simulation is employed to calculate the performance of a SEPS design, this process becomes computationally very expensive. Selection is a process in which the fittest individuals are selected to reproduce offsprings for the next generation. There are many approaches to conduct "survival of the fittest" operations. Some common approaches are: fitness proportional selection, ranking selection and tournament selection. The recombination or crossover operator is responsible for exchanging the features of the selected parents for the generation of new individuals with the intention of improving the fitness of the individuals in the next generation. The last operator needed to generate a population of the new generation is called mutation. The function of mutation is to keep the diversity of a population and promote searching in the solution space that cannot be represented by the strings of the parent population. One of the most common form of mutation is uniform mutation that adds a uniform random number to each component of an individual's vector with a probability of $p_c$.

### 3.4.2 Handling of Multi-objective Problems

Several different methods exist which can handle the multi-objective problems [25]. The most widespread and classical way is the weighted sum, where each objective is assigned a weight and these weighted objectives are added together into a single objective. This is one of the simplest methods and quite efficient for problems having convex Pareto front. Weighted sum objective function for '$M$' objectives $(f_1(\vec{x}), f_2(\vec{x}), ..., f_M(\vec{x}))$ is formulated as:

$$F(\vec{x}) = \sum_{j=1}^{M} w_j f_j(\vec{x}) \tag{3.6}$$

where $w_j \geq 0$ is the weighting coefficient representing the relative importance of the $j^{th}$ objective function. By choosing different weightings, $w_j$, for different objectives, the preference of the decision maker is taken into account. $w_j$ are selected such that:

$$\sum_{j=1}^{M} w_j = 1$$

This method has the advantage of generating a single compromised solution. However, to get a proper set of Pareto optimal solutions, many runs of optimization, with repeatedly changing the weights, are required. Another disadvantage of this approach is that it fails to produce solutions on non-convex parts of Pareto front.

Evolutionary algorithm based multi-objective optimization methods deal simultaneously with a set of possible solutions (population). They facilitate the finding of an entire set of Pareto optimal solutions in a single run of the algorithm. This feature enables the designer to get a clear picture of how different objectives are trading off against each other, and helps in selecting solution where decision maker has no pre-defined preferences. Additionally EAs are less susceptible to the shape or continuity of the Pareto front while finding an optimum solution.

In this work, we will make use of NSGA-II, as it has been applied to many optimization problems with promising results [34], [35]. It uses elitism[1] and a crowded comparison operator that keeps diversity without specifying any additional parameters and it is computationally more efficient [36].

[1] Elitism is the approach in MOEAs that employs an external set to store best solution and to add them in the next generation. With this method, best individuals of each generation are always preserved

#### 3.4.2.1 Non-Dominated Sorting Genetic Algorithm-II

There are numerous versions of the MOEAs as discussed in section 2.3. In these approaches, a simple evolutionary algorithm is extended to maintain a diverse set of solutions with the emphasis on moving toward a true *Pareto-optimal* region. The non-dominated sorting GA (NSGA) proposed by Srinivas and Deb [37], is one of the first such algorithms. It is based on several layers of classification of the individuals. Non-dominated individuals get a certain dummy fitness value and then are removed from the population. This process is repeated until the entire population has been ranked. It is a very effective algorithm but it has been criticized for its computational complexity, lack of elitism and its requirement for specifying sharing parameters in the algorithm. Based on these issues, a modified version of the NSGA, named NSGA-II [36] was developed. In [36] a comparison of NSGA-II with the two other powerful algorithms: Pareto-archived evolution strategy and strength pareto is presented which shows that NSGA-II out performs its competitors when used for solving truly diverse problems.

Two distinct entities are calculated in the NSGA-II to validate the quality of a given solution. The first is a domination-count where the number of solutions that dominate a given solution are tracked. The second keeps track of how many sets of solutions a given solution dominates. In the process, all the solutions in the first non-dominated front will have their domination count set to zero. The next step is to select each solution in which the non-domination count is set to zero and visit all other solutions in the solution set and reduce the domination count by one. In doing so, if the domination count of any other solution becomes zero, this solution is grouped in a separate list. This list is flagged as the second non-dominated front. This process is then continued with each member of the second list until the next non-dominated front is identified. The process is continued until all fronts are identified. Based on the non-domination count given to a solution, a non-domination level will be assigned. Those solutions that have higher non-domination levels are flagged as non-optimal and will never be visited again. One of the key requirements of a successful solution method is ensuring that a good representative sample from all possible solutions is chosen. Introduction of a density estimation process and a crowded-comparison operator has helped NSGA-II to address the above need. The crowding-distance computation requires sorting of a given population according to each objective function value in ascending order of magnitude. Once this is done, the two boundary solutions with the

largest and smallest objective value are assigned distance values of infinity. All other solutions lying in between these two solutions are then assigned a distance value calculated by the absolute normalized distance between each pair of adjacent solutions. After each population member is assigned a crowding-distance value, a crowded-comparison operator is used to compare each solution with the others. This operator considers two attributes associated with every solution which is the non-domination rank and the crowding-distance. Every solution is rated with others based on the non-domination rank. Solutions with lower ranks are deemed better in this attribute. Once solutions that belong to the best front are chosen based on the non-domination rank, the solution that is located in a lesser-crowded region is considered better and forms the basis of the NSGA-II algorithm. The flow chart depicting the NSGA-II algorithm is shown in Figure 3.9.

### 3.4.3 Constraint Handling

There are several methods described in the literature that are used to handle design constraints in optimization problems [38], [39]. Penalty functions are the most common method that is used with meta-heuristics techniques. In this approach, the constrained optimization problem is converted into an unconstrained formulation where a penalty is added to the value of the objective function when constraint is violated, the function under consideration is transformed to:

$$F(\vec{x}) = \begin{cases} f(\vec{x}) & x \in feasible\,region \\ f(\vec{x}) + penatly(\vec{x}) & x \notin feasible\,region \end{cases} \tag{3.7}$$

In this work, a linear exterior penalty function approach is implemented to handle the constraint and is described by:

$$p(\vec{x}) = f(\vec{x}) + \sum_{j=1}^{J} c_j\, max[0, g_j(\vec{x})]^{\beta} + \sum_{k=1}^{K} c_k \left| h_k(\vec{x}) \right|^{\gamma} \tag{3.8}$$

where $\beta$ and $\gamma$ are commonly 1 or 2. Here,$f$ is the unconstrained function that needs to be minimized, $h$ is the equality constraint, $g$ is the inequality constraint and $c_j$ and $c_k$ are penalty parameters. The formation of equality and inequality constraints is shown in Equations 3.9 and 3.10 respectively.

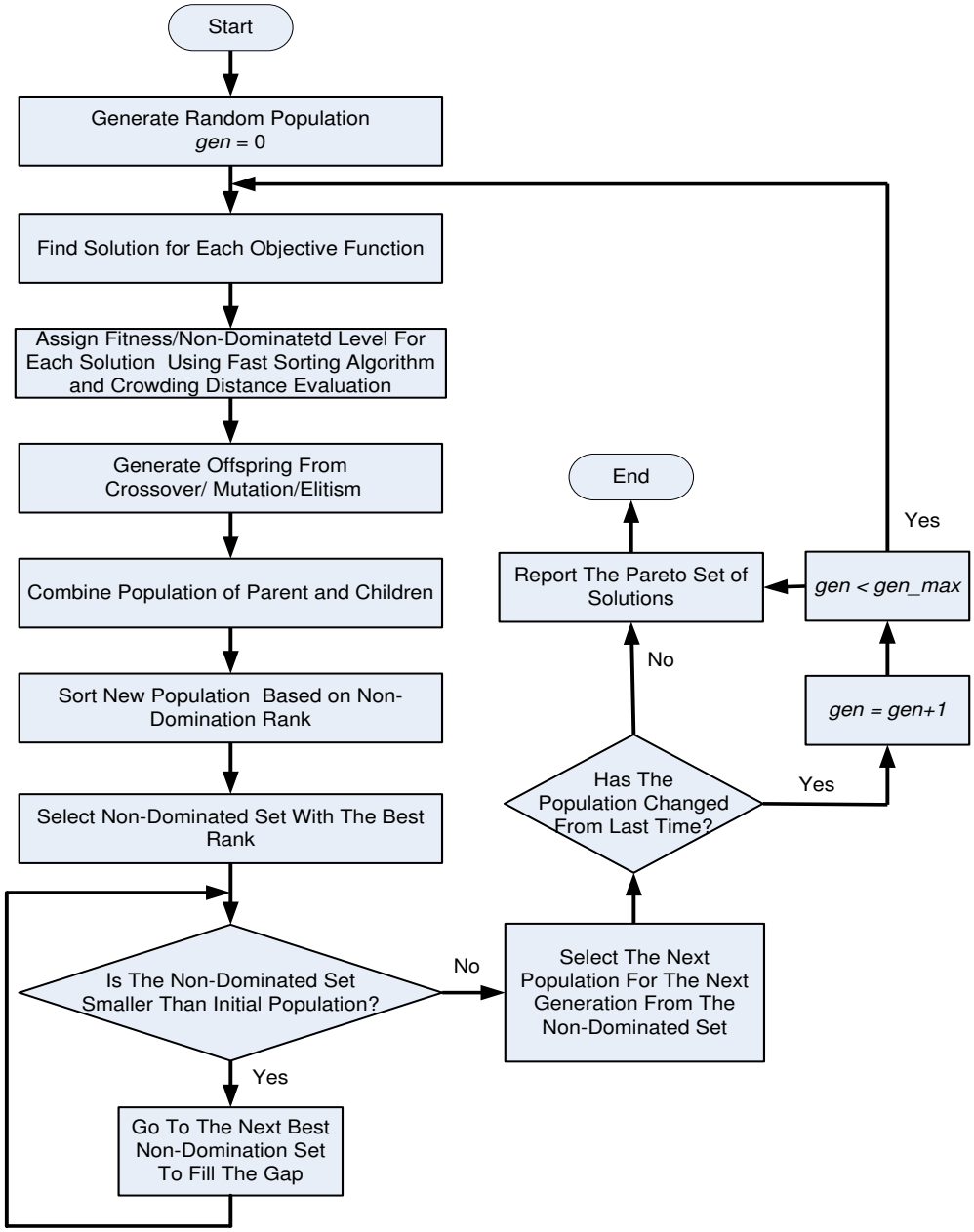


FIGURE 3.9: Flow Chart Representation of NSGA-II Algorithm.

$$h(\vec{x}): \quad \frac{Response}{Limit} - 1 \quad = 0 \tag{3.9}$$

$$g(\vec{x}): \quad \frac{Response}{Limit} - 1 \quad \leq 0 \tag{3.10}$$

The penalty multipliers $c_j$ and $c_k$ are selected through prior work on this problem. This is a disadvantage of the penalty method because they demands prior knowledge of the penalty multipliers that can achieve fast convergence. A general guideline is that the multiplier should add penalties for violated constraints of the same order of magnitude as the objective function [33].

## 3.5 SEPS Design Optimization

### 3.5.1 Practical Aspects of Engineering Design Optimization

Many aspects have to be taken into account when reformulating the design problem as an optimization problem. These include:

- Which design variables should be chosen?
- What are the objectives and what are the constraints?
- Often a mix of design variables exist (continuous, discrete).
- Almost always several objectives exist.

In practice, the choice of design variable is often given by the fact that not all the design parameters can be changed. Even if all the design parameters can be changed, only those which have significant effect on the design should be chosen as design variables.

In a practical problem, it is often difficult to decide what the objectives and constraints are. If several objectives exist, the formulation might be a multi-objective optimization problem. If some of the objectives may be formulated as constraints instead, this is preferable since the problem will, in general, become easier to solve.

An optimization problem with only discrete design variables is a combinatorial problem with a finite set of solutions. If some design variables are of continuous type, the search space is a set of infinitely many solutions. Many real-world design problems involve mixed types of design variables.

Before formulation of the problem is done, it is always good to get as much information as possible about the system. The strategy used by author in this thesis is summarized as follows:

- Selection of design variables
- Optimization problem formulation
- Development of required tools
- Optimization runs
- Post-optimal analysis

### 3.5.2 SEPS Conceptual Design-Problem Formulation

The goal of a system engineering design project is to integrate the design activities to provide quantitative support to high level decision making in all stages of the project. It is most important in the preliminary design phase where trade-offs and design decisions that characterize the performance of the whole system are made. This study focuses on the application of evolutionary computation (EC) to the spacecraft power system, the emphasis being on multi-objective design.

#### 3.5.2.1 Selection of Design Variables

In the case of SEPS, the system design consists of a number of decisions. The total number of decisions or design variables is very large for the preliminary design. For the current research purpose, the design variables are chosen at the top level, leaving out details regarding power management and the focus is only on major design variables. For a spacecraft power system design quite a number of factors influence the design. The total number of decision variables can be very large. Table 3.5 summarizes the selection of design variables for this work. Maximum battery discharge rate is also considered as design variable as this is a factor in determining battery size (capacity). Battery discharge rate is defined in terms of battery capacity C (Ampere-hour). If we say the battery is to be discharged at 1C rate, it means that the battery can provide C amperes of current for one hour. For space applications usually a discharge rate of C/2 to C/3 can be used.

| Variable | Variable Name | Possible Value |
|---|---|---|
| 1 | Solar cell type | Si<br>High-$\eta$Si<br>GaAs/Ge SJ<br>GaInP$^2$/GaAs/Ge DJ<br>GaInP$^2$/GaAs/Ge TJ<br>Ultra triple junction UTJ<br>Hybrid 1 (High-$\eta$ Si + GaAs/Ge SJ)<br>Hybrid2 (Si + GaInP$^2$/GaAs/Ge TJ) |
| 2 | Solar array type | Rigid planar<br>Flexible planar |
| 3 | Battery cell choice | NiCd<br>$NiH_2$<br>Li-ion |
| 4 | Bus voltage | 28V<br>50V<br>100 |
| 5 | No. of batteries | 1, 2, 3, 4,6 (LEO)<br>1,2,4,(GEO) |
| 6 | No. of cells per battery | Values are selected on<br>the basis of bus voltage<br>(Table 3.4) |
| 7 | Maximum battery discharge rate | 0.5C -<br>0.67C |

TABLE 3.5: Design parameter trade space.

#### 3.5.2.2 Objective Function

Previous studies on SEPS design followed the approach to minimize cost and mass [2]. In these cases, fewer design variables were considered, no consideration of technology choices was provided and also performance matrix consisted only of the performance of the batteries. Also only the cases of two deep space missions were evaluated. In the current problem, optimization is to be applied which minimizes cost and mass for maximum performance for both the solar array and the battery under the constraints of technologies available in the market and the battery performance criteria. The problem is designed for earth orbiting spacecraft, both in LEO and GEO.

In this case, the objective function is defined using MATLAB programming environment. The function makes use of a sizing tool for algebraic operations and an analysis tool for modelling and simulation.

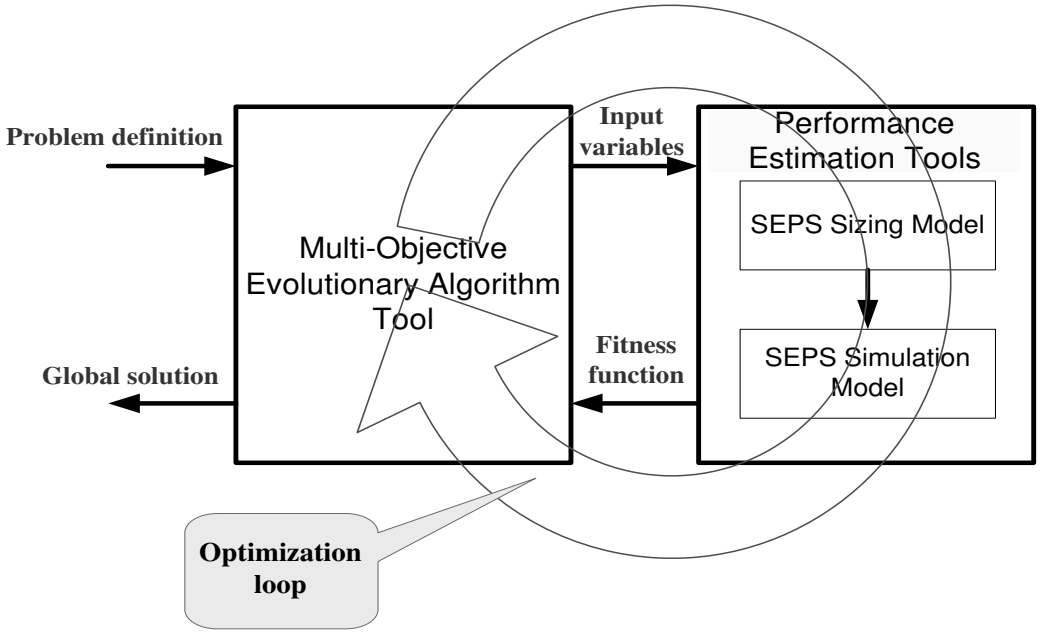


FIGURE 3.10: Summary of SEPS design optimization approach and computational tools.

### 3.5.3 Implementation Tools

In any space system design, there are usually several design objectives that interest system architects. Traditionally, the spacecraft power system design matrices include mass, size, and performance. Other requirements that play an important role in the system architecture are the acquisition cost and reliability.

The approach of this research, with emphasis of multi-objective design, is to facilitate the system architect to integrate design optimization with modelling and simulation. The focus, here, is on power systems for spacecraft in a low earth or geosynchronous orbit. This can also be used for a medium earth orbit, although with some levels of uncertainty. This is based on a subset of the above mentioned performance matrices, namely mass, cost and performance. The design variables under consideration are technology options. Figure 3.10 summarizes the approach implemented in this work.

The different blocks shown in the figure represent the different tools which are developed or implemented as part of the complete SEPS design optimization framework. To evaluate the performance of alternative designs, a SEPS sizing model is developed based on approaches given in the literature [28, 40], along with some knowledge of common space industry practices. Sometimes the designs generated

by simple relations, given in the literature may not come up with what is available in industry thus rendering the designs as infeasible. To take this factor into account, such knowledge has been incorporated as constraints. The design relations in this sizing tool mimic the preliminary design budget which includes system mass, cost, reliability and solar array figure of merit. This framework also mimics the analysis tool which, as a response, does performance analysis and mimics a performance budget.

To implement the design optimization, the third part of the framework consists of an optimizer. Two variations of the GA are used as optimization techniques. One approach makes use of the classical weighted sum GA approach. In the second one, a non-dominated sorting genetic algorithm is implemented to address the multi-objective nature of the problem. All the computational tools developed or used in the work are discussed in chapter 4.

# Chapter 4

# SEPS Design Optimization Methodology

In this chapter, the methodology adopted and the tools developed for design optimization of spacecraft power system, are discussed. The study in this research is focused on the development of a single platform based for the application of evolutionary algorithms to spacecraft power system design search and optimization. In chapter 3, we have seen that, in order to achieve this goal we need three tools to be designed or developed. These include sizing-, analysis- and optimization-tools. The methodology adopted here is applicable for spacecrafts both in GEO and LEO having circular orbits. This can also be applied to the MEO missions but as enough data about the environment and technology heritage for MEO missions are not available, we do not expect accurate results.

There are several system approaches that can be used in spacecraft power system design. The primary functions of such systems are common to all of these designs. There are few areas that need to be identified before sizing any spacecraft power system. These include total spacecraft power, system losses, solar array degradation over mission life, orbit profile, spacecraft bus voltage, and battery charging profile.

The sizing tool predicts the subsystem level parameters for the spacecraft such as mass, size and cost. The sizing tool is based on knowledge gained from previous experience and literature [40],[28], [41]. The sizing tool is coded as MATLAB scripts. Many of the following design estimating relationships and scaling factors are used to correlate the predictions with the actual data taken from industry and

existing database of satellites. Some of the data is proprietary and may not be shared here.

An analysis tool is required to evaluate the design of SPS during optimization run. There are a few proprietary tools available for such analysis, but no such tool is available in public domain that can fulfill the purpose of this research. Therefore, a considerable part of this research deals with the development of such an analysis tool. The analysis tool will predict the SEPS performance using the sizing parameters calculated by the sizing tool. The meta-heuristics based optimizer will then make use of the results of both the sizing tool and analysis tool to get *near-optimal* solutions.

The first part of the chapter describes the SEPS sizing model that predicts system mass, cost and size based on spacecraft's mission and power requirements.

The second part of this chapter describes the SPS analysis model. This model is developed as part of complete design and optimization framework. The model is then integrated with both sizing and optimization models.

Third part of this chapter describes evolutionary algorithm based optimization tool. The different optimization techniques used are explained in this section.

## 4.1 Spacecraft Power System Sizing Model

As spacecraft power system design and sizing model is developed, in order to assess the relative performance of solar cell, array technology, battery design, and bus voltage. This model calculates the mass and size of solar array, battery capacity (Ah), and mass of battery depending upon the technology of the solar array, solar cell, battery and battery configuration (number of batteries and number of cells per battery). Mission data including average power, maximum power required from power subsystem and orbital parameters are provided as input. Orbital parameters include orbit altitude, worst case sun angle and maximum beta angle (angle between orbit and sun-earth line). This information is used to determine the orbit's sunlight and eclipse time. Based on the information of altitude and sun-orbit-plane angle ($\beta$), eclipse duration is calculated. Approximate eclipse duration ($T_e$) for a circular orbit is given by [40]:

$$T_e = \frac{T_p}{\pi}\left[cos^{-1}\left[\frac{\sqrt{1-\left(\frac{R_e}{R_e+h}\right)^2}}{cos\beta}\right]\right] \quad \text{where} \quad \frac{R_e}{R_e+h} > sin\beta \tag{4.1}$$

Maximum eclipse duration will occur for a minimum $\beta$ which corresponds to $\beta = 0$. Here $T_p$ is orbital time period and is given as:

$$T_p = 2\pi\sqrt{\frac{(R_e+h)^3}{\mu}} \tag{4.2}$$

where $R_e$ is radius of earth, $h$ is satellite altitude and $\mu$ is the product of the universal gravitational constant and mass of earth.

Solar array sizing is performed on the basis of spacecraft average load power ($P_{avg}$) requirement. The total power to be generated by solar array ($P_{sa}$), is sum of the load-power required by spacecraft and battery charge power. Considering direct energy transfer system, $P_{sa}$ is given as:

$$P_{sa} = \frac{\frac{T_d}{X_d} + \frac{T_e}{X_e}}{T_d} \times P_{avg} \tag{4.3}$$

where $P_{sa}$ is the solar array power required at the end of mission life. $T_d$ is sun-light time duration, $X_d$ is efficiency of solar array system and is given by 0.85 for a direct energy transfer system and $X_e$ is round trip efficiency of battery and depends on battery technology and is related to battery characteristics by relation given as:

$$X_e = \frac{energy\ output\ over\ full\ discharge}{enery\ input\ required\ to\ restore\ full\ charge} \tag{4.4}$$

In this work, the value of $X_e$ is taken to be 0.85, 0.80 and 0.9 for NiCd, $NiH_2$ and Li-ion respectively.

### 4.1.1 Solar Array Sizing

The solar array sizing model calculates the size, mass and cost of the solar array, to be used by optimizer, as well as the layout of solar array, which is to be used by analysis model. The main inputs for solar array design are:

- sunlight and eclipse duration
- spacecraft power profile
- array type
- solar cell type
- solar cell efficiency
- temperature coefficients of solar cell
- radiation degradation factor
- assembly mismatch factor
- thermal cycling degradation
- packing factor
- bus voltage

The methodology adopted for sizing is shown in Figure. 4.1.

The beginning of life power ($P_{BOL}$) for the solar array to give required power by end of life is given as:

$$P_{BOL} = \frac{P_{sa}}{F_{loss}} \tag{4.5}$$

where $F_{loss}$ represents the power loss factor for the solar array power due to temperature, radiation and sun light offset effects along with life time degradation. Collectively, it is given as:

$$F_{loss} = [1 - (T_0 - 28) \times T_{Coeff}] \times P_{Coeff} \times I_d \times |cos\theta| \times (1 - L_d)^N \tag{4.6}$$

where $T_{Coeff}$ is the temperature factor determined by type of solar cell, and array, $P_{Coeff}$ is radiation degradation factor determined primarily by the type of orbit

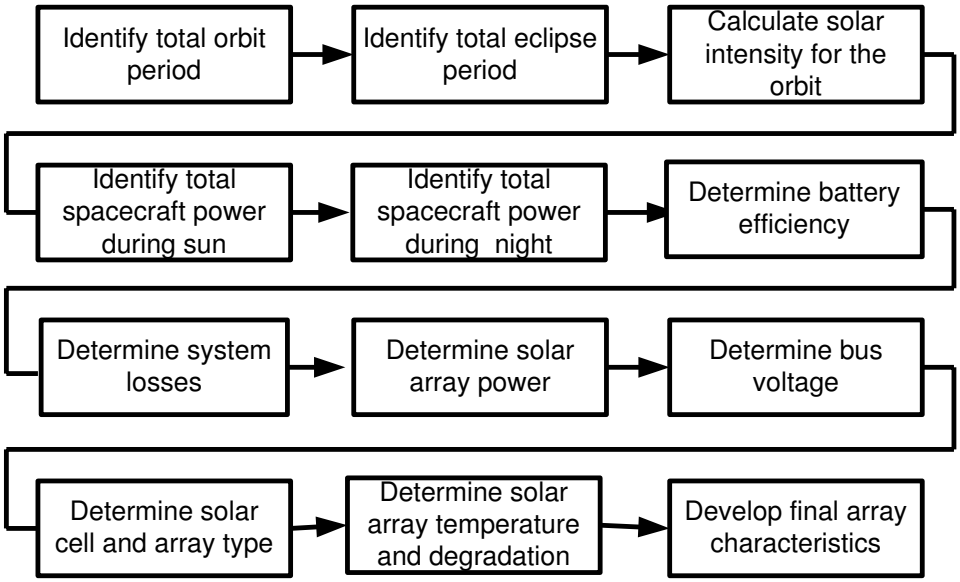


FIGURE 4.1: Spacecraft solar array sizing methodology

and mission life along with the type of solar cell and array and N is mission life in years. $I_d$ is inherent degradation factor due to design, assembly, cell mismatch and shadowing because of appendages of spacecraft. Its value varies between 0.49-0.88. Here this value is taken as 0.77. $L_d$ is performance degradation factor due to thermal cycling, having a value of 3.75% per year for Si and GaAs and 2.75% per year for multijunction cells. In addition to these factors, 5% reliability margin is also added. In the case of flexible array, additional power losses are to be taken into account due to large thermal gradient across the array. For standard cells, i.e., Si and GaAs, it is assumed to be 3% and for multijuntion cells, it is taken to be 5% [28].

Solar cell area is determined by calculating number of cells in series ($N_S$) and parallel ($N_P$) required to meet the array voltage ($V_{sa}$) and power specifications.

$$N_S = \frac{V_{sa}}{V_{scell}} \tag{4.7}$$

$$N_P = \frac{I_{sa}}{I_{scell}} \tag{4.8}$$

where $V_{scell}$ and $I_{scell}$ are the cell load voltage and current at operating temperature. Here the values of $N_S$ and $N_P$ are calculated to the nearest integer value.

Then the total solar cell area ($A_{sctotal}$) is calculated as:

$$A_{sctotal} = N_S \times N_P \times A_{scell} \tag{4.9}$$

where $A_{scell}$ is area of individual cell. Solar cells are available in different sizes i.e., 2x2 cm, 2x4 cm, etc. Although there is a provision in sizing and analysis tool to define size of the solar cell for different technologies, we have considered a value of 2x4 cm solar cell size.

Total area of solar array ($A_{sa}$) is calculated as:

$$A_{sa} = \frac{A_{sctotal}}{PF} \tag{4.10}$$

where PF is solar array packing factor. Here its value is taken as 0.9.

### 4.1.2 Battery Sizing

The battery sizing model calculates the mass and cost of the battery. The methodology of achieving this is described in Figure 4.2. Battery sizing depends on mission requirements i.e. power required during eclipse ($P_e$), duration of eclipse ($T_e$) and the frequency of eclipse. So before starting sizing we should know the energy required by batteries for spacecraft operation during eclipse. Battery sizing starts with the selection of electro-chemistry and number of batteries. The characteristics, that are associated with the chemistry of the battery have been summarized in Table 3.3. The main inputs for the battery sizing model are:

- capacities available for each technology
- cell average discharge voltage ($V_{avg}$)
- Maximum allowable discharge rate
- mission life in years.

Total number of charge-discharge cycles is determined from mission life and mission type. For LEO, an average number of charge discharge cycles is taken to be 5000 cycles per year. For GEO, this value is 90 cycles per year [42]. Maximum

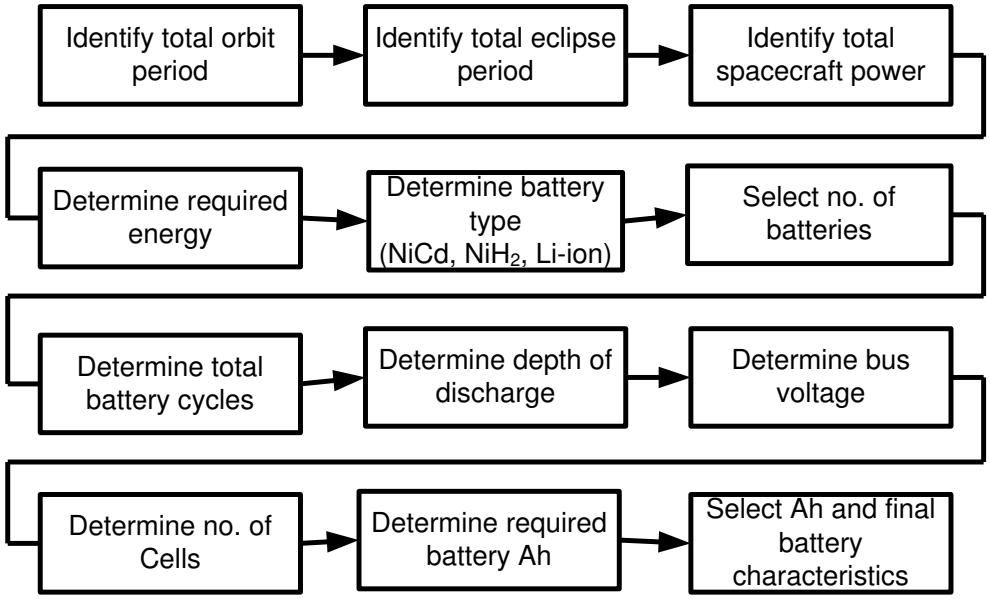


FIGURE 4.2: Spacecraft battery sizing methodology.

allowable depth of discharge (DOD) varies with the battery type and the mission life (number of charge-discharge cycles). It is determined by the interpolation of the graphs given in Figure 4.3 [43].

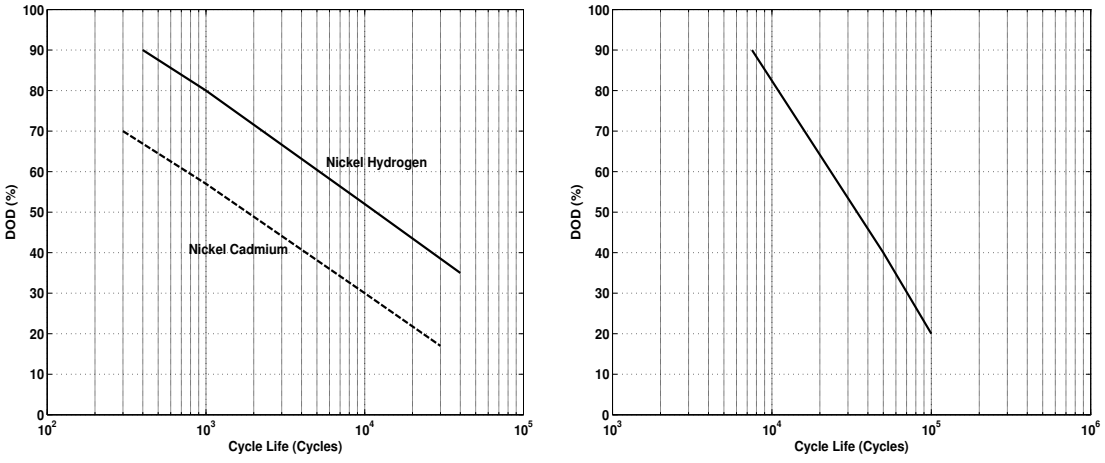


(a) NiCd and $NiH_2$

(b) Li-ion

FIGURE 4.3: DOD vs. cycles life for NiCd, $NiH_2$, and Li-ion batteries (adapted from [43])

The graph for Li-ion shown in Figure 4.3, does not comply with the figures of DOD given in the literature [44],[45]. Keeping this in view, a graph between cycle life and DOD for Li-ion has been reconstructed and is shown in Figure 4.4.

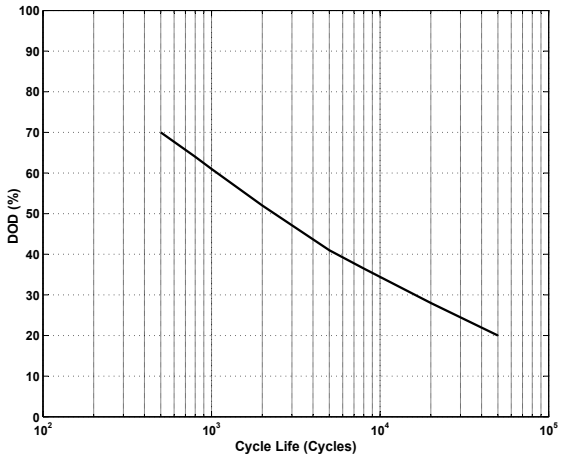


FIGURE 4.4: DOD vs. cycles life for Li-ion batteries

Number of cells per battery is selected depending upon the bus voltage. Ampere-hour capacity of battery ($Ah_{batt}$) is calculated using two methods; one is based on watt-hours required and the other is on maximum steady state power required during eclipse ($P_{dis}$). The relations for both methods are given as:

$$Ah_{batt} = \frac{P_e \cdot T_e}{N_{batt} \cdot \eta_{discharge} \cdot \{(N_{cell} - 1) \cdot V_{avg} - V_d\} \cdot DOD} \tag{4.11}$$

$$Ah_{batt} = \frac{P_{dis}}{N_{cell} \cdot V_{avg} \cdot C_{rate} \cdot N_{batt}} \tag{4.12}$$

where $N_{cell}$ is the number of cells in series, $N_{batt}$ is the number of batteries in parallel, $V_d$ is voltage drop across diode, $\eta_{discharge}$ is battery efficiency during discharge and $C_{rate}$ is battery discharge rate in terms of battery capacity. The battery with Ah-capacity closest to available capacity is selected for further testing against battery design constraints. $N_{cell}$ is selected keeping one cell redundancy in mind.

### 4.1.3 Calculation of System Mass

The mass of SEPS is determined from mass of solar array, battery and power control unit.

$$M_{eps} = M_{sa} + M_{batt} \times N_{batt} + M_{PCU} \tag{4.13}$$

| Bus voltage (V) | Normalized mass | |
|---|---|---|
| | Box | Cabling |
| 28 | 1 | 1 |
| 50 | 0.65 | 0.55 |
| 100 | 0.55 | 0.25 |

TABLE 4.1: Normalized mass of PMAD components for different bus voltages

where $M_{array}$, $M_{batt}$, $M_{PCU}$ are mass of solar array, battery and PCU respectively. The total solar array mass is sum of solar cell mass, substrate, deploying mechanism and interconnections. The values of mass of solar array (substrate and cover glass) are given in Table 3.2.

$$M_{sa} = (M_{scell} \times A_{sctotal}) + (M_{areal} \times A_{array}) \tag{4.14}$$

Mass of the battery is then determined from battery cell energy density ($\rho_{cell}$), as sum of battery cell and battery structure which is taken to be 10% of the mass of battery cells. Mass of single battery is calculated as:

$$M_{batt} = 1.1 \times (Ah_{batt} \times N_{cell} \times V_{avg} \times \rho_{cell}) \tag{4.15}$$

Mass of power management and distribution unit (PMAD) is an indirect estimation. It is calculated as sum of mass of power management and distribution boxes ($M_{box}$) and cables ($M_{cable}$). Linear relationships assumed for 28V bus are given as:

$$M_{box} = 0.01 \times P$$

$$M_{cable} = 0.02 \times P$$

The summary of normalized mass estimates for different bus voltages used here is given in Table 4.1.

### 4.1.4 Calculation of System Cost

Cost of the system is the sum of solar array cost ($C_{sa}$) and battery cost($C_{batt}$). The cost of PMAD is not being added here directly as it depends highly on detailed design. But it will not affect the purpose of selecting bus voltage as the effect

of voltage is translated here in terms of PMAD mass and effective launch cost. Overall system launch cost due to SPS (Solar array, battery and PMAD) is also to be considered in order to increase the effectiveness of design. Launch cost factor ($R_{launch}$) for GEO is taken to be \$22k/Kg and for LEO it is \$11k/Kg [29].

$$C_{eps} = C_{sa} + C_{batt} \times N_{batt} + M_{eps} \times R_{launch} \tag{4.16}$$

The cost of solar array ($C_{sa}$) is sum of cost of solar cell ($C_{scell}$) and cost of array structure ($C_{areal}$). The cost of array other then cell material is taken to be 41,300 $\$/m^2$ [46].

$$C_{sa} = C_{scell} \times A_{sctotal} + C_{areal} \times A_{sa} \tag{4.17}$$

The cost of battery ($C_{Batt}$) is calculated as:

$$C_{batt} = C_{Ah} \times Ah_{batt} \tag{4.18}$$

where $C_{Ah}$, the cost of battery per unit Ampere-hour, is taken as \$4.02K/Ah for NiCd, \$7.4K/Ah for NiH2 and \$10K/Ah for Li-ion. Because of manufacturer's policy to keep cost data confidential, it is hard to predict actual cost. Therefore, the cost information, used here, is only representative in nature, and is calculated on the basis of data collected from different space-qualified battery suppliers.

### 4.1.5 Calculation of System Reliability

System reliability will be calculated as part of determining the overall system performance. The reliability of SEPS ($R_{eps}$) is calculated as:

$$R_{eps} = R_{scell} \cdot R_{sa} \cdot R_{batt} \tag{4.19}$$

where $R_{scell}$, $R_{sa}$, and $R_{batt}$ represents the reliability factors for solar cell, solar array and battery respectively. The figure of reliability factor for individual technology has been assumed on the basis of their heritage and current status.

## 4.2 SPS Analysis Model

The spacecraft power system analysis model has been developed in Matlab/Simulink. The MATLAB/Simulink schematic of this model for the standard solar array is shown in Figure. 4.5. Modified version of the same model for the solar array with hybrid composition is shown in Figure 4.6. In the following sections, the models for orbit, solar array, battery and power control unit are discussed in detail.

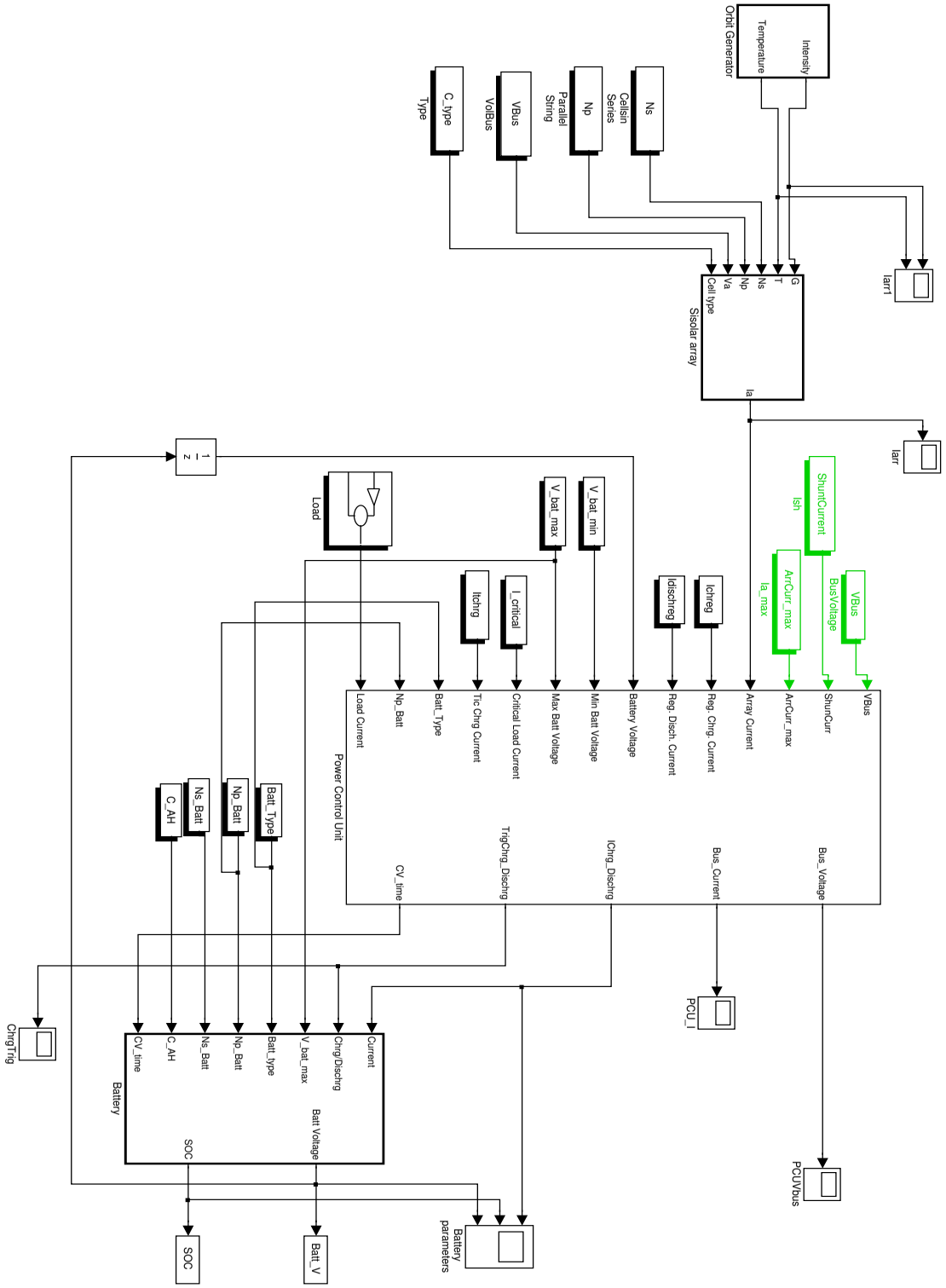


FIGURE 4.5: Simulink schematic of SEPS analysis tool

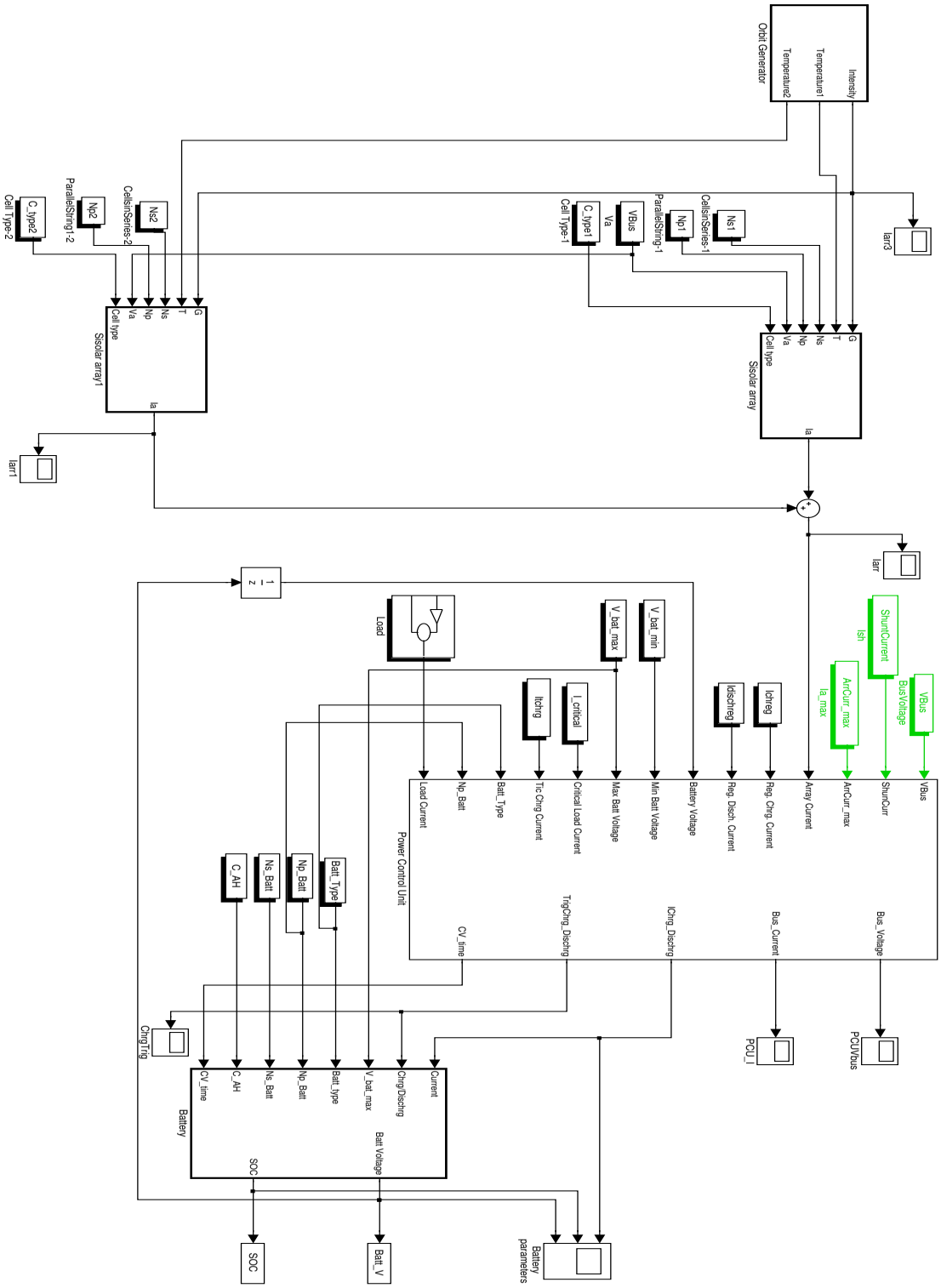


FIGURE 4.6: Simulink schematic of SEPS analysis tool for hybrid solar array system

### 4.2.1 Orbit Generator

The purpose of this block is to simulate the behavior of orbit (illumination) over a given period of time. The model predicts whether or not the satellite is in sunlight or eclipse and also the variation in illumination, if any, based on the orbit parameters. In addition, this model also predicts the temperature of solar array.

#### 4.2.1.1 Mathematical description of Model

The main inputs to the model are:

- semi-major axis, $a$
- inclination, $i$
- right ascension of the ascending node, $\Omega$
- argument of perigee, $w$
- true anomaly, $v$
- eccentricity, $e$=0 (as we assume circular orbits)

This model consists of two components: one is to predict whether the satellite is in eclipse or not and the second is to predict the illumination intensity, if not in eclipse.

The components that are used for eclipse prediction are based on algorithm presented in [47]. Figure 4.7 shows the schematic representation of satellite-earth-sun geometry and shadow regions. As the Sun disk is not a point, it does not cast a sharp shadow. There are actually two areas of shadow, the cone, where no portion of the sun's surface can be seen, is referred to as the umbra (the tail of this cone reaches over a million kilometers beyond the earth). And the shadow cone where only part of the sun's disk is obscured by the earth is referred to as penumbra. This region is not completely dark but in a transition from full light to full darkness and vice versa. In current program, we are interested only in umbra shadow, as in near earth orbits the time of penumbra is quite short and can be neglected.

To predict the shadow conditions, we need to know the satellite-earth distance ($\vec{d_{se}}$), satellite to sun distance($\vec{d_{sS}}$), and earth to sun distance ($\vec{d_{eS}}$). These distance

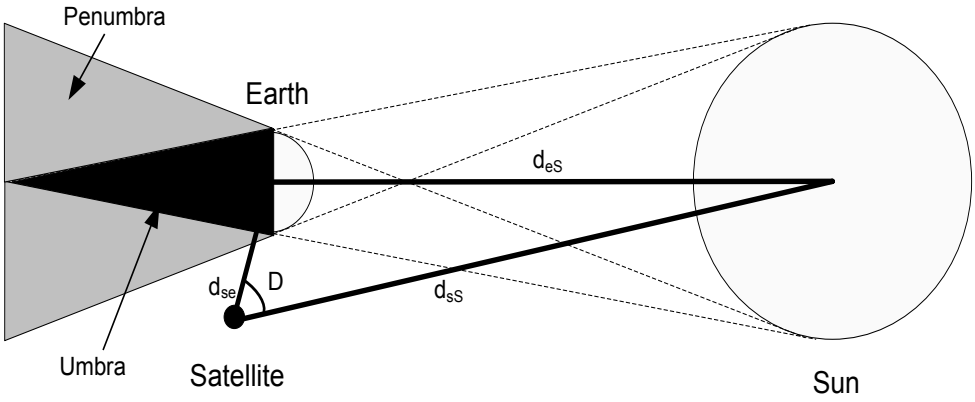


FIGURE 4.7: Schematic of satellite-earth-sun geometry and shadow regions

vectors are determined from knowledge of the position of the satellite and the sun in the ECI (Earth-Centered Inertial)coordinate system. The necessary conditions for umbra eclipse in terms of semi-diameters of sun ($D_S$) and earth ($D_e$) are:

$$D_e > D_S$$

and

$$D < (D_e - D_S)$$

where D is angle between centers of sun and earth. The values of these terms can be calculated as

$$D_e = sin^{-1}\left(R_e/d_{se}\right) \tag{4.20}$$

$$D_s = sin^{-1}\left(R_S/d_{sS}\right) \tag{4.21}$$

$$D = cos^{-1}\left(\vec{d_{se}} \cdot \vec{d_{sS}} \,/ d_{se}d_{sS}\right) \tag{4.22}$$

The second component is to calculate the *effective solar intensity, (S)*, which is incident upon the solar cells. This model is essentially based on theory and formulas described in [48, 49]. A depiction of orbit is shown in Figure 4.8. The effective solar intensity as a function of array-sun distance $d$(in unit of AU) and angle of incidence $\Gamma$ is given as

$$S' = \left(\frac{S}{d^2}\right) cos\ \Gamma \tag{4.23}$$

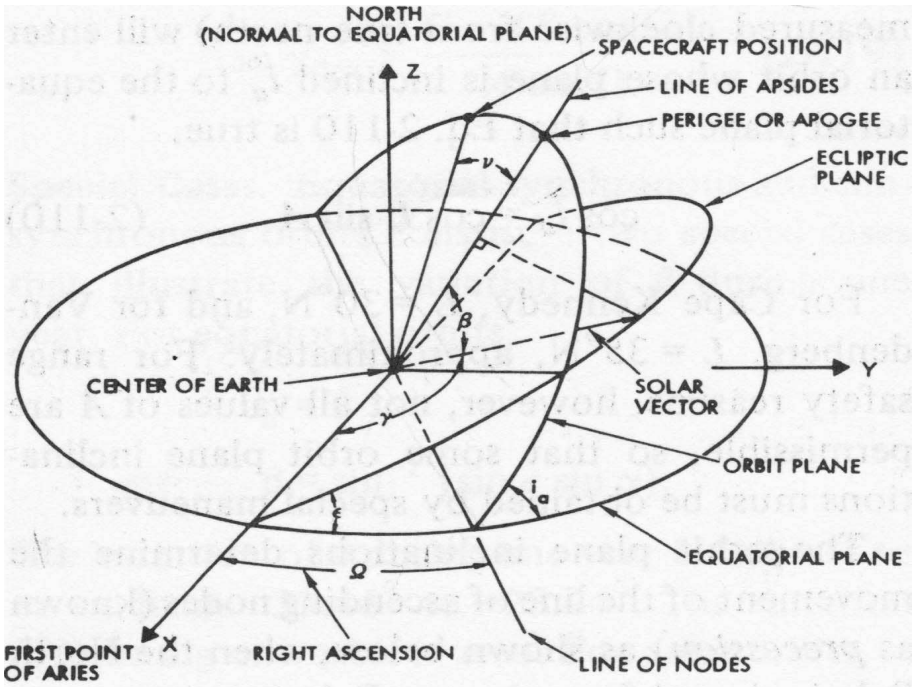


FIGURE 4.8: Schemtic of orbit plane (courtesy of [48])

where $S$ is solar intensity at 1AU, which is taken to be $1371 W/m^2$. For sun-pointed flat solar array and assuming that the illumination over whole panel is uniform, we can say that $\Gamma$ is equal to sun angle $\theta$, and further that $\theta$ is equal to $\beta$. Hence we can say that:

$$\Gamma = \beta$$

Based upon launch information, the time of previous equinox is calculated. For solar cell array conceptual design, we are interested in angle of incidence on the orbit plane. This angle, $\beta$, is known as sun-orbit-plane angle. The relationship between $\beta$ and other orbit angles are given as:

$$sin\beta = sin\ \gamma\,(sin\ i \cdot cos\Omega \cdot cos\ e - cos\ i \cdot sin\ e) - sin\ i \cdot sin\ \Omega \cdot cos\ \gamma \qquad (4.24)$$

where $e$ is fixed angle between ecliptic plane and equatorial planes having a value of $23.45^o$. The sun central angle, $\gamma$, is measured in ecliptic plane from the X-axis to the earth-sun line and has a value of 0 deg at vernal equinox. If $\gamma_0$ is a known value of $\gamma$ at some specific time, $t_0$, then $\gamma$ at any later time $t$ is given by:

$$\gamma = \gamma_0 + (t - t_0)\,\frac{d\gamma}{dt} \qquad (4.25)$$

The value of the rate of change of sun central angle, $d\gamma/dt$, is given approximately as $0.98565^o/day$. Using last vernal equinox as a reference, for which the value of $\gamma$ is 0, the gamma at any time $t_{eq}$ (in days), since last vernal equinox can simply be calculated as:

$$\gamma = t_{eq} \times 0.98565 \tag{4.26}$$

The value of $\Omega$ at time $t$ is given as:

$$\Omega = \Omega_0 + t\,(d\Omega/dt) \tag{4.27}$$

Approximate value of $d\Omega/dt$ for a circular orbit is given as:

$$d\Omega/dt = -\frac{JR^2\mu^{1/2}cos\ i}{(R_e + h)^{7/2}} \tag{4.28}$$

where $J$ is the general coefficient of gravitational harmonics. The values of $J$ and $\mu$ are given as:

$J = 1.624 \times 10^{-3}$

$\mu = 3.986 \times 10^5/Km^3 \cdot sec^{-2}$

The orbit model within optimization frame work is part of spacecraft power system analysis under worst case scenario, and it is desirable to run the simulation over a limited orbit duration such as for two complete orbits in our work. We need to determine the worst case conditions before hand. For this purpose a dedicated MATLAB program is used which calculates the maximum and minimum eclipse durations for a mission along with date and orbit parameters at that time. This information is then used by main optimization framework.

### 4.2.2 Solar Array

The purpose of this block is to simulate the behavior of the solar array over given simulation time. The inputs to the model are array configuration and illumination conditions. The central entity of this block is the model of solar cell. In this work, a novel approach, for modelling of the solar cell using meta-heuristics, has been developed. This model and details of the algorithm that have been used to predict the solar array behavior are explained in chapter 5.

### 4.2.3 Battery

The next important element of a PV-power system is rechargeable battery. The battery is necessary to make sure that spacecraft system can work properly during eclipse as well. As the main purpose of the analysis tool is to perform the trade analysis, we need models for batteries that are commonly used in space applications. In current work, we consider three types of batteries; NiCd, $NiH_2$, and Li-ion. In the next sections, we will briefly discuss different approaches that have been used for battery modelling and how the batteries are being modeled for this work.

#### 4.2.3.1 A brief review

There are several approaches that have been used for battery modelling. Simple empirical modelling approaches based on extensive cell data have been used to model NiCd and $NiH_2$ battery [50, 51]. In some of the approaches, the models make use of electrochemical relations for computing cell reactions [52]. Here the model parameters are calculated on the basis of the best fit of calculated data on the experimental data. Mathematical modelling approaches have also been used for modelling of $NiH_2$ and Li-ion [53, 54]. These approaches are based on a set of mathematical equations representing the behavior of battery. This is a very effective method but requires a lot of information about cell properties which are hard to avail in our case. There has been a lot of work on modelling of Li-ion batteries because of its application in portable electronics [55–57].

#### 4.2.3.2 Description of Model

The battery model implemented in this work is based on empirical approach. The main reasons for choosing this approach are: firstly, it is simple in it implementation, secondly, the model can be developed on the basis of set of the battery characteristic curves, and because it was hard to get any data related to electrochemistry of battery as the author could not even get true test data from industry in-spite of all her effort. The battery module predicts a number of battery parameters, which includes battery state of charge (SOC), and battery voltage based on test data as function of charge/discharge current, temperature, previous state

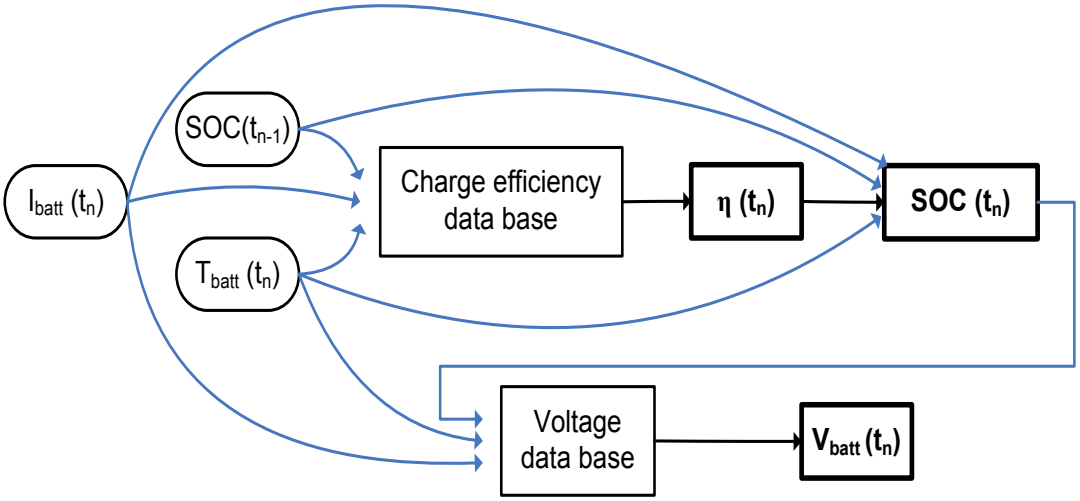


FIGURE 4.9: Schemtic of battery model

of charge and coulombic efficiency. The Models for NiCd , $NiH_2$ and Li-ion are developed using same approach. The inputs to the model are:

- Charge/discharge current
- Battery capacity
- Temperature

The database to model a battery consists of set of battery test curves which include: voltage against SOC for different charge/discharge rates and temperature, and coulombic efficiency against SOC for different charge currents and temperatures. The functional diagram of the model is shown in Figure 4.9.

A battery's SOC is calculated in terms of the actual capacity from ampere-hour integration. This is also called coulomb counting [57], counting the current flowing into or out of battery. Battery's SOC is calculated using following equation:

$$SOC(t_n) = \begin{cases} SOC(t_{n-1}) + \eta_{charge}\left(\frac{I\ dt}{C}\right) & Charging \\ SOC(t_{n-1}) - \left(\frac{I\ dt}{C}\right) - dSOC_{selfdescharge} & Disharging \end{cases} \tag{4.29}$$

where $\eta_{charge}$ is battery cell efficiency during charge process, and $dSOC_{selfdescharge}$ is the change in battery cell's SOC due to self discharge. $dSOC_{selfdescharge}$

is calculated from average self discharge rates, which are taken as 20% per month for both NiCd and $NiH_2$ [28].The battery cell efficiency during discharge is assumed to be 100%. During charge process, $\eta_{charge}$ is function of battery charge rate, previous state of charge and temperature of the battery. For NiCd and $NiH_2$, it is calculated from set of efficiency curves. Figure 4.10 shows a set of efficiency curve for NiCd. Same efficiency curves are used for $NiH_2$. Charge efficiency and self discharge rate factors are negligible in the case of Li-ion, and are ignored in this work. After SOC at a given instance has been calculated, the battery voltage

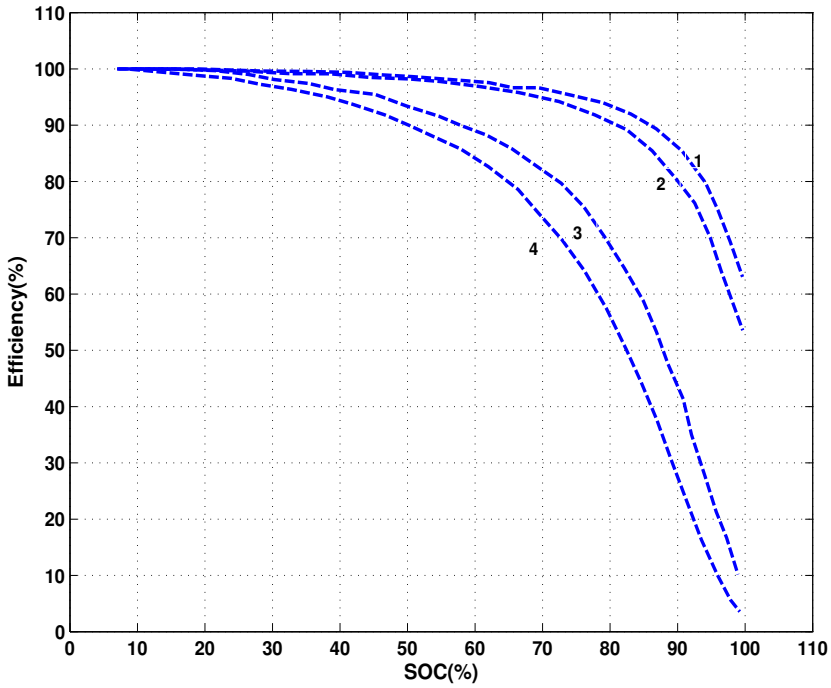


FIGURE 4.10: Efficiency Vs. DOD at different charging rates (reproduced from [50]): (1) C/3, (2) C/10, (3) C/50, (4) C/10

is determined as a function of SOC, temperature and charge or discharge current using linear interpolation of stored data. As this model is based on data taken from literature, it has some limitations. The model can predict the performance of battery fairly good for charge-discharge range of C/10 to 3C for Li-ion and C/10 to 1C for NiCd and $NiH_2$. No thermal modelling for the batteries is taken in to consideration for this work. Although the model is able to simulate the battery behavior over a range of temperature, for the sake of efficiency to keep computational cost low, we assumed that battery is operating in a temperature controlled environment, and the battery performance is simulated for constant temperature. For NiCd and Li-ion this is taken as $25^0$C and for $NiH_2$ this value is taken to be $10^o$C.

Battery overcharge protection is extremely important for maintaining the battery temperature, and it has strong influence on battery life. The battery, when fully charged, reaches the maximum voltage beyond which all input power is converted into heat. Most common approach is voltage temperature control. Here the end of charge voltage is determined from set of V-T curves over an age period stored in data base. When the full charge is approached, battery current is tapered down to trickle charge. Trickle charge is selected on the basis of electro-chemistry and mission. For Li-ion it is taken to be zero, as we have already assumed negligible self discharge.

#### 4.2.3.3 Model Validation

The model is implemented in MATLAB/Simulink. The program calculates all parameters at each designated time step. The inputs to the model are charge/discharge current and temperature, at each time step $t$. Based in this information, and the previous state of charge and time interval between two samples ($dt$), the state of charge at time $t$ is determined. Along with the inputs described before, the model makes use of efficiency vs SOC information during charge phase and self-discharge rate information during discharge phase. The simulation results of the model for NiCd are presented in Figures 4.11(a) and 4.11(b). Figure 4.11(a) shows the profile of voltage vs SOC during charge at a rate of C/10 and C/3, and Figure 4.11(b) shows discharge behavior under same conditions. The results here resemble with the ones given in [58].

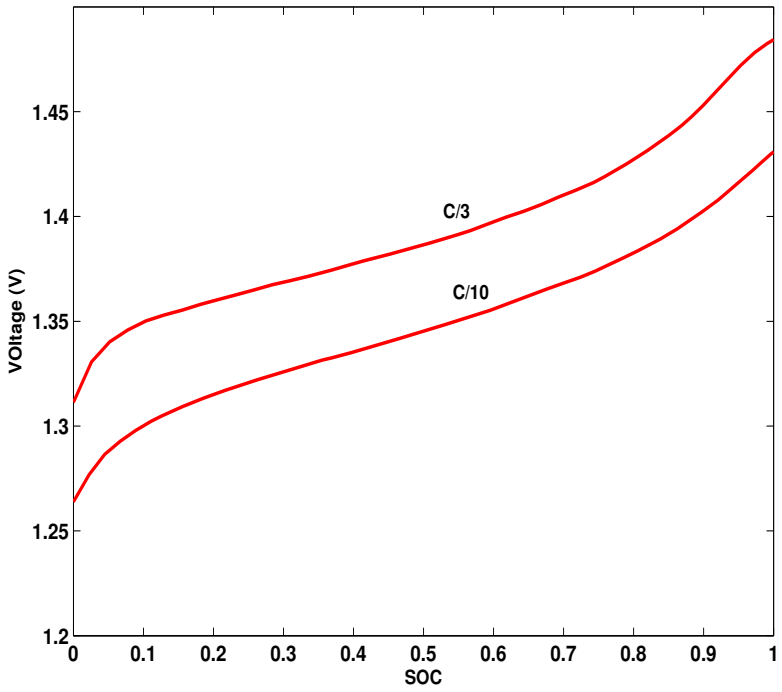


(a) Charging at different rates

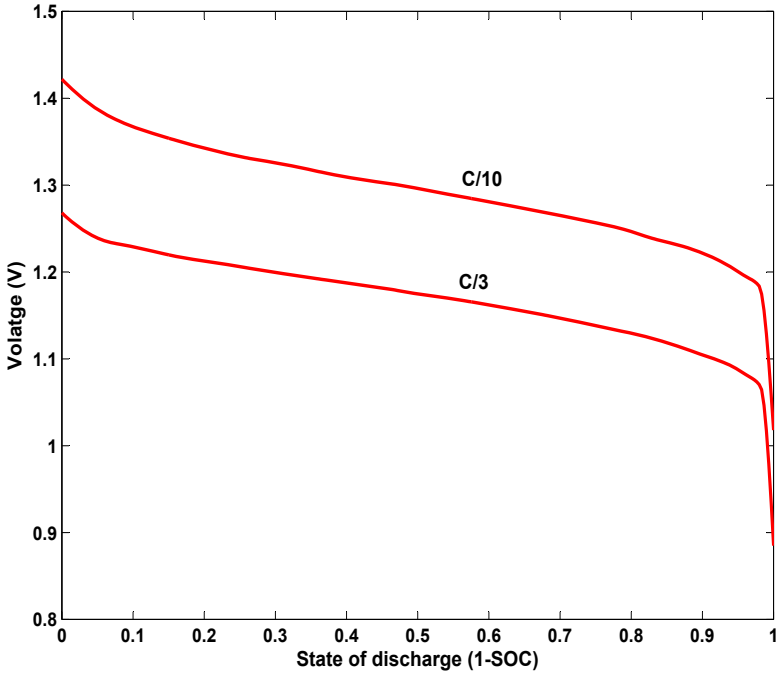


(b) Discharge at different rates

FIGURE 4.11: Cell voltage vs. state of charge

### 4.2.4 Power Control Unit

The main function of power control unit is to deliver appropriate voltage and current levels to different loads or components as identified in mission requirements. The power sources are always over-sized to fulfill the power requirements till the end of mission life. Hence there is surplus power at the start of mission which needs to be dissipated. A shunt regulator is used to dissipate this surplus power and also to compensate the changes that arise from changing load demands. Charge and discharge controllers are responsible for maintaining life time operation and reliability of the battery unit. Figure 4.12 represents the Simulink schematic of power control unit. It includes battery charge/discharge regulator and shunt regulator.

The power system considered in this study is based on DET architecture. DET system can be further divided into: i) the fully regulated and, ii) the sun regulated bus. The main difference among the two types is that there is no battery discharge regulator in sun regulated bus. Power control unit has different modes of operations:

- Shunt mode: When the power from solar array exceeds the load and battery charge requirements, the shunt mode is turned on to dissipate the excess power. During this phase, the battery charging mode is also on, and the battery is charged at full, partial or trickle charge rate.
- Charge cut back mode: When battery's end of charge voltage is detected, the charge rate is cut back to lower rate called trickle charge. This mode is also on, during sunlight when solar array power is just enough to fulfill load power requirements.
- Discharge mode: During the eclipse period, the battery discharge mode is on. In the fully regulated bus, the bus voltage is maintained through a battery discharge regulator. As with discharge, the battery voltages fall, the duty cycle of the discharge converter also increases. Consequently battery discharge current increases with time. In the sun regulated system bus, the voltage follows the battery voltage.

Next, a detailed discussion of main components of power control unit of a fully regulated power unit is given.

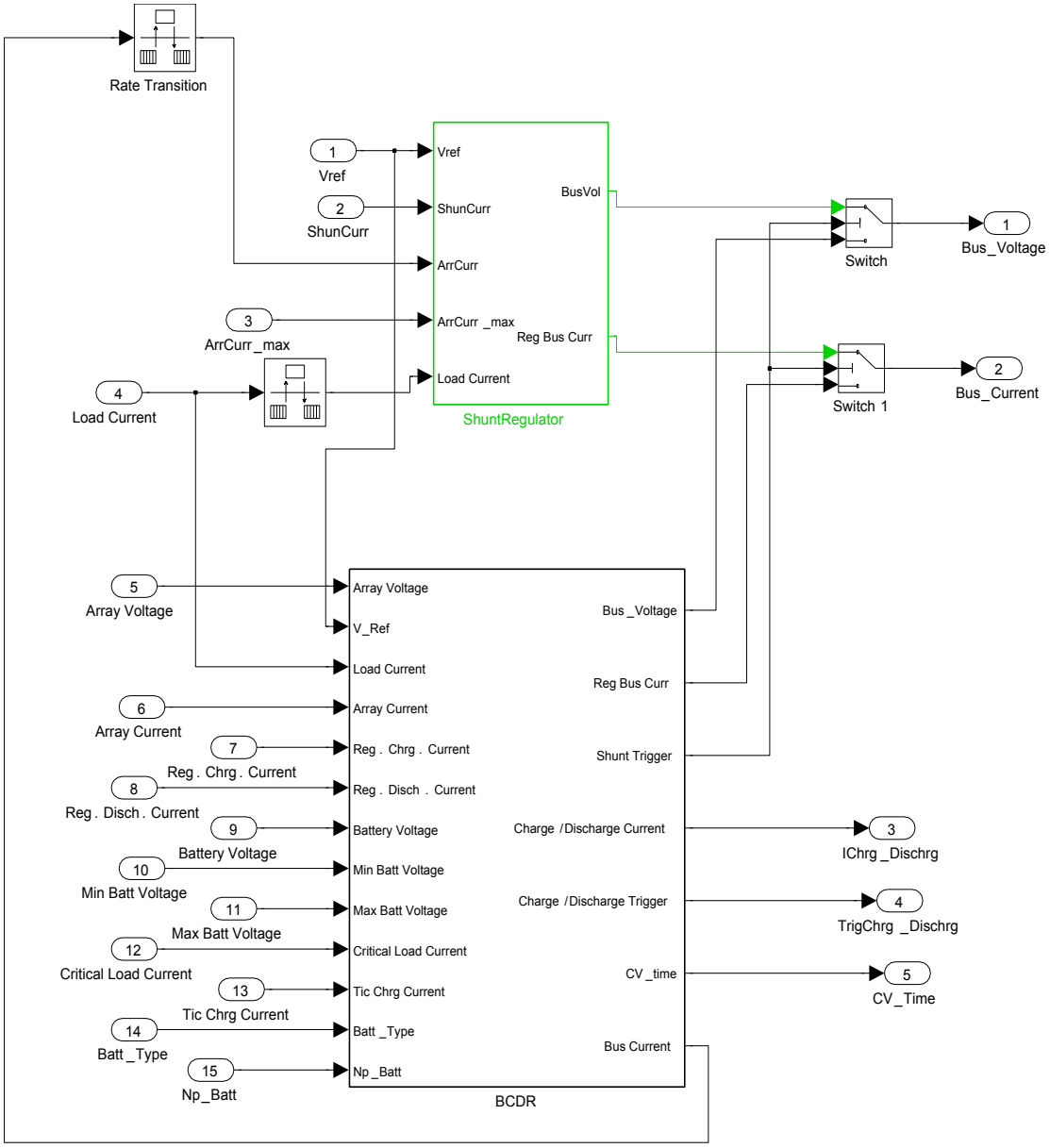


FIGURE 4.12: Simulink schematic of power control unit

#### 4.2.4.1 Shunt regulator

The function of the shunt regulator is to limit the bus voltage within defined levels by dissipating excess solar array power. Out of many forms of the shunt regulators, sequential switching shunt regulator (S3R) is the most popular and is implemented here. The schematic of S3R is shown in Figure 4.13 [59]. In S3R scheme, the solar array is divided into N number of strings. For any given load current, certain numbers of strings are connected to bus, while rest are set in short-circuit. Fine current adjustments are achieved through pulse width modulated (PWM) switching of one of the sections. In this work, S3R is implemented using

only a single PWM section. Figure 4.14 shows the schematic of working principle for a single PWM section approach.

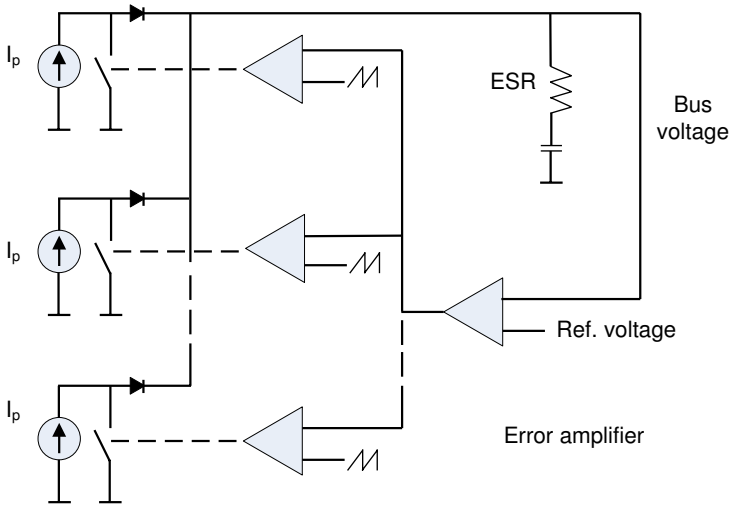


FIGURE 4.13: Sequential switching shunt regulator unit (adapted from [59])

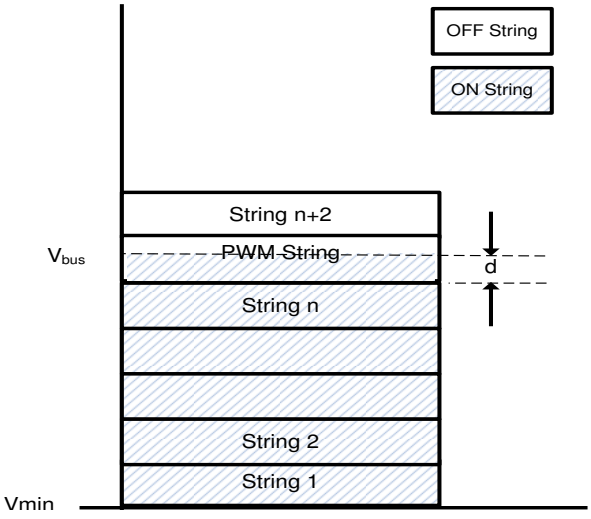


FIGURE 4.14: Sequential switching shunt with single PWM section (adapted from [60])

#### 4.2.4.2 Description of Model

The Simulink schematic of S3R is shown in Figure 4.15. Here output1 of the main error amplifier (EA3) is the total current of "ON" shunts and output2 is the

signal to PWM. The total number of shunts, N, is calculated on the basis of total bus current and maximum current per shunt (each shunt is assumed to have same current rating).

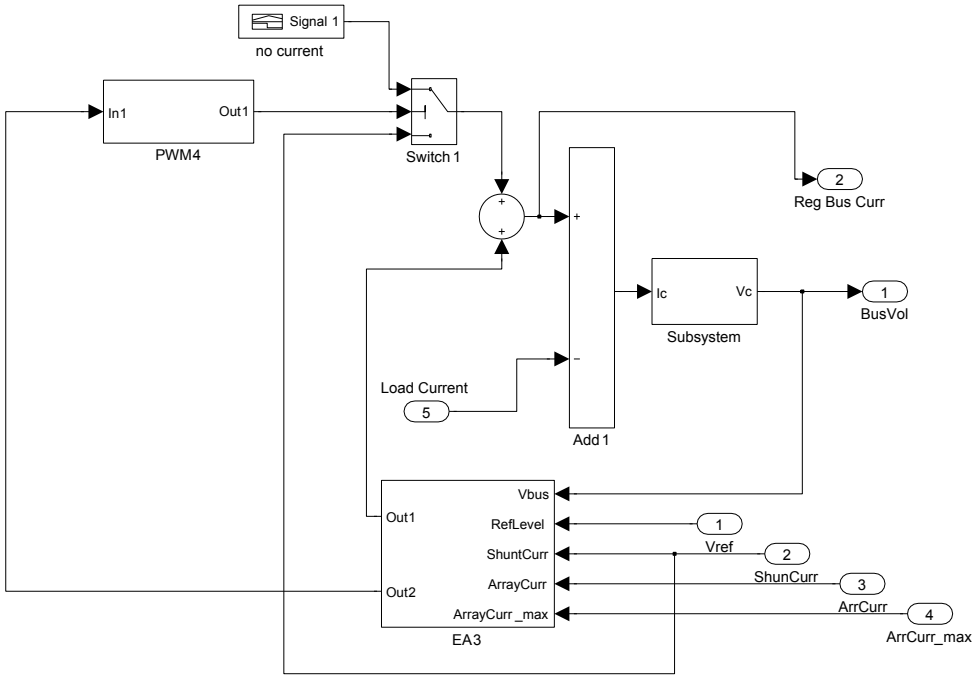


FIGURE 4.15: Simulink schematic of S3R

The inputs to the model are:

- Reference voltage ($V_{ref}$)
- Bus voltage ($V_{bus}$)

The outputs of the model are bus voltage and bus current, which is the sum of the currents of 'ON' shunt and 'PWM' shunt. For the condition when $V_{bus}$ is less than $V_{min}$, all the shunts are open, and when $V_{bus}$ is greater than $V_{max}$ all the shunts are shorted. For the intermediate conditions, one section is in switching mode, which we call as 'PWM' shunt and the others are either 'ON' or 'OFF'. The model calculates, the no. of 'ON' shunts and the duty cycle of the 'PWM' shunt on the basis of bus voltage and reference voltages. These two are calculated as:

$$N_{on} = int\left\{\frac{V_{bus} - V_{min}}{V_{max} - V_{min}}\right\} N \tag{4.30}$$

$$d = \frac{V_{bus} - (N_{on}\,(V_{max} - V_{min}) + V_{min})}{V_{max} - V_{min}} \tag{4.31}$$

where $V_{max}$ and $V_{min}$ are user defined and are usually taken as % of $V_{ref}$.

The transient response of S3R for a 50 volt bus is shown in Figure 4.16. The upper and lower voltage limits in this case are 50.25 and 49.75 respectively. Here a load step is applied at 0.45 sec. At this point, the bus voltage restarts to fluctuate around the lower voltage value.

#### 4.2.4.3 Battery Charge/Discharge Controller

For battery charge control, the controller makes use of the constant current-constant voltage method. The inputs to the model are battery voltage, battery current and temperature. During charging phase, the battery is charged till the battery voltage is built up to $V_{BattMax}$, defined as voltage-limit, and is temperature compensated. After $V_{BattMax}$ has reached, the controller switches to the constant voltage charging phase. During this phase, current is tapered such that battery voltage remains constant. Taper current is calculated using double exponential equation:

$$i = i_0(Ae^{-t/a} + Be^{-t/b}) \tag{4.32}$$

where $i_0$ is the initial current at the start of constant voltage phase. The values of constants are determined using curve fitting methods. During discharge phase, the current is drawn from the battery at defined rate. In case the battery voltage drops below the preset minimum battery voltage ($V_{battMin}$), the controller can output the signal to disconnect all non-critical loads.

In Figure 4.17, the dynamic simulation of Li-ion battery consisting of 11 cells in series integrated with satellite simulation model is shown. As battery enters the charging phase at the beginning of sunlight, the battery voltage rises under constant charge rates. At the point, where maximum voltage is detected, the charge rate starts tapering and reduce to trickle charge rate in order to maintain full voltage. During discharge, we can see that battery discharge current rises as the battery voltage drops. This is due to the fact that battery voltage drops with discharge.

Battery charge and discharge regulators (BCR, BDR) are represented by their steady state continuous conduction mode equations [6]. For BCR, the relations

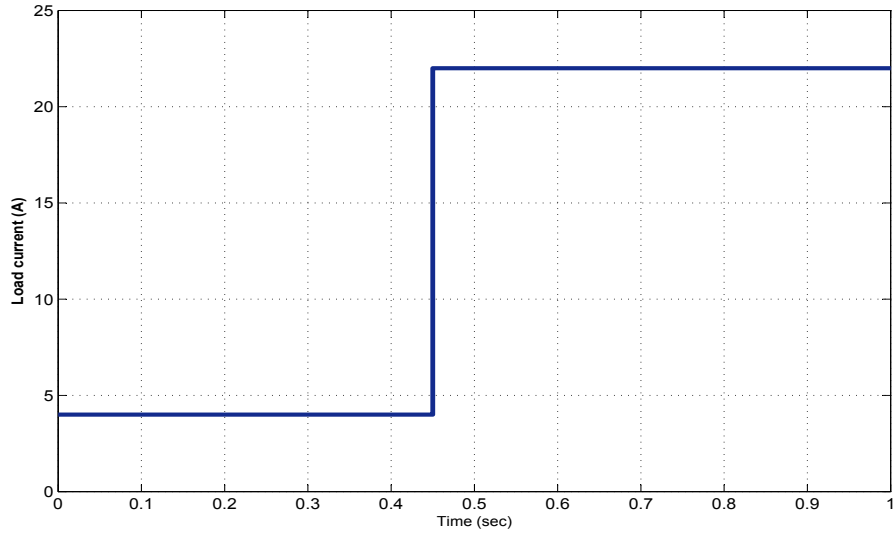


(a) Load current

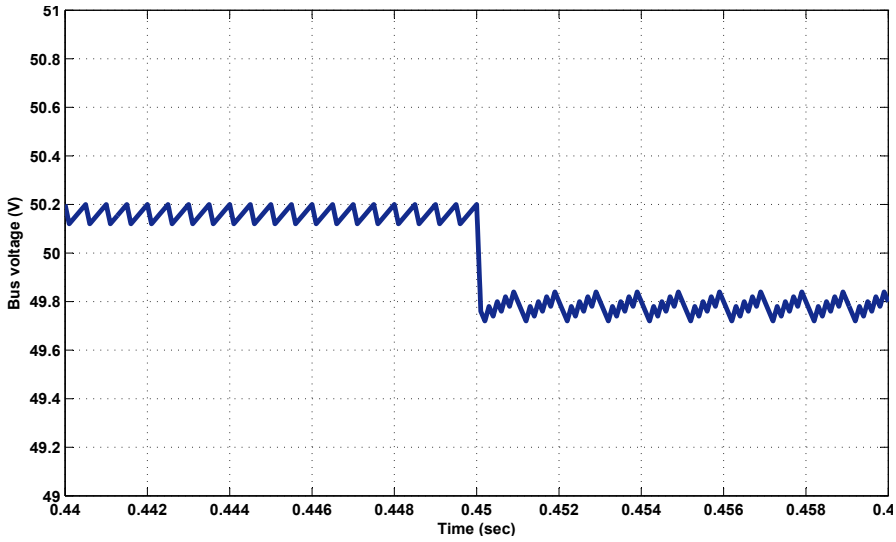


(b) Output bus voltage (a closer look)

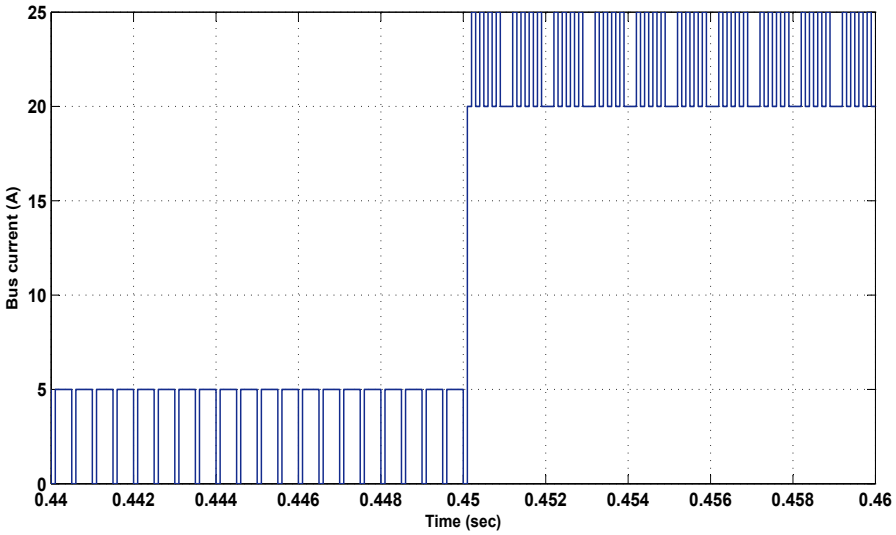


(c) Bus current(a closer look)

FIGURE 4.16: S3R operation and dynamic response

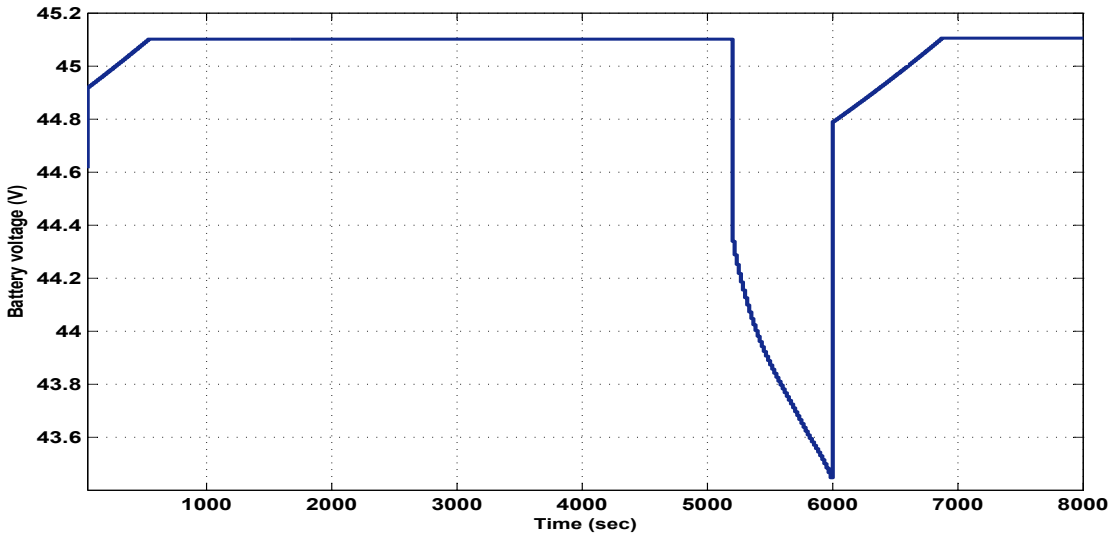


(a) Battery voltage (V)

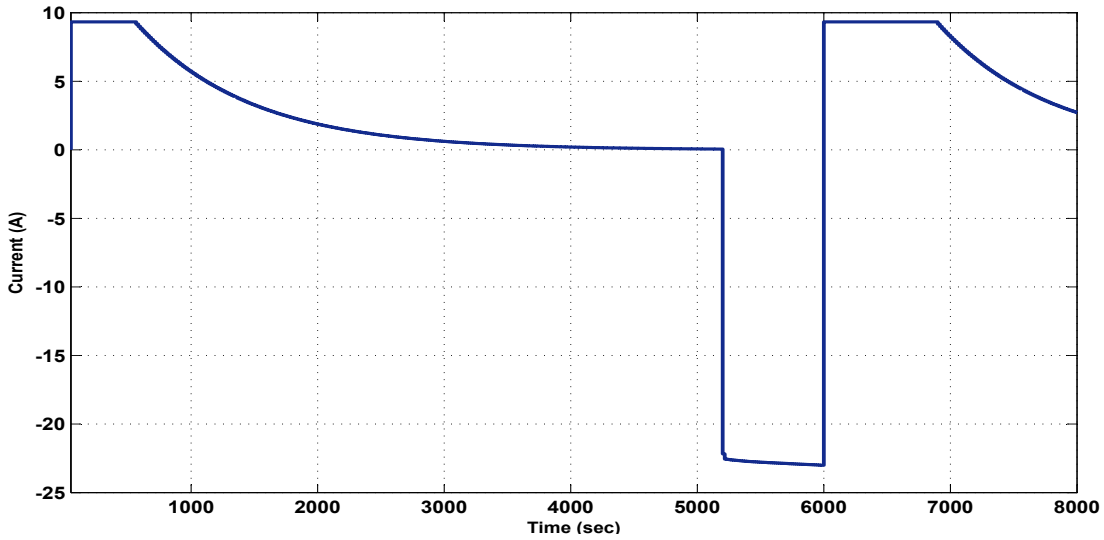


(b) Battery current (A)

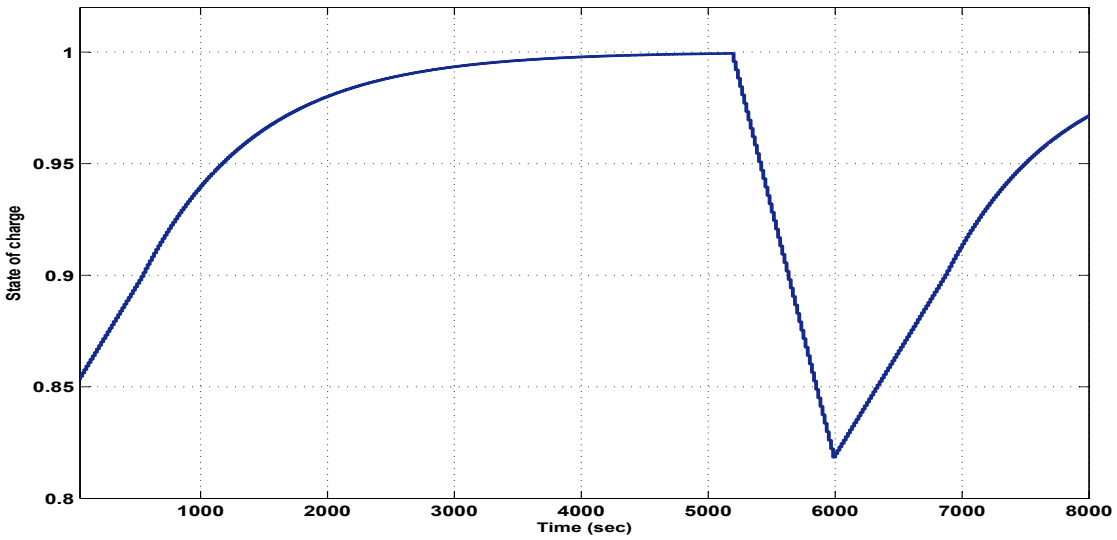


(c) Battery state of charge

FIGURE 4.17: Dynamic response of Li-ion battery

for duty ratio (D) and output current are given as:

$$D = V_{out}/V_{in} \tag{4.33}$$

$$I_{out} = \left(\frac{1}{D}\right) I_{in} \tag{4.34}$$

For BDR, these relations are as follows:

$$\frac{V_{out}}{V_{in}} = \frac{1}{1-D} \tag{4.35}$$

$$I_{out} = (1-D)\, I_{in} \tag{4.36}$$

.

## 4.3 Optimization Tool

The third component of the SEPS design optimization frame work is the optimization tool. This block is also based on MATLAB. Two different approaches for multi-objective optimization (MOO) have been applied, one is a conventional weighted sum genetic algorithm and the other is NSGA-II. The reasons for choosing these two are: i) the weighted sum approach is very simple in its implementation and, ii) in problems where we can define the relative weights to the objectives, it proves to be very effective. In MOO methods based on Pareto-optimality, NSGA-II is proven to be very effective as compared to other techniques.

In this research, three design objectives are considered: i) minimization of SEPS mass, ii) minimization of cost, and iii) maximization of performance. In case of the weighted sum approach, the three objectives are combined, to make it a single objective problem, and this single objective problem is then solved using GA toolbox.

The main MATLAB code for NSGA-II has been taken from the work done by Aravind Seshadri [61], and has been modified by the author for this application.

# Chapter 5

# Solar Array Modelling

The simulation of solar array involves modelling of solar cells while taking into account the influence of illumination and temperatures along with representation of the network resulted from the panel's series parallel call assembly. Here we deal with different types of solar cells that are commonly used in space applications. The objective is to design a tool which can automatically update the values of solar cell parameters if there is any change in environment conditions. Under these conditions, we need a model which is applicable for all major types of space solar cells.

Solar cell models are commonly used for analysis of solar cell behavior. The most common approach to solar cell modeling is the use of a single diode solar cell equivalent circuit [62], shown in Figure 5.1. The current-voltage relation of a solar cell is described by:

$$I = I_{ph} - I_{sat}\left(e^{\frac{V+IR_S}{V_t}} - 1\right) + \frac{V - IR_s}{R_p} \tag{5.1}$$

where $V_t$ is given by:

$$V_t = \frac{AkT_K}{q}$$

Because of the nonlinearity and the implicit nature of these equations, determination of the parameters demands significant computational effort. In most cases, the model includes only the variations of photo-current and diode saturation current while the values of other parameters are kept constant or adjusted for better

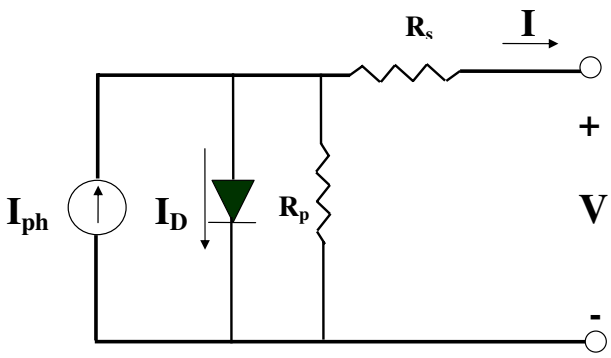


FIGURE 5.1: Solar cell equivalent circuit.

curve fitting [63]. However, it is known that solar cell parameters are affected by temperature and irradiance which further affects solar cell performance curves. Hence, for accurate modeling of a solar cell, it is essential to incorporate all of these effects. Various analytical methods have been proposed for the determination of junction parameters [64] but applications of these methods are limited to the availability of test data and require significant computation. Progress has been reported in Ref. [65], where a genetic algorithm has been implemented for solar cell parameter determination. This method requires an extensive set of I-V characteristic data as input.

In this work, we have implemented a simulated annealing based optimization method for the determination of A and $R_s$ for any set of conditions using a set of data at standard test conditions, obtained from the manufacturer's data sheet. Hence, it eliminates the requirement of having a set of I-V curves of the cell beforehand. Simulated Annealing was introduced by S. Kirkpartick et. al. [66]. It is a global optimization method that can distinguish between different local optima and has the capability of escaping local optima. Hence, it can be used for optimization of complex non-linear functions.

As this model is basically developed to simulate the behavior of a solar array over a number of orbit cycles, the primary motivation is to develop a model that can be applied to all major types of solar cells (single and multi-junction) in space applications. Therefore, the requirement is to design a tool which can automatically update the values of solar cell parameters if there is any change in environmental conditions.

The model also makes use of an additional diode factor for multi-junction solar cells making it suitable for both single and multi-junction solar cells, with almost the same accuracy. Another attractive feature of this model is that it makes use of data-based approach i.e., the data set of current and voltage values of solar cell at any standard environmental condition will be enough for the model to work for any environmental condition.

Application of the model for the determination of I-V characteristics of solar cell after degradation under radiation fluence has been described in section 5.2.1. In addition, an algorithm to use this model in solar array simulation under varying environmental conditions has also been presented in section 5.3.

## 5.1 Description of Model

### 5.1.1 Solar Cell Equivalent Circuit Model Equations

The current model is based on a simplified single-diode model [63] to describe the electrical characteristics of solar cell. The behavior of the solar cell is determined from the cell characteristics given in the cell data sheet. An adapted version of this model is implemented using MATLAB. The inputs to the model are:

- Voltage across cell/array
- Illumination intensity
- Operating temperature.

The simplified single-diode model ignores the effect of leakage currents eliminating the last term of Equation 5.1. In addition for multi-junction cells, the concept of considering a multi-junction solar cell as a series connected diodes, is used. These serially connected diode are replaced by a single equivalent diode, using an additional factor $\lambda$, representing the number of junctions in solar cell [67]. So Equation 5.1 can now be rewritten as:

$$I = I_{ph} - I_{sat}(e^{\frac{V+IR_s}{V_t}} - 1) \tag{5.2}$$

where $V_t$ is given by:

$$V_t = \lambda \frac{AkT_K}{q}$$

The current model needs the following four parameters; $V_{oc}$(open circuit voltage), $I_{sc}$(short circuit current), $I_{mpp}$(current at maximum power point) and $V_{mpp}$ (voltage at maximum power point) along with their respective temperature coefficients which are represented by $dV_{oc}$, $dI_{sc}$, $dI_{mpp}$, and $dV_{mpp}$. The effect of variations in temperature and illumination on different operating conditions is given as follows:

- Short Circuit Condition

$$I_{ph} = I_{sco}\frac{G}{G_o} + dI_{sc}(T - T_o) \tag{5.3}$$

- Open Circuit Condition

$$I_{sat}(G,T) = \frac{I_{ph}(G,T)}{(e^{\frac{V_{oc}(T)}{V_t(T)}} - 1)} \tag{5.4}$$

$$V_{oc} = V_{oco} + V_t\ ln\left(\frac{G}{G_o}\right) + dV_{oc}(T - T_o) \tag{5.5}$$

which is generally true for illumination intensity less than 100 $W/m^2$. For illumination intensity greater than 100 $W/m^2$, following relationship is used:

$$V_{oc} = V_{oco} + V_t ln\left(\frac{G}{100}\right) ln\left(\frac{G}{G_o}\right) + dV_{oc}(T - T_o) \tag{5.6}$$

- Peak Power Point

$$I_{mpp}(G,T) = I_{mpps}\frac{G}{G_o}\left(1 + dI_{mpp}(T - T_o)\right) \tag{5.7}$$

$$V_{mpp} = \begin{cases} V_{mppo} + V_t ln\frac{G}{100} ln\frac{G}{G_o} + dV_{mpp}(T - T_o) & \text{if } G \geq 100W/m^2 \\ V_{mppo} + V_t ln\frac{G}{G_o} + dV_{mpp}(T - T_o) & \text{if } G < 100W/m^2 \end{cases} \tag{5.8}$$

### 5.1.2 Simulated Annealing

Simulated annealing is a stochastic heuristic technique to find a global minimum for continuous-discrete-integer, and non-linear programming problems [68], [69]. The basic idea of the method is to generate a random point and evaluate the problem functions. If the trial point is infeasible, it is rejected and a new trial point is generated. If the trial point is feasible and the cost function value is smaller than the current best record, then the point is accepted, and the record for the best value is updated. If the point is feasible but the cost function is higher than the best value, then the point is sometimes accepted and sometimes rejected. The acceptance is based on value of the probability density function of the Boltzman-Gibbs distribution. If this function has a value greater than a random number, then the trial point is accepted as the best solution even if its cost function value is higher than the recorded best value. In computing the probability, a parameter called the temperature is used. For the optimization problem, this temperature can be a target value (estimated) for the cost function corresponding to a global minimum. Initially, a larger target value is selected. As the trials progress, the target value is reduced (this is called the cooling schedule), and the process is terminated after a fairly large number of trials. The acceptance probability steadily decreases to zero as the temperature is reduced. Thus in the initial stages, the method is likely to accept worse designs while in the final stages, the worse designs are almost always rejected. This strategy avoids getting trapped at a local minimum.

### 5.1.3 Simulated Annealing Based Parameter Prediction

Equations (5.3-5.8) represent the change in solar cell parameters with respect to temperature and irradiance. The coefficients of temperature for current and voltage are usually provided in the manufacturer's data sheet. So, the change in the values of $I_{ph}$ and $I_{sat}$ can be determined linearly if an accurate value of A and $R_s$ is known. The main effect of A and $R_s$ is on the shape of the curve around maximum power point, and hence on the determination of the maximum power point under that operating condition. Because of this reason, in most of the cases, the values of these parameters are usually obtained from I-V curves.

In Ref. [70], it has been shown that the value of A and $R_s$ are best when the difference between the value of $\frac{dI}{dV}$ at maximum power point and $\frac{I_{mpp}}{V_{mpp}}$ is minimal. Using this as our objective function, we define a search and optimization problem for determination of optimal values of A and $R_s$. Adaptive Simulated Annealing (ASA) is implemented for the objective minimization optimization problem where the objective function is defined as:

$$J = -\frac{dI}{dV}\bigg|_{V=V_{mpp}} + \frac{I_{mpp}}{V_{mpp}} \tag{5.9}$$

where

$$\frac{dI}{dV}\bigg|_{V=V_{mpp}} = \frac{\frac{I_{sat}}{V_t} e^{\left(\frac{V_{mpp}+IR_s}{V_t}\right)}}{1 + \frac{I_{sat}R_s}{V_t} e^{\left(\frac{V_{mpp}+IR_s}{V_t}\right)}}$$

The model developed in this work consists of mainly two parts: (i) one simulated annealing based optimizer and (ii) single diode based cell modeler. Both of these have access to the set of basic parameters ($V_{oc}$, $I_{sc}$, $I_{mpp}$ and $V_{mpp}$ ) at standard test conditions along with their respective temperature coefficients for different types of cells. This set of data can be upgraded to accommodate any type of cell. The model is called for a specific cell type with environmental conditions. Upon the call, both of the modules (optimizer and modeler) are loaded with the specific cell data. Then the optimizer calculates the optimal (near optimal) values of A and $R_s$ using cell data and environmental conditions (temperature and illumination intensity). These values are then given to the modeler which generates the I-V curves for the cell or array, whatever the case be.

## 5.2 Model Validation

A Matlab/Simulink based model is used to demonstrate the performance of the modeling process and has been tested for various types of cells. Figures. 5.2, 5.3, and 5.4 show the result of the simulation of I-V curves for Si, dual junction (DJ) and advanced or ultra triple junction (UTJ) solar cells respectively at standard conditions, and are compared with the data points taken from I-V curve given in the manufacturer's data sheet. Along with this, the model has been checked for its performance at various environmental conditions. The effect of illumination on the

I-V curve of advanced triple junction is demonstrated in Figure. 5.5. These cells are used in NPSAT1 satellite. The results shown in Figure. 5.5 show very close resemblance with those, taken experimentally in [71]. The effect of temperature variation on single junction GaAs/Ge cells are presented in Figure 5.6. And the results have been compared with the points taken from the results in Ref. [72].

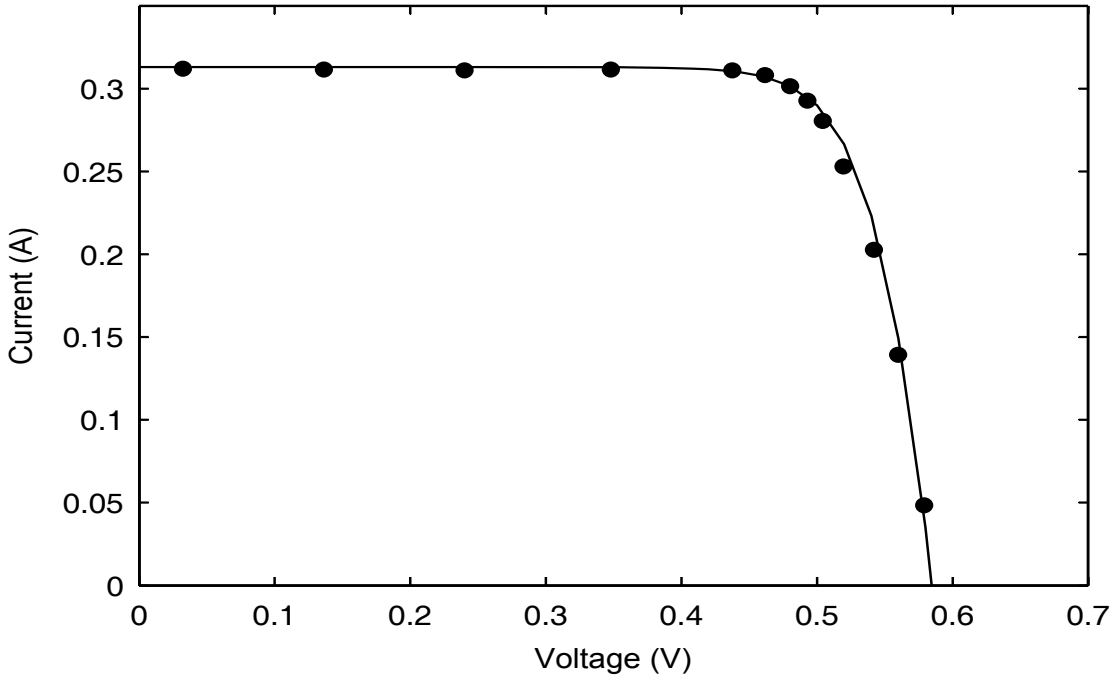


FIGURE 5.2: Simulated I-V curve for Si solar cell, compared with the discrete points taken from manufacturer's data sheet

### 5.2.1 Solar Cell Performance Evaluation After Degradation

In the previous section, we have discussed and evaluated the model for varying temperature and illumination. For spacecraft applications, the users are more interested in end of life (EOL) characteristics rather than the beginning of life (BOL). The model presented here can also be equally useful in predicting EOL characteristics after radiation degradation. In space environment, radiations of different types are main environmental degradation factor. For theoretical and experimental purposes, the radiation effects due to electron and proton fluxes are integrated into equivalent 1MeV electron flux (fluence). The equivalent fluence for a particular mission depends on the given solar cell and solar array type along

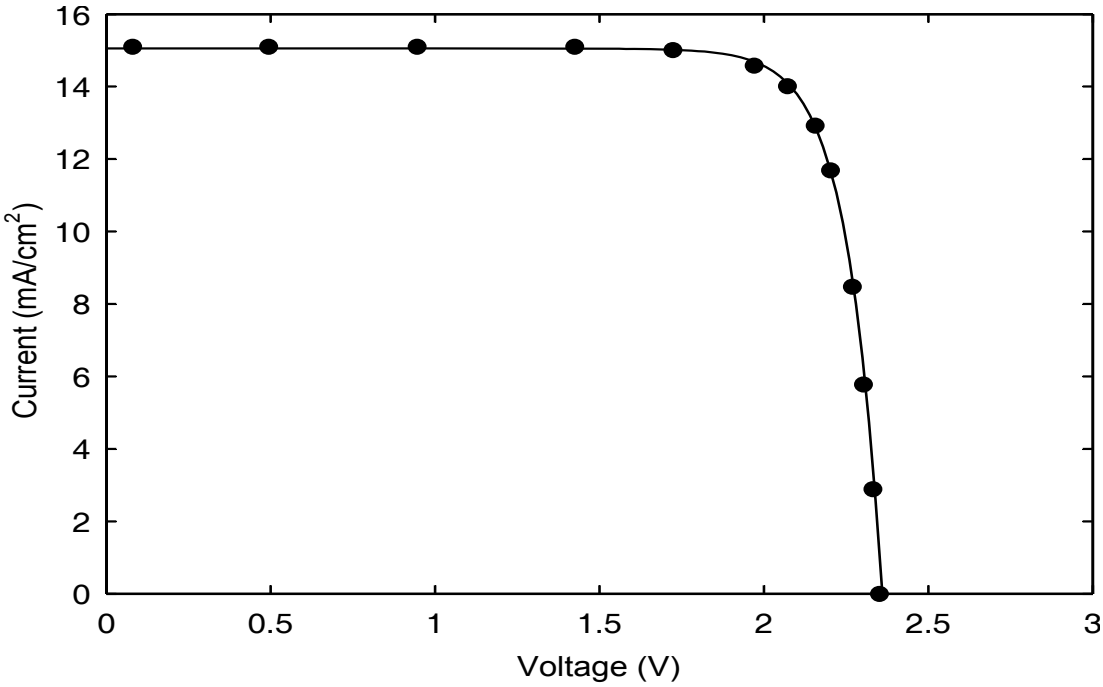


FIGURE 5.3: Simulated I-V curve for DJ solar cell compared, with the discrete points taken from manufacturer's data sheet

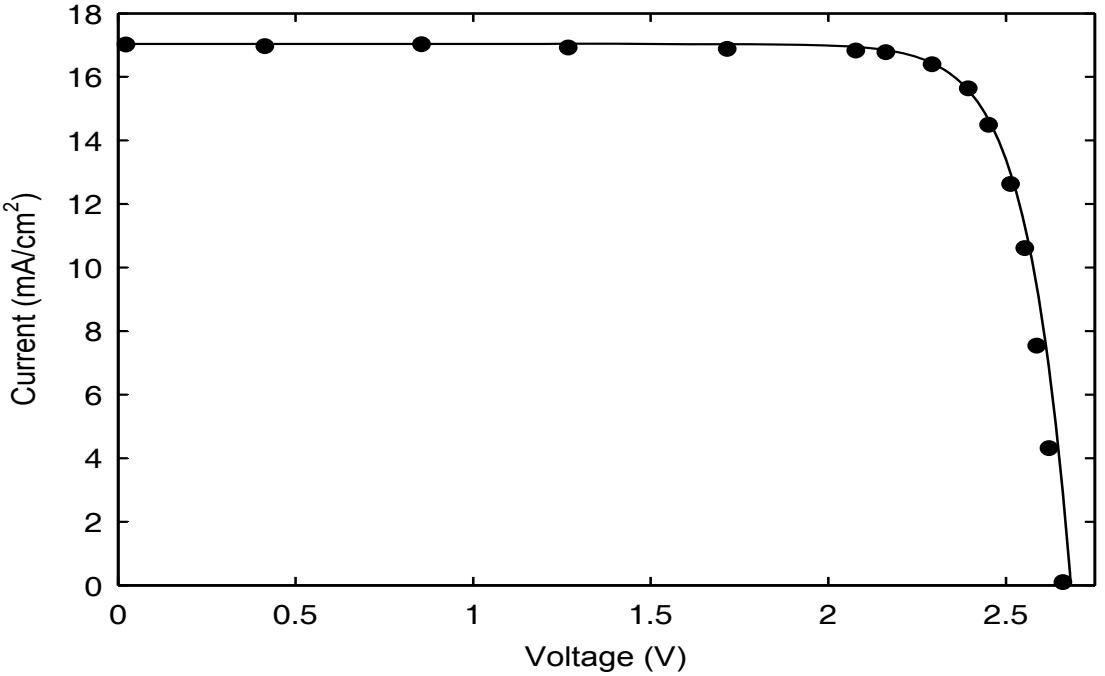


FIGURE 5.4: Simulated I-V curve for UTJ solar cell compared, with the discrete points taken from manufacturer's data sheet

with orbit parameters and mission duration. Let the radiation degradation factors for $V_{oc}$ , $V_{mpp}$, $I_{sc}$ and $I_{mpp}$ under given equivalent fluence ($\phi$) be $K_{voc}$, $K_{vmpp}$, $K_{Isc}$ and $K_{Impp}$, respectively. The temperature coefficients of the solar cell in this case are given as $dV_{oc\phi}$ , $dV_{mpp\phi}$, $dI_{sc\phi}$ and $dI_{mpp\phi}$. These factors can be determined from manufacturer's data sheet for the given set of fluences or can be calculated by interpolating the given data. The solar array characteristics are then determined by modifying Equations 5.3- 5.8 as follows:

$$I_{ph} = I_{sco}K_{Isc}\frac{G}{G_o} + dI_{sc\phi}(T - T_o) \tag{5.10}$$

$$V_{oc} = V_{oco}K_{voc} + V_t\ ln\left(\frac{G}{G_o}\right) + dV_{oc\phi}(T - T_o) \tag{5.11}$$

$$V_{oc} = V_{oco}K_{voc} + V_t ln\left(\frac{G}{100}\right) ln\left(\frac{G}{G_o}\right) + dV_{oc\phi}(T - T_o) \tag{5.12}$$

$$I_{sat}(G,T) = \frac{I_{ph}(G,T)}{(e^{\frac{V_{oc}(T)}{V_t(T)}} - 1)} \tag{5.13}$$

$$I_{mpp}(G,T) = I_{mpps}K_{Impp}\frac{G}{G_o}\left(1 + dI_{mpp\phi}(T - T_o)\right) \tag{5.14}$$

$$V_{mpp} = \begin{cases} V_{mppo}K_{vmpp} + V_t ln\frac{G}{100} ln\frac{G}{G_o} + dV_{mpp\phi}(T - T_o) & \text{if } G \geq 100W/m^2 \\ V_{mppo}K_v mpp + V_t ln\frac{G}{G_o} + dV_{mpp\phi}(T - T_o) & \text{if } G < 100W/m^2 \end{cases} \tag{5.15}$$

The effect of radiation fluence over Si solar cell characteristics under standard temperature and illumination conditions is given in Figure 5.7. To establish the accuracy of this approach, the simulation results for BOL and EOL of triple junction solar cells are compared with the experimentally measured results [73] in Figure 5.8. The simulated characteristics show very close resemblance to experimental values. This verifies that the presented model can predict the solar cell characteristics at EOL with a high level of accuracy.

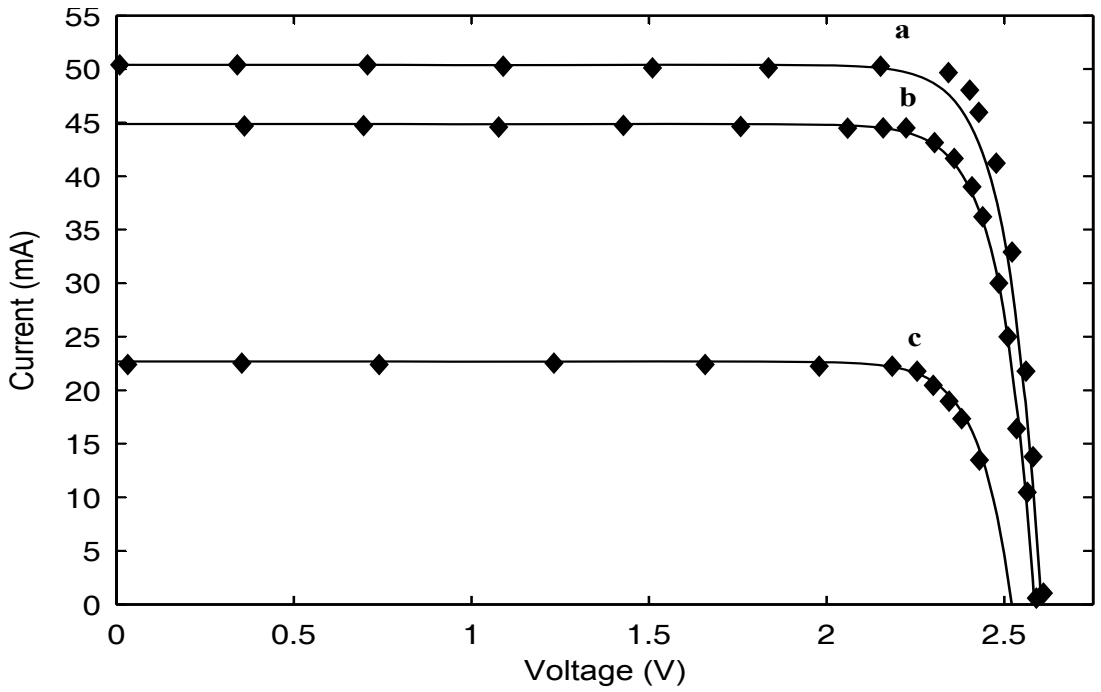


FIGURE 5.5: Simulated I-V curves for UTJ solar cell for illumination intensity of 1000W/$m^2$ and various incident angles:(a) 0 deg, (b) 30 deg, (c) 60 deg. The discrete points shown are taken from [71]

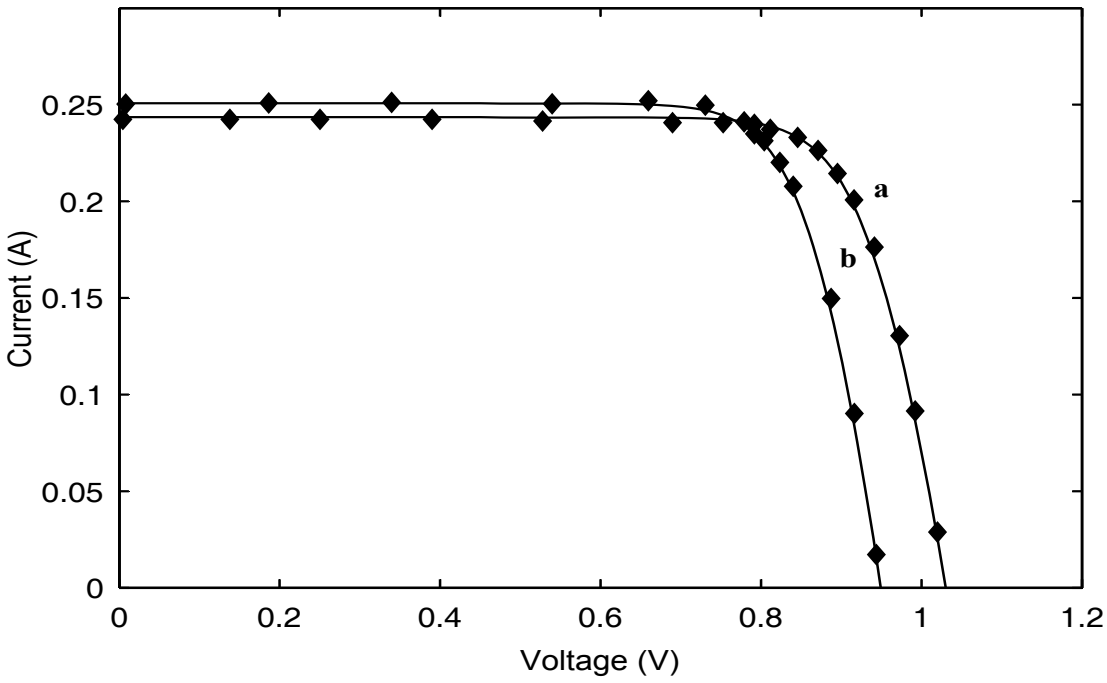


FIGURE 5.6: Simulated I-V curves of single junction GaAs/Ge cell at various temperatures: (a) 25 $^oC$, (b)70$^oC$. The discrete points shown are taken from [72]

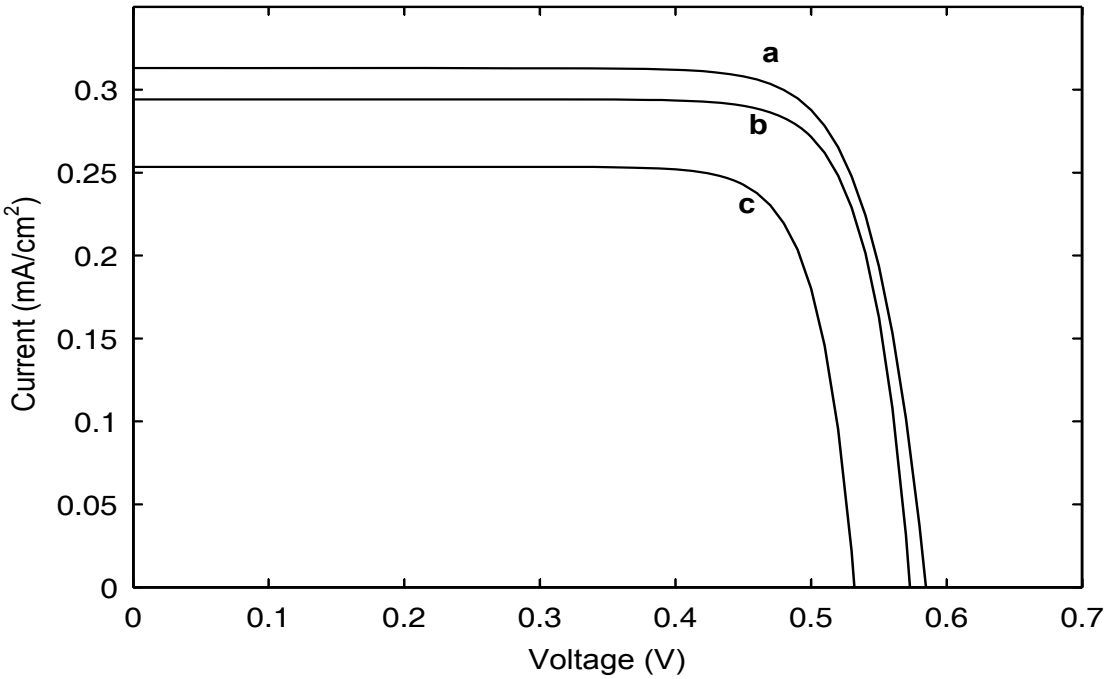


FIGURE 5.7: Simulated I-V curves of Si solar cell: (a) BOL, (b) EOL at Flunece of $1 \times 10^{14} e/cm^2$, (c)EOL at Flunece of $1 \times 10^{15} e/cm^2$

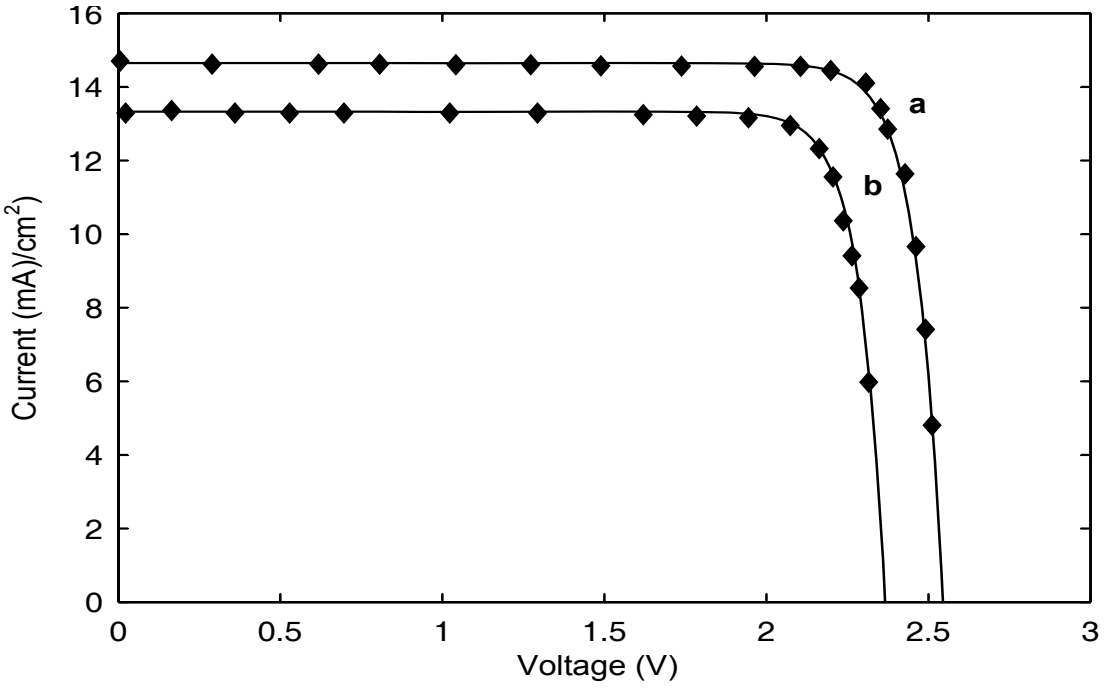


FIGURE 5.8: Simulated I-V curves of triple junction solar cell: (a) BOL, (b) EOL at Flunece of $5 \times 10^{14} e/cm^2$. The discrete points shown are taken from [73]

## 5.3 Solar Array Performance Calculation in Varying Environment

As solar array consists of number of solar modules composed of series-parallel combination of cells. Consider an array consisting of M number of modules, and each module consisting of $N_p$ number of parallel strings, and each string having $N_s$ no. of cell connected in series. Assuming that all cells are identical, current-voltage relationship will be given as:

$$I(V) = M\left[N_p I_{ph} - N_p I_{sat}\left[e^{\left(\frac{V/N_s + IR_s/N_p}{V_t}\right)} - 1\right]\right] \tag{5.16}$$

This model has capability to calculate the current voltage relation in an environment where illumination and temperature are varying as in the case of spacecraft solar array. An algorithm to demonstrate its application for solar array analysis over a simulation period of $t_p$ is described in Figure 5.9.

This algorithm is very effective and efficient, if the model is to be run once, as is the case for general SEPS design analysis. In current work, we have to use this model as part of optimization problem, where analysis model has to be run repetitively, while illumination pattern remain same for given mission parameters. In order to keep the computational time low, a modified version of the above algorithm has been developed and used in the final analysis model. This new algorithm is shown in Figure 5.10. Here the values of A and $R_s$, for the given illumination and temperature condition, are stored in a table for future reference. When there is a change in the temperature or illumination, the entries of the table are checked against these. If a match is found, the values of A and $R_S$ are taken from table and the value of current is calculated. Otherwise the new values of A and $R_S$ are calculated and same are fed to the table. This modification reduces the optimization run time by a factor of 10.

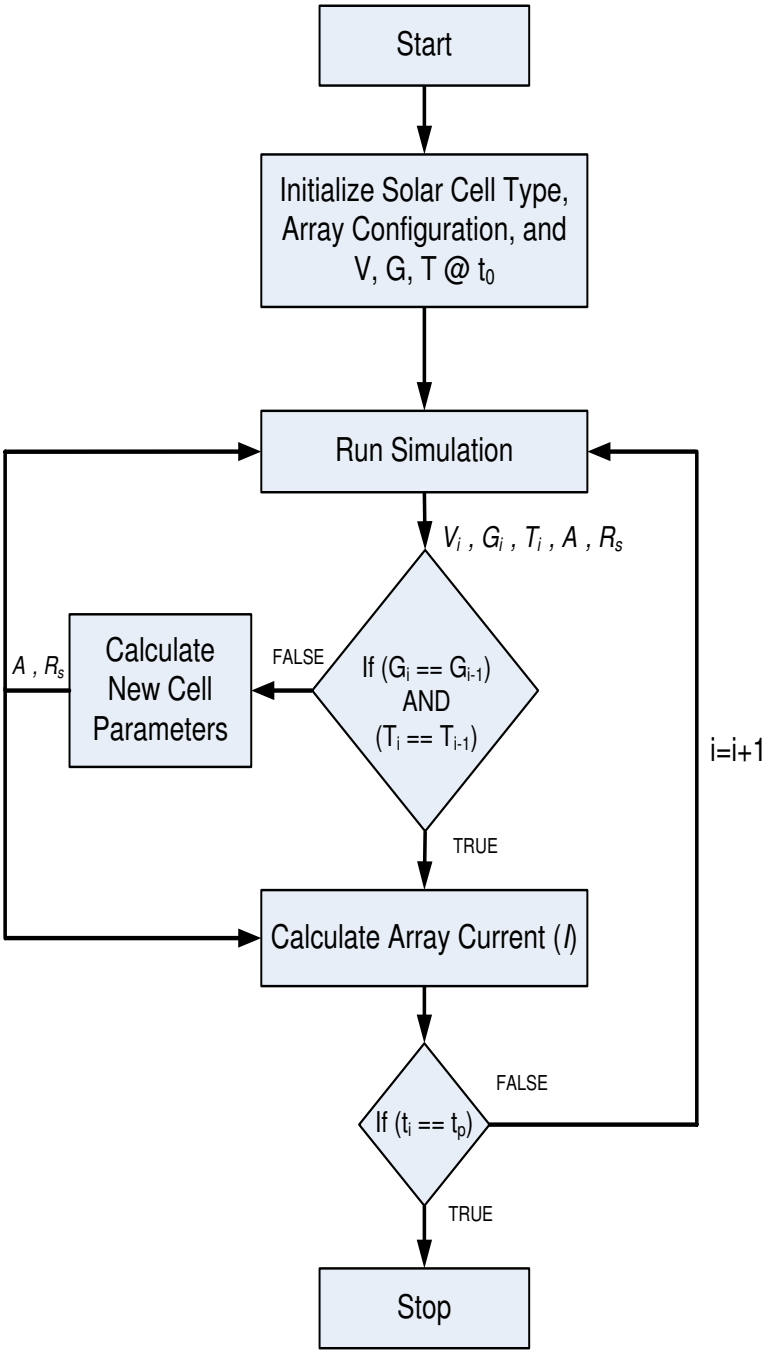


FIGURE 5.9: Original algorithm for single run

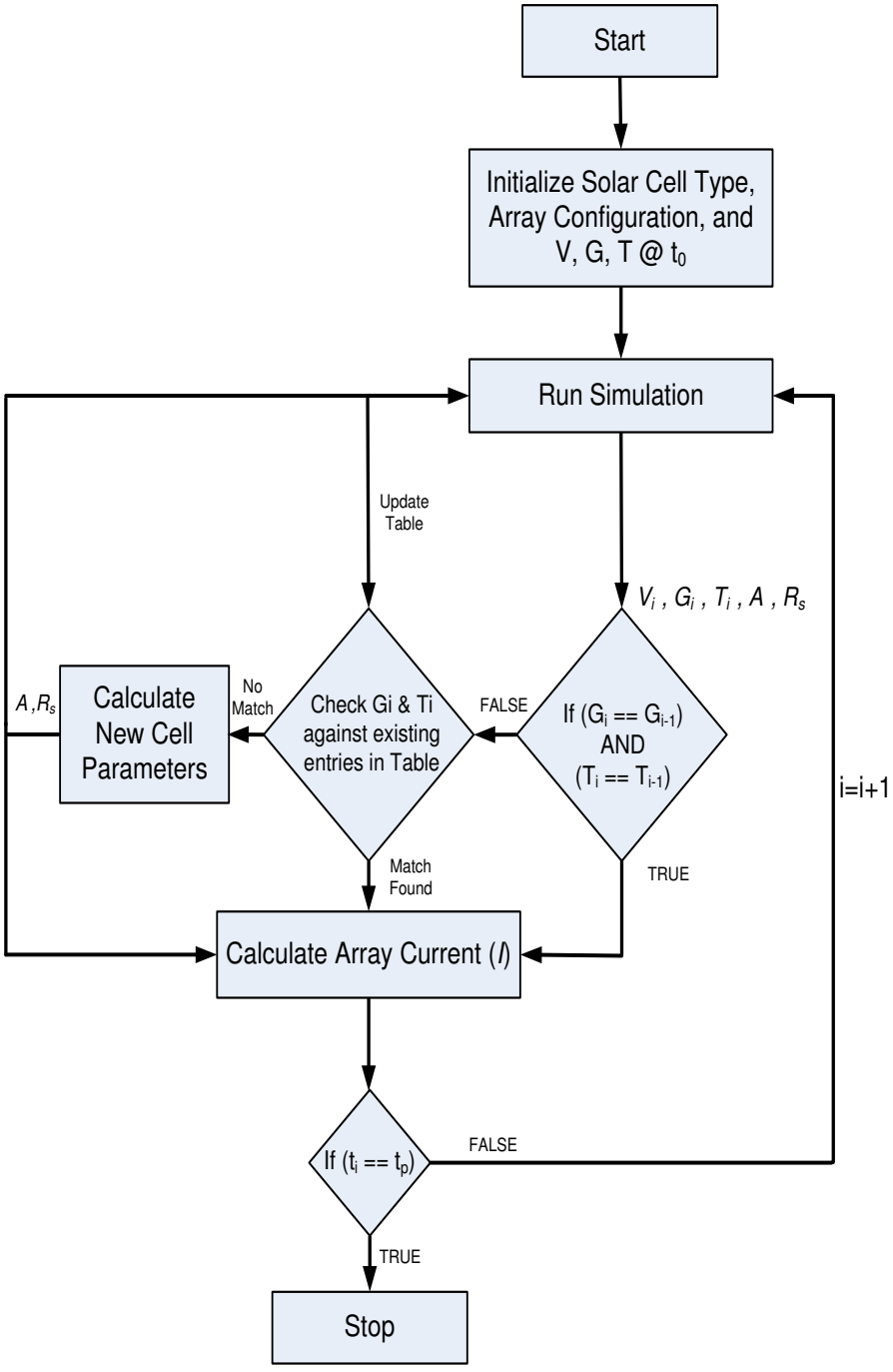


FIGURE 5.10: Modified algorithm for multi-run applications

# Chapter 6

# SEPS Conceptual Design Optimization

In this chapter, we describe the application of GA as a search and optimization tool for spacecraft power system design . The aim here is to analyze the behavior of GA and to compare the results when two techniques are applied to an automated design of spacecraft power system, with an improvement over the original baseline design.

The problem is sought by conducting two case studies. The optimization framework in case-1, is composed of the sizing model and optimizer only. Here, the *dynamic simulation model* of the spacecraft power system is not included. In case-2, the problem is extended to complete framework consisting of sizing, analysis and optimization.

## 6.1 Problem Statement

In this work, a LEO mission with medium power requirement is considered as a design optimization problem to be solved using genetic algorithms. The parameters of our mission along with the power requirements are given in Table 6.1. These requirements are coupled with a sizing tool to design our SEPS with minimum mass and cost, while targeting maximum performance.

| Parameter name | Value |
|---|---|
| Orbit altitude | 798 km |
| Inclination angle | $68^o$ |
| Mission life | 3Yrs. |
| Day light power requirements | 2kW |
| Eclipse power requirements | 2kW |

TABLE 6.1: List of mission parameters.

### 6.1.1 Design Variables

Seven different design variables are considered in this problem. These variables are selected for two reasons; first, to evaluate the impact of these variables on the system performance and, secondly, to consider the range of the solutions available with the industry in order to avoid the extra cost incurred as a result of development of new solutions. These design variables include both discrete and continuous parameters. Table 3.5 summarizes these design variables. The first three design variables describe the technology of solar cell-, the battery- and array-types. The solar cell choices are shown in Table 3.1. The three battery choices available are NiCd, $NiH_2$ and Li-ion. The forth variable is the bus voltage, and choices for this are 28V, 50V and 100V. The fifth and sixth variables are the choices of battery configuration i.e., number of the batteries and number of the cells per battery. The battery capacities and configurations required to fulfill the mission requirement are traded off against battery mass, cost and battery performance. These variables are chosen keeping in view the general practice and availability in the market. The seventh variable is maximum discharge rate. Maximum allowable discharge rate for the battery is given either by battery manufacturer or selected by designer depending upon mission and battery type. For GEO and LEO missions, this value is usually between C/2 and C/1.5, where C is battery capacity in ampere-hour.

### 6.1.2 Constraints

The constraints account for the allowable operational ranges of a specific battery for a given mission. These constraints are defined as:

- The battery should approach maximum allowable DOD as close as possible.

- The battery discharge current should not exceed maximum allowable rate of discharge.
- The battery operation should be energy efficient i.e., it should have an efficiency value higher than required ( a value usually defined by the user).

These constraints are handled differently as the battery SOC over a given period cannot be calculated in the first case, where only the mathematical relations are taken into consideration. To evaluate SOC, the battery must be subjected to charge/discharge cycles over a certain period similar to the ones encountered on real missions.

#### 6.1.2.1 CASE 1: Optimization using the sizing tool only

In this case, only one equality constraint is used to calculate the penalty function. The constraint is calculated as follows:

$$h_1(x) = \frac{DOD}{DOD_{maxallowable}} - 1 = 0 \tag{6.1}$$

#### 6.1.2.2 CASE 2: Optimization incorporating the analysis tool

Here, one equality and two inequality constraints are applied to the SEPS design problem. An external penalty function approach is implemented to account for the design, as described in section 3.4.3. These constraints ensure that the design of the battery is within allowable operation limits. These constraints can be described mathematically as:

$$h_1(x) = \frac{DOD}{DOD_{max}} - 1 = 0 \tag{6.2}$$

$$g_1(x) = \frac{SOC_{avg}}{SOC_{avg-desired}} - 1 \leq 0 \tag{6.3}$$

$$g_2(x) = \frac{I_{disrate}}{I_{disratemax}} - 1 \leq 0 \tag{6.4}$$

where $SOC_{avg}$ is calculated as average of fractional SOC over the simulation period and the $SOC_{avg-desired}$ is user defined target battery efficiency.

### 6.1.3 Objective Function Formulation

The problem we are considering belongs to the class of multi-objective (MO) problems. This MO problem is first reduced to a weighted sum problem in this chapter as discussed in section 3.4.2. It is solved initially using the sizing tool only, and the same problem is then solved using complete framework which includes the analysis tool as well. In both of these cases, the problem is solved for three different objectives. The objective functions for both of the cases are same. The difference lies in the formation of the function because the constraints are considered differently as discussed above. The objective functions used in the optimization process are based on the minimization of the system mass ($W_m$), cost ($W_c$) and inverse performance index ($W_{ipi}$) which means maximization of the performance of the SEPS. The objective function is given as:

$$J = w_m W_m + w_c W_c + w_p W_{ipi} \tag{6.5}$$

where $w$ represents the weight given to each objective, W represents the value of individual objectives. The subscripts $m$, $c$, and $ipi$ represent mass, cost and inverse performance index respectively. The SEPS performance index is a measurement of system performance. It takes into account the solar array figure of merit ($FoM_{sa}$), system reliability ($R_{eps}$), and system performance constraints. As the current problem has been formulated as minimization problem, we use inverse of performance index. Individual objectives are calculated as follows:

$$W_m = M_b + M_{sa} + M_{PMAD} \tag{6.6}$$

$$W_c = C_{batt} + C_{sa} + C_{eff-launch} \tag{6.7}$$

$$W_{ipi} = \frac{1}{FoM_{sa}} + \frac{1}{R_{eps}} + Pen \tag{6.8}$$

where penalty value ($Pen$) takes into account all the penalty factors, $R_{eps}$ is overall system reliability and is calculated as described in section 4.1.5. The solar array figure of merit is defined as ratio of the solar array EOL power with solar array

mass and area, and is calculated for LEO and GEO missions as [29]:

$$FoM_{sa} = \begin{cases} \frac{P_{arr}}{A_{sa}^3 \times M_{sa}^2} & LEO \\ \\ \frac{P_{arr}}{A_{sa}^2 \times M_{sa}^2} & GEO \end{cases} \tag{6.9}$$

## 6.2 Results and Discussion

### 6.2.1 Case-1

In the weighted sum approach, the three objectives are reduced to one as described by Equation 6.5. This single objective problem is then solved using the MATLAB GA toolbox. In these runs, only the sizing tool is used to calculate the mass, the cost and the figure of merit of solar array design. To evaluate the constraints, the SOC condition of the selected battery configuration is checked against maximum allowable for the given technology.

The problem is solved for population sizes of 50 and 70 generations. Two different selection methods namely, i) the tournament selection and ii) the remainder selection, are used in the evolutionary computations. The results generated by both of these are summarized in Table 6.2 against the baseline values.

A closer look at these results reveals that, although the technology for solar array and battery is same, the selection of bus voltage and number of battery cells makes a significant effect on collective as well as individual-objectives. Thus the results generated by GA are optimized in the sense of mass, cost and performance. In addition, the design engineer will have confidence that the resultant design is realizable and stays within the design options available in the industry.

The evolutionary progress of the GA over the course of different generations for the tournament and the remainder selection processes is given in Figure 6.1 and Figure 6.2 respectively. It is clear from the results that the remainder selection gives better results in a lesser no. of generations, so all further optimization runs in this chapter are conducted using remainder selection process.

| Design Variable/ Parameter | Baseline | Optimization Results | |
|---|---|---|---|
| | | Remainder Selection | Tournament Selection |
| Solar cell technology | GaAs | ATJ2 | High-$\eta$ Si |
| Battery technology | $NiH_2$ | $Li-ion$ | Li-ion |
| Array type | Rigid | Rigid | Rigid |
| Bus voltage (V) | 50 | 100 | 50 |
| No. of batteries | 2 | 1 | 2 |
| No. of cells per battery | 22 | 52 | 10 |
| Maximum Discharge rate ($\times$C) | 0.5 | 0.506 | 0.5296 |
| Battery capacity (Ah) | 52 | 50 | 50 |
| Array area ($m^2$) | 71 | 42.290 | 75.50 |
| SPS mass (kg) | 378.88 | 220.55 | 255.192 |
| Total cost factor($10^4$\$) | 1531.0 | 1023.8 | 786.668 |
| Inverse performance index | 4058.30 | 189.696 | 592.9913 |
| WS objective | 1987 | 477.554 | 545.229 |

TABLE 6.2: Comparison of baseline and optimized design

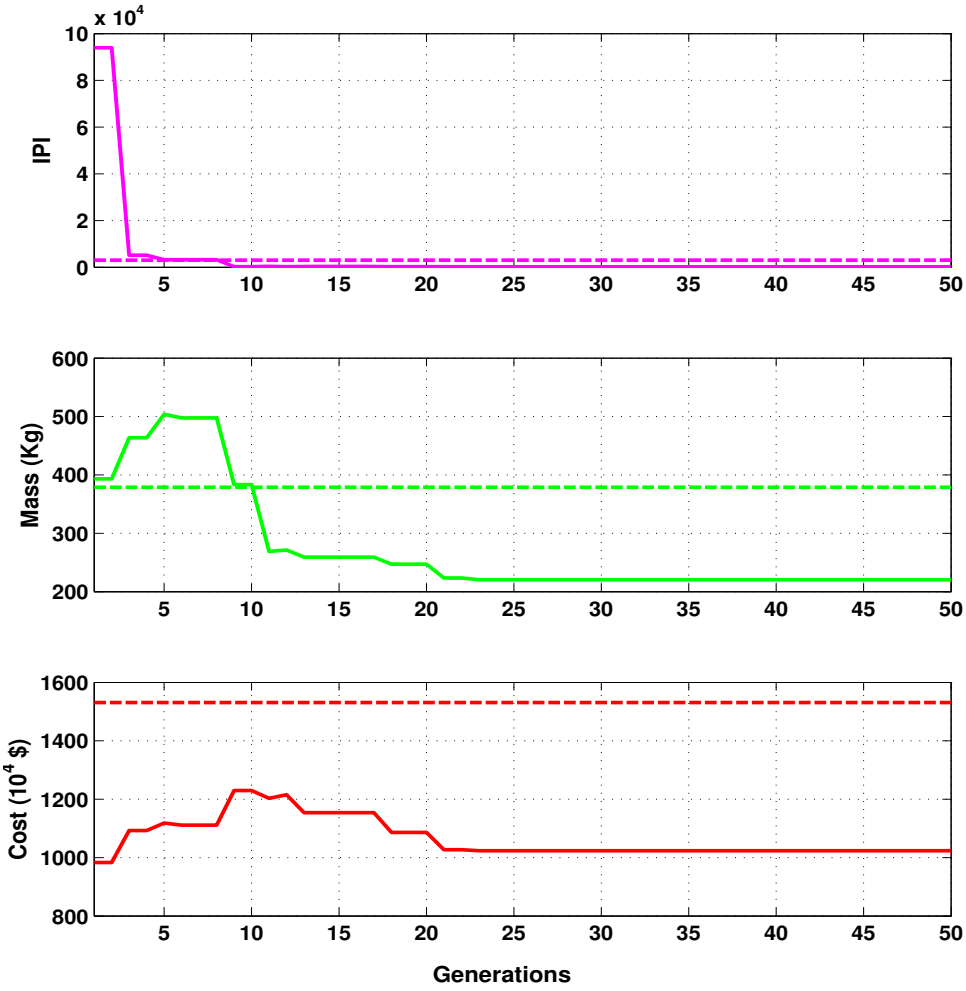


(a)

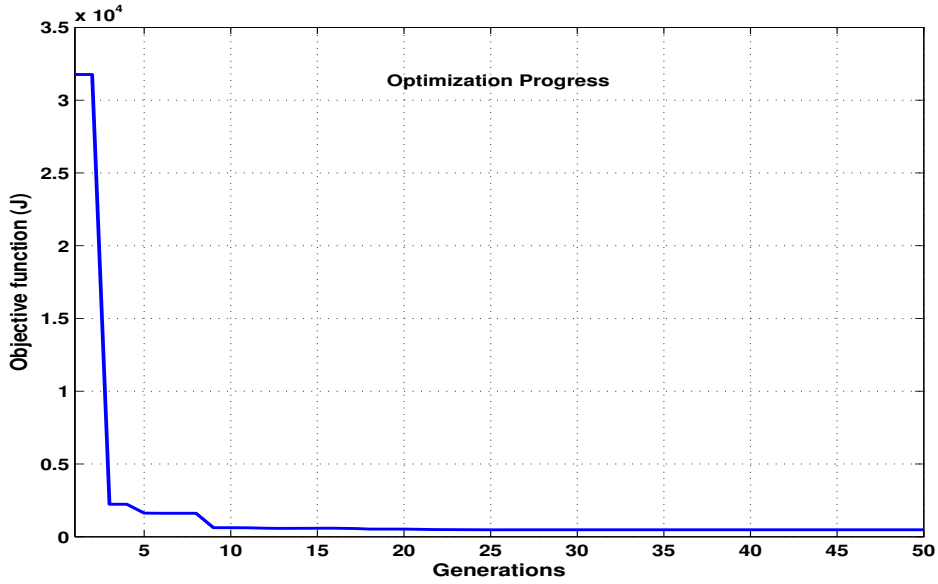


(b)

FIGURE 6.1: Fitness values of individual and weighted sum objective over optimization run using tournament selection method

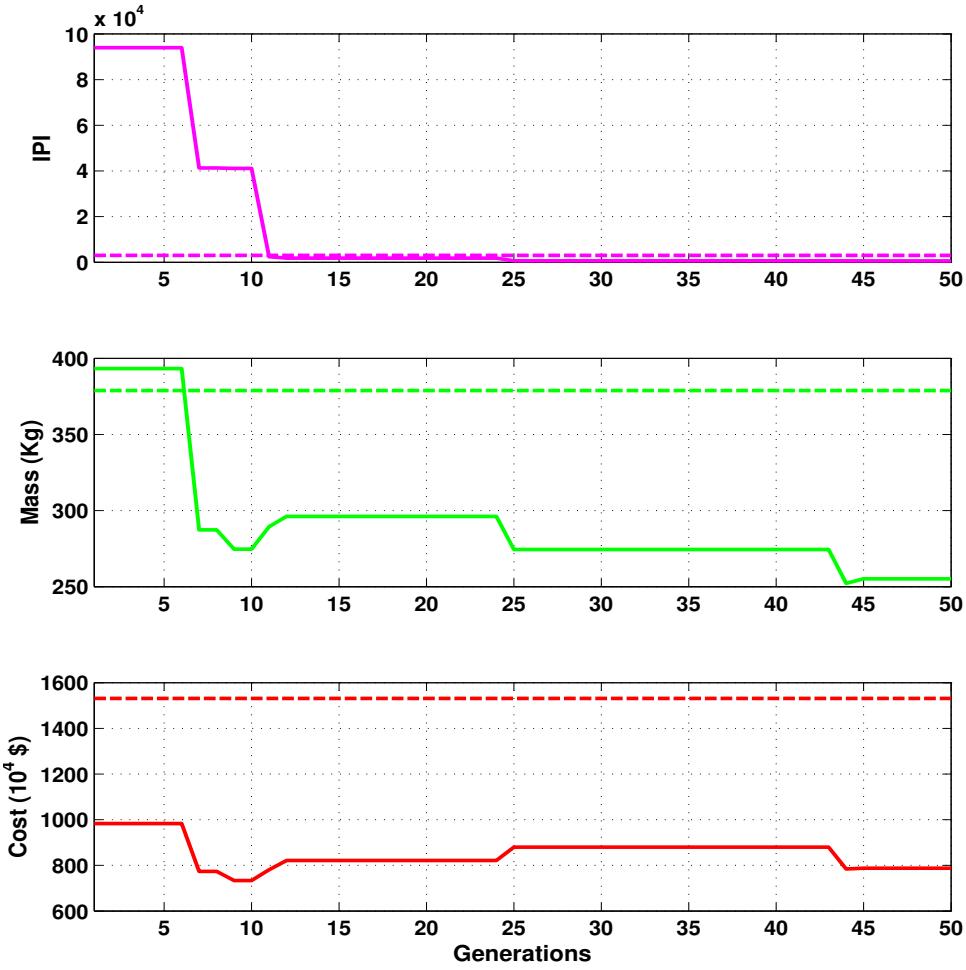


(a)

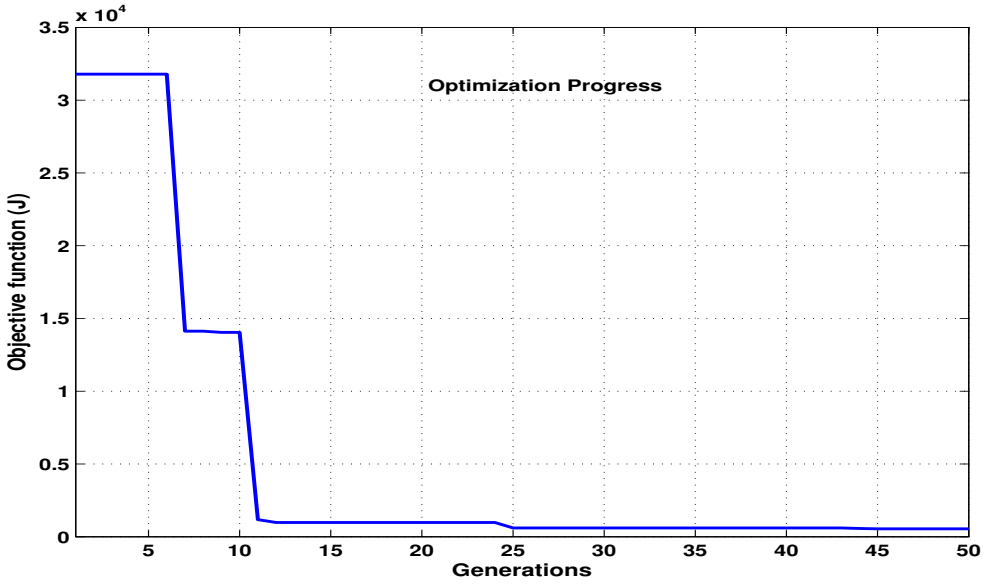


(b)

FIGURE 6.2: Fitness values of individual and weighted sum objective over optimization run using remainder selection method

| Design variable/ parameter | Baseline | Optimization results |
|---|---|---|
| Solar cell technology | GaAs | UTJ |
| Battery technology | $NiH_2$ | $Li-ion$ |
| Array Type | Rigid | Rigid |
| Bus voltage (V) | 50 | 100 |
| No. of batteries | 2 | 1 |
| No. of cells per battery | 22 | 56 |
| Maximum discharge rate | 0.5 | 0.6039 |
| Battery capacity (Ah) | 52 | 39 |
| Array area ($m^2$) | 71 | 42.290 |
| SPS mass (kg) | 378.88 | 215.693 |
| Total cost factor($10^4$\$) | 1530.0 | 1007.5 |
| Inverse performance index | 4058.0 | 196.660 |
| WS objective | 1987.0 | 472.8037 |

TABLE 6.3: Comparison of baseline and optimized design using complete framework

### 6.2.2 Case-2

For the optimization of the SPS design using the complete framework, the scenario of using same weights for all objectives has been used. The results given here are almost same as above. The results along with some parametric analysis in Table 6.3 give a summary of main parameters for both baseline and optimal (near optimal) designs.

Figure 6.3 shows how the objective function progresses toward its minimum. The optimal solution here is attained in $18^{th}$ generation. The dynamic simulation results for the optimal solution are shown in Figure 6.4. It can be seen that the battery goes to a minimum of 70.13% while it was allowed for a minimum of about 51%. Hence, although the constraint of SOC does not exceed the maximum allowed limit, the battery failed to utilize itself efficiently, and the system design will be penalized for this.

As one single optimization run gives one optimal solution at the Pareto front, to find other solutions at the Pareto front we need multiple optimization runs with different weight combinations. Here we do it for three different cases, low IPI, low mass and low cost. The results of these different optimizations are summarized in Table 6.4. From these results, we can see that UTJ solar cells are best choice for low IPI and mass, hence the same comes as selection for equal weights. Similarly

| Design Variable/ Parameter | Optimization Results | | |
|---|---|---|---|
| | High IPI Weight | High Cost Weight | High Mass Weight |
| Solar cell technology | UTJ | High-$\eta$ Si | UTJ |
| Battery technology | *NiCd* | Li-ion | Li-ion |
| Array type | Rigid | Rigid | Rigid |
| Bus voltage (V) | 100 | 50 | 50 |
| No. of batteries | 2 | 3 | 2 |
| No. of cells per battery | 54 | 11 | 11 |
| Maximum Discharge rate (×C) | 0.603 | 0.58 | 0.65 |
| Battery capacity (Ah) | 29 | 28 | 39 |
| Array area ($m^2$) | 42.29 | 75.50 | 41.90 |
| SPS mass (kg) | 334.703 | 249.979 | 221.442 |
| Total cost factor($10^4$\$) | 1376.6 | 765.9344 | 1046.40 |
| Inverse performance index | 178.24 | 594.593 | 226.5776 |

TABLE 6.4: Comparison optimized designs for different weight options

for battery choice Li-ion is the selection for low cost and low mass, so, it comes out as selection where all objectives are given equal weights. The design variables like array type, battery configuration and maximum discharge rate play an important role in the refinement of the optimal design selection. How the objective functions evaluate over the optimization run is shown in Figure 6.5.

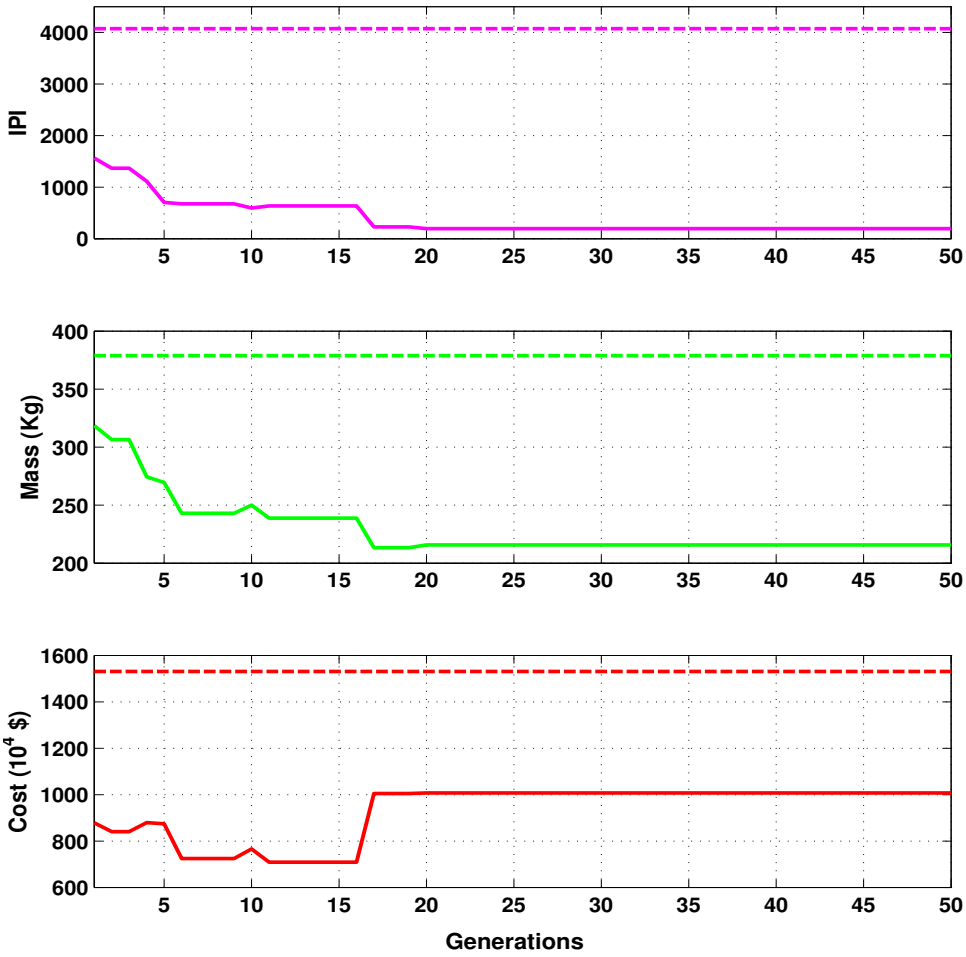


(a)

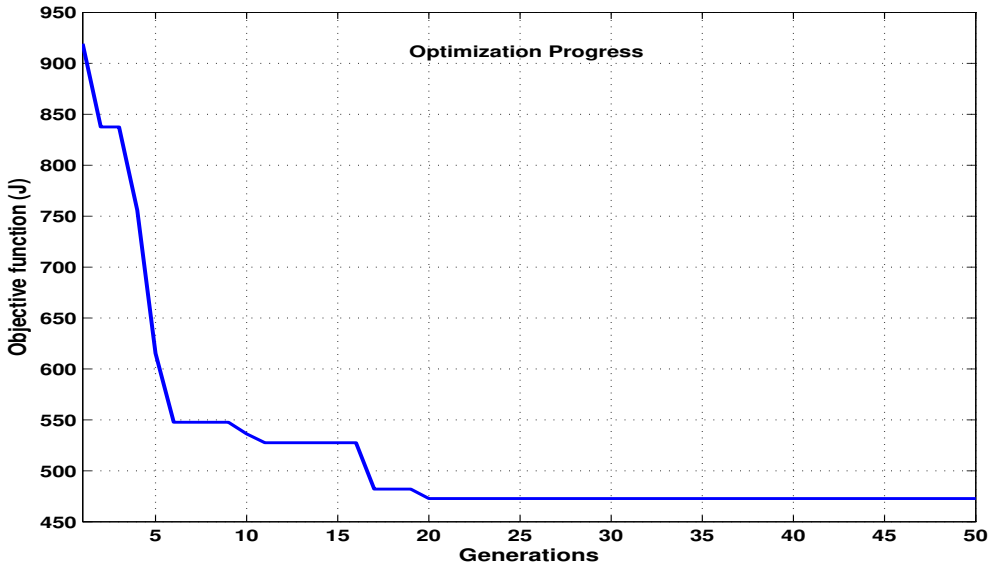


(b)

FIGURE 6.3: Fitness values of individual and weighted sum objective over optimization run

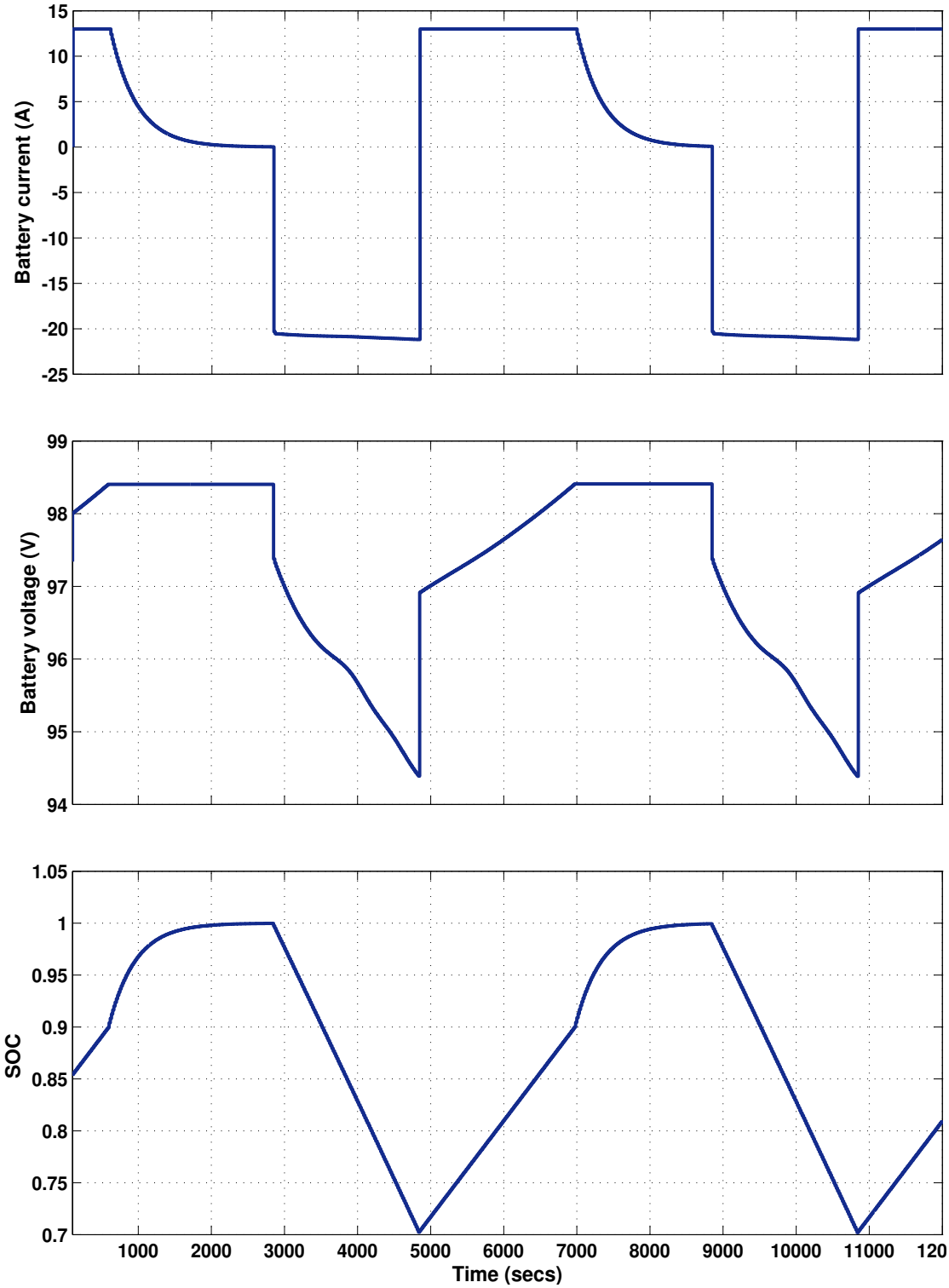


FIGURE 6.4: Dynamic simulation of optimized design

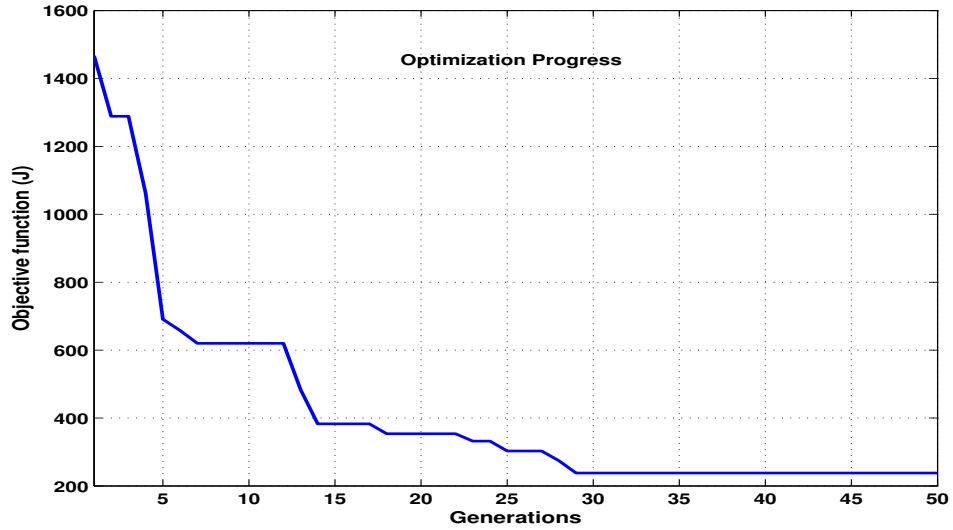


(a) High IPI weight

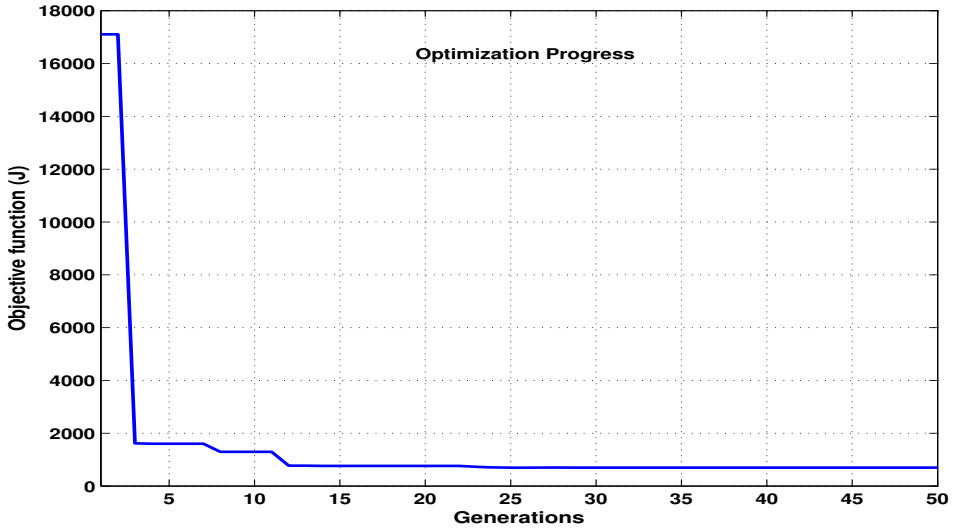


(b) High Cost weight

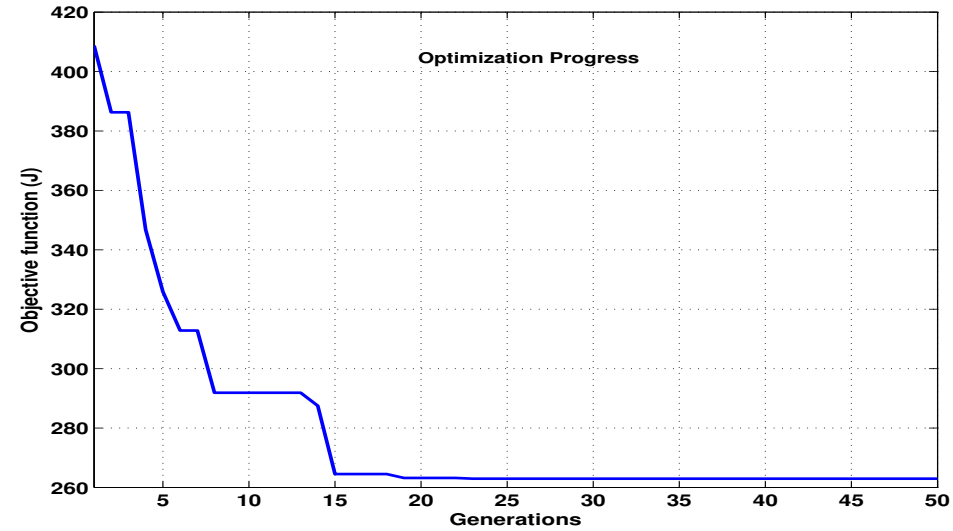


(c) High Mass weight

FIGURE 6.5: Fitness values of weighted sum objective over optimization run

# Chapter 7

# Multi-Objective Design Optimization

In spacecraft systems design, there are usually more than one design objectives, which a design team should take into account. These objectives involve system performance measures like mass, size, cost, reliability, power efficiency and system robustness. In a good design procedure, the tradeoffs between competing objectives should be incorporated so that the design team can make an informed decision.

In the previous chapter, we have seen the application of the classical weighted sum approach in solving the design search and optimization of a spacecraft power subsystem problem. In the weighted sum approach, the weighting of the different objectives into a single objective is necessary which require prior weights of objectives. This approach finds one solution in one run, and requires a large number of function evaluations and several optimization runs to find the set of Pareto optimal solutions. Whereas, multi-objective optimization treats each objective independently, and does not require any prior weights. Secondly, multi-objective optimization generates a set of Pareto optimal solutions in one single run, and the designer can identify the trade-off between competing objectives.

This chapter presents the application of multi-objective optimization to the spacecraft power subsystem design search and optimization. In the previous chapters, we have discussed that spacecraft power subsystem design is multi-objective where we try to minimize the mass and cost and maximize system performance (minimizing inverse performance index) at the same time. To understand the application

of the multi-objective nature of optimization problem, we have gone from a bi-objective to a tri-objective application. In bi-objective problems, the trade-offs between two objectives are sought while third is not taken into account. In this research, a modified version of the non-dominated sorting genetic algorithm is used to find a set of Pareto optimal solutions. NSGA-II has performed very well here, and is able to give converging Pareto fronts. The test results performed on the problem, discussed in last chapter, show that the computational time of NSGA-II is comparable to that of weighted sum genetic algorithm (WSGA).

## 7.1 Problem Statement

In this chapter, two case studies are made: in the first case study, the power subsystem design is investigated for the LEO mission parameters which are given in chapter 6, using NSGA-II. In the second case study, the problem for the design of power subsystem for a communication satellite will be evaluated. This problem has been encountered during author's work experience and is being solved after going through a long traditional trade-off study and consultations.

The three objectives are the same as defined in chapter 6. These objectives are:

- Minimization of SPS mass

$$J_1 = min(M_{eps}) \tag{7.1}$$

- Minimization of cost.

$$J_2 = min(C_{eps} + C_{eff-lauch}) \tag{7.2}$$

- Minimization of inverse performace index

$$J_3 = min(\frac{1}{FoM_{sa}} + \frac{1}{R_{eps}} + Pen_{batt}) \tag{7.3}$$

## 7.2 Results and Discussion

### 7.2.1 Case-1

NSGA-II is implemented for multi-objective optimization. The problem of SEPS design for LEO missions is analyzed in two different ways.

#### 7.2.1.1 Bi-Objective Optimization

Before solving the multi-objective problem for three objectives, it is solved as a bi-objective problem. To this end, individual optimization runs are made for three bi-objective problems, which are designed as, IPI-mass, IPI-cost and mass-cost optimization problems. The Pareto fronts for bi-objective optimizations of these bi-objective problems are determined. The Pareto optimal solutions for IPI/Cost are shown in Figure 7.1. The results shown in Figure 7.1(a) are obtained with a population size of 70, while the results shown in Figure 7.1(b) are obtained with a population size of 110. As we can see the number of solutions obtained in second case are greater than what we get in case-1, but increasing the population size further does not have any significant effect on the number of solutions obtained. Hence, it can be said that the population size of 110 (about 15 times number of variables involved) is optimal. In Figure 7.1(b), we can see three regions of a Pareto front. Region I contains the solutions with very low IPI and very high cost, whereas Region-II contains the solution with clear trade-off between the IPI and cost. Region III contains the solutions with lowest costs and very high IPI. The progress of the minimum of each objectives along the generations for IPI/Cost is shown in Figure 7.2. The Pareto fronts for IPI/Mass and Mass/Cost are shown in Figures 7.3 and 7.5 respectively. The progress of the minimum of each objectives vs. the generations is shown in Figures 7.4 and 7.6

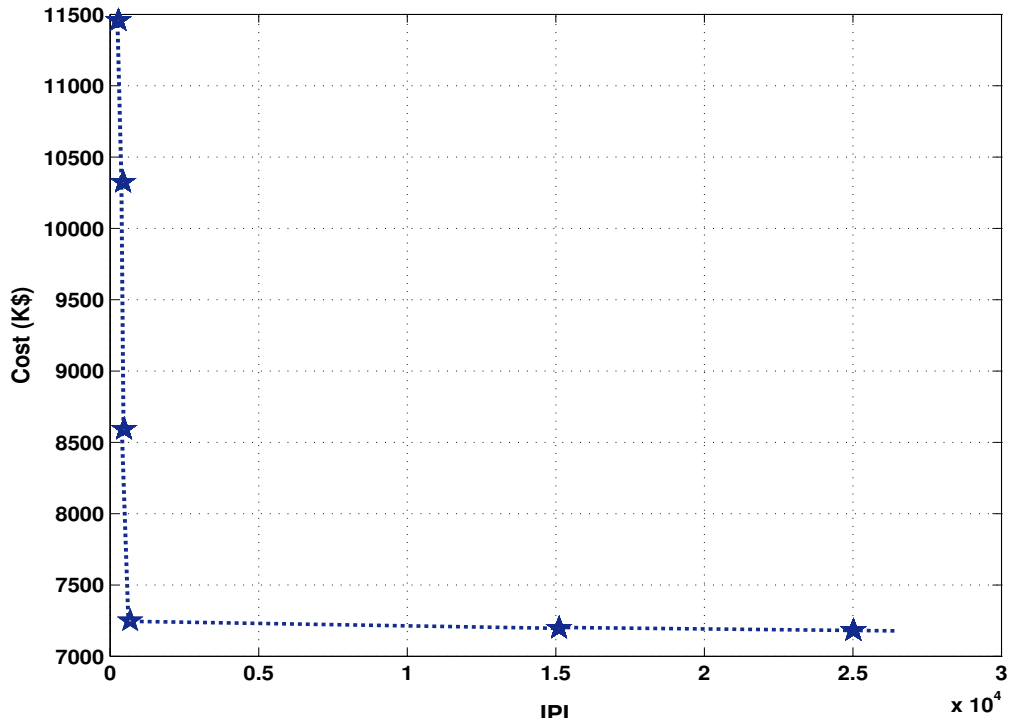


(a) Results with a population size of 70

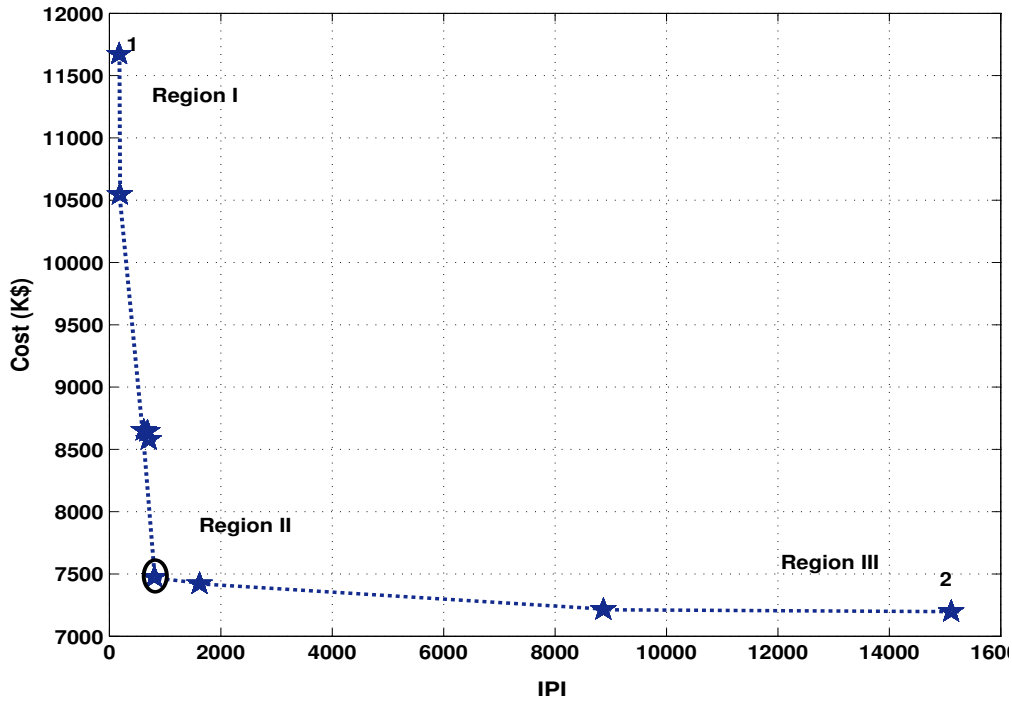


(b) Results with a population size of 110

FIGURE 7.1: Pareto set for IPI/Cost

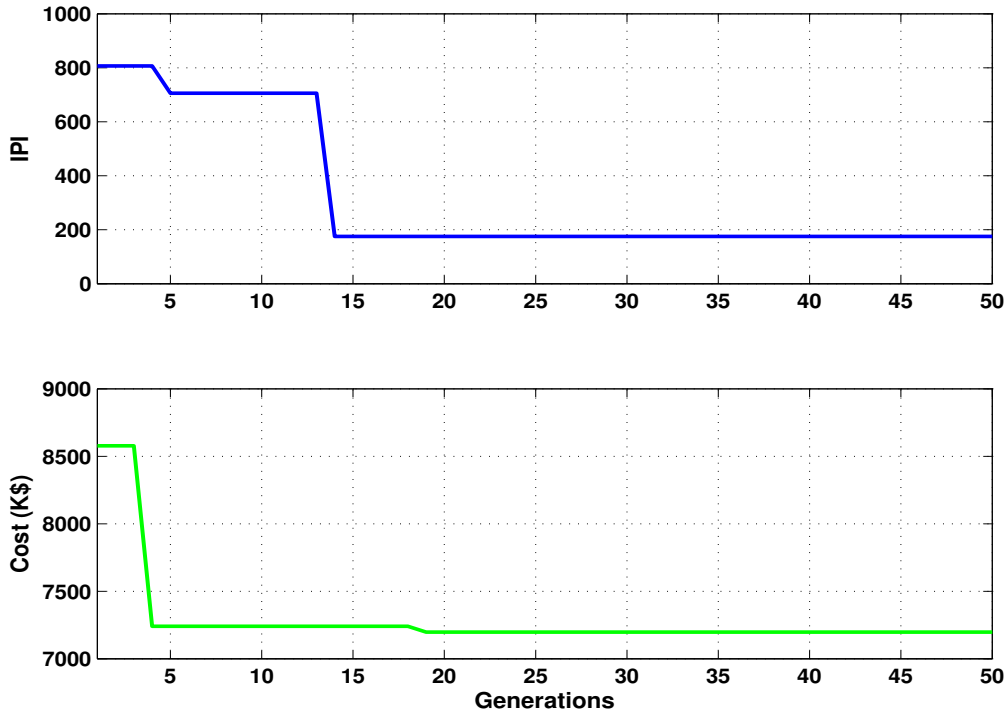


FIGURE 7.2: Progress of minimum achieved for each objective vs. no. of generations for IPI/Cost problem

In Figure 7.1, we can see that NSGA-II has produced results representing the tradeoff between the inverse performance index and cost, which are well distributed around the imaginary Pareto front (represented by the dashed line). Point-1 represents the design with minimum IPI but maximum cost while point-2 represents the design having maximum inverse performance index with minimum cost. A similar situation can be seen for IPI/Mass and Mass/Cost cases. The points between the extremes are the results showing a clear trade-off between the two objectives being optimized. To analyze this trade off phenomenon, we do a comparison of extreme- and compromised- (encircled) solutions. This comparison is given in Tables 7.1, 7.2 and 7.3. From the results for IPI/cost optimization given in Table 7.1, we can see that, for the current problem, selecting Li-ion can provide a low cost system. Also, it is clear that although the UTJ solar cell can give the best performance fit, high-$\eta$ Si solar cells can give better results for low cost. From Table 7.2, we can see that when it comes to performance-mass trade off UTJ is the best choice in both cases. Whereas when it comes to mass/cost trade-off (Table 7.3) NiCd with high-$\eta$ Si results in lowest cost system. To understand what does is meant by low and high IPI, the performance of battery system for the extreme solutions from

| Parameter | Minimum IPI | Minimum Cost | Compromised solution |
|---|---|---|---|
| IPI | 175.189 | 15110.227 | 806.929 |
| Cost (k$) | 11672.277 | 7197.506 | 7473.266 |
| Solar cell technology | UTJ | High-$\eta$ Si | High-$\eta$ Si |
| Battery technology | *NiCd* | *Li – ion* | *Li – ion* |
| Array Type | Rigid | Rigid | Flexible |
| Bus voltage (V) | 100 | 50 | 100 |
| No. of batteries | 3 | 1 | 1 |
| No. of cells per battery | 52 | 11 | 22 |
| Maximum discharge rate | 0.501 | 0.624 | 0.595 |

TABLE 7.1: Comparison of value limits of Pareto set (IPI/Cost)

| Parameter | Minimum IPI | Minimum Mass | Compromised solution |
|---|---|---|---|
| Mass (kg) | 346.715 | 212.321 | 223.512 |
| IPI | 334.756 | 14704.242 | 765.691 |
| Solar cell technology | UTJ | UTJ | UTJ |
| Battery technology | *NiCd* | *Li – ion* | *Li – ion* |
| Array Type | Flexible | Rigid | Rigid |
| Bus voltage (V) | 100 | 50 | 100 |
| No. of batteries | 3 | 1 | 1 |
| No. of cells per battery | 60 | 11 | 24 |
| Maximum discharge rate($\times$C) | 0.563 | 0.547 | 0.50 |

TABLE 7.2: Comparison of value limits of Pareto set (IPI/Mass)

IPI/cost trade off is given in Figures 7.7 and 7.8. Here we can see that, in the system with low IPI, the battery is well approaching the maximum state of discharge (0.7). While in the system with high IPI, the battery is discharging far beyond the maximum allowed limit (0.6), and it can also be seen that if same behavior continues over a number of charge/discharge cycles, the battery may exceed the end of discharge limits. Hence the systems with high IPI are the worst choice.

| Selection | Minimum mass | Minimum cost | Compromised |
|---|---|---|---|
| Mass (kg) | 211.07 | 279.94 | 245.71 |
| Cost (k$ ) | 10023.94 | 7392.95 | 755.24 |
| Solar cell technology | UTJ | High-$\eta$ Si | High-$\eta$ Si |
| Battery technology | $Li-ion$ | $NiCd$ | $Li-ion$ |
| Array Type | Rigid | Rigid | Flexible |
| Bus voltage (V) | 100 | 50 | 50 |
| No. of batteries | 1 | 1 | 2 |
| No. of cells per battery | 20 | 30 | 10 |
| Maximum discharge rate ($\times$C) | 0.666 | 0.614 | .665 |

TABLE 7.3: Comparison of value limits of Pareto set (Mass/Cost)

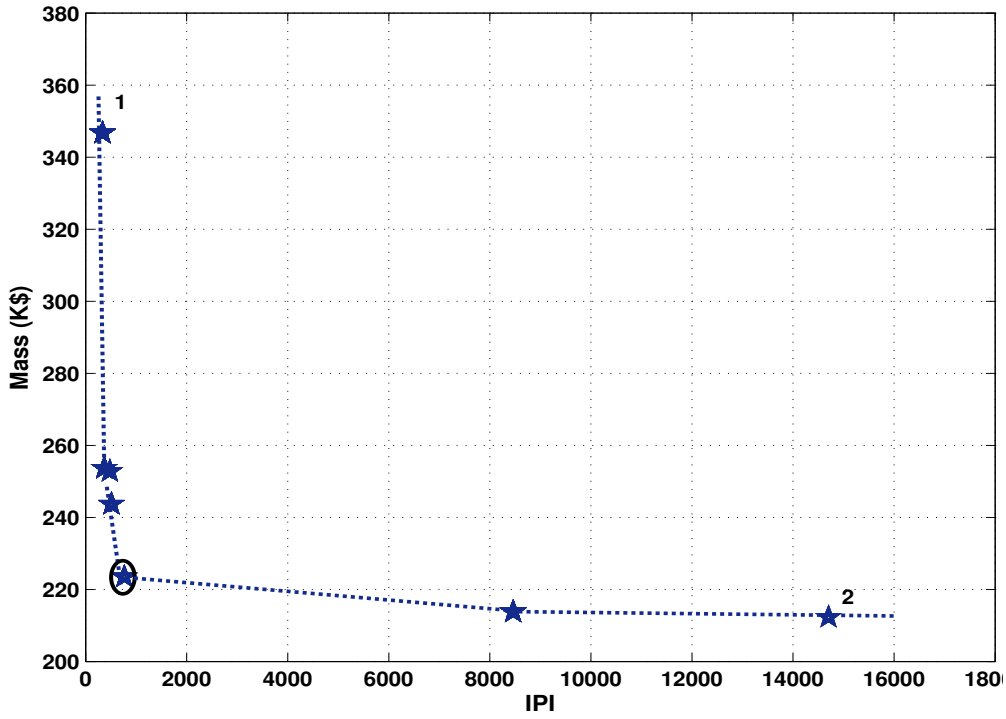


FIGURE 7.3: Pareto set for IPI/Mass

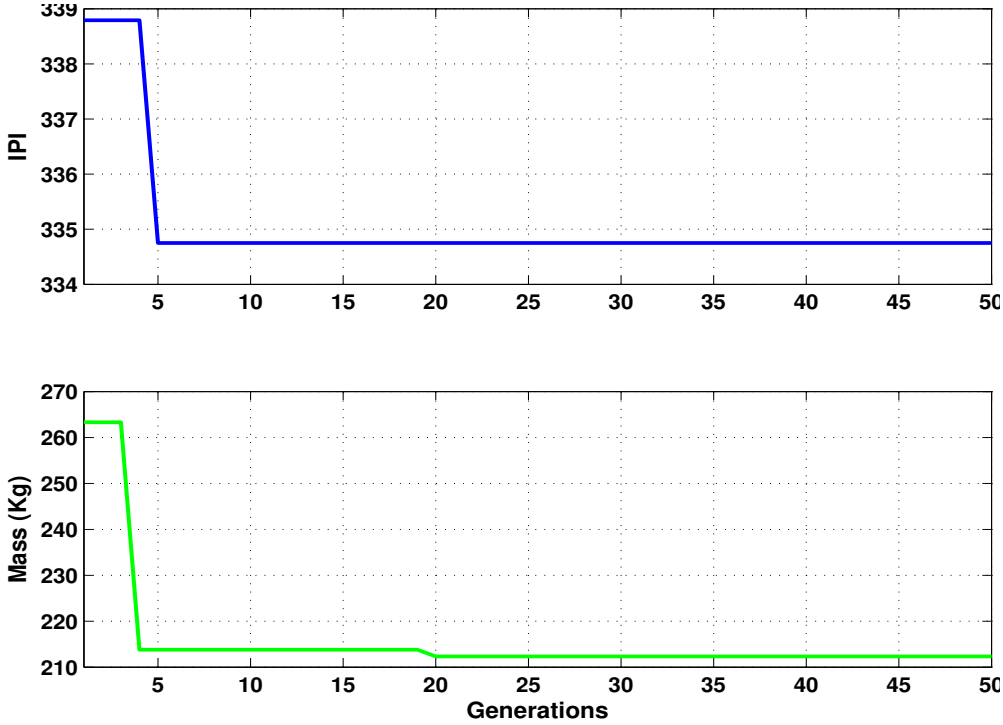


FIGURE 7.4: Progress of minimum achieved for each objective vs. no. of generations for IPI/Mass problem

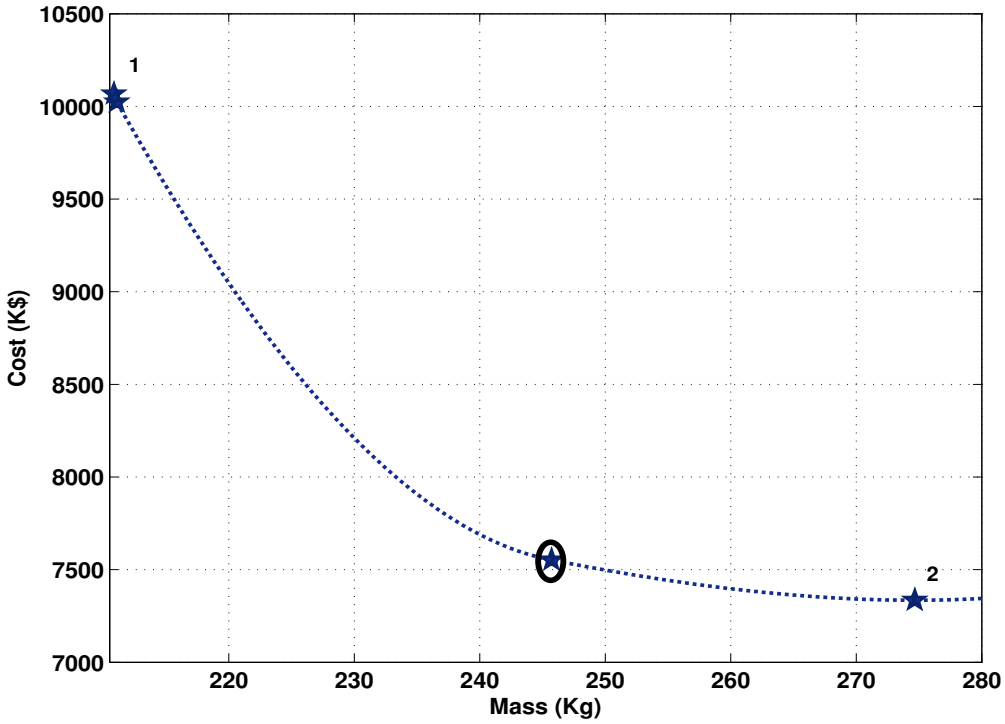


FIGURE 7.5: Pareto set for Mass/Cost

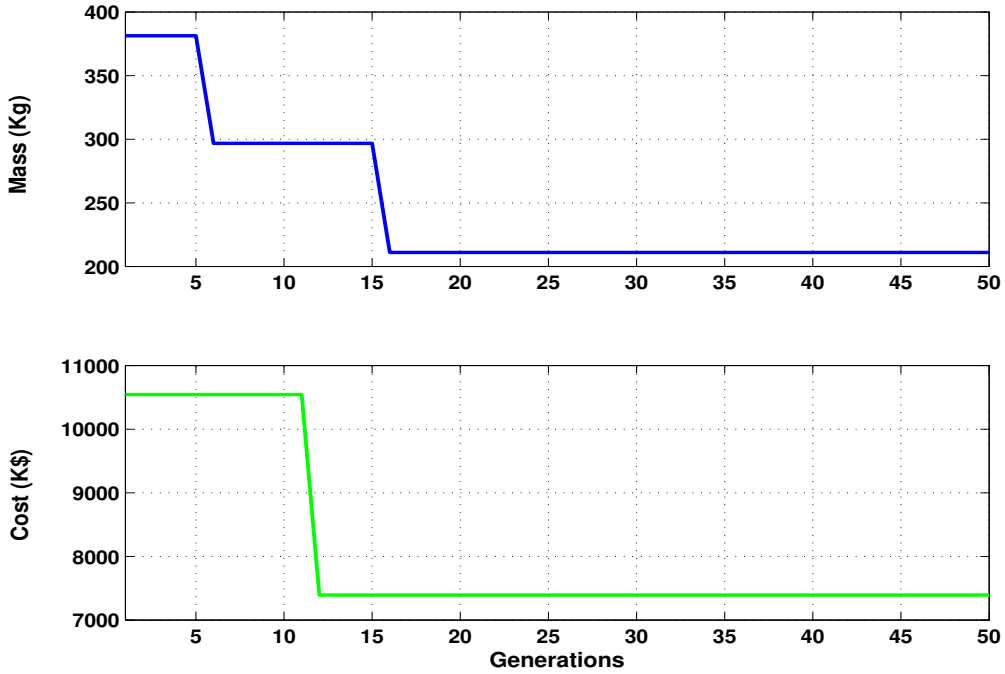


FIGURE 7.6: Progress of minimum achieved for each objective vs. no. of generations for Mass/Cost problem

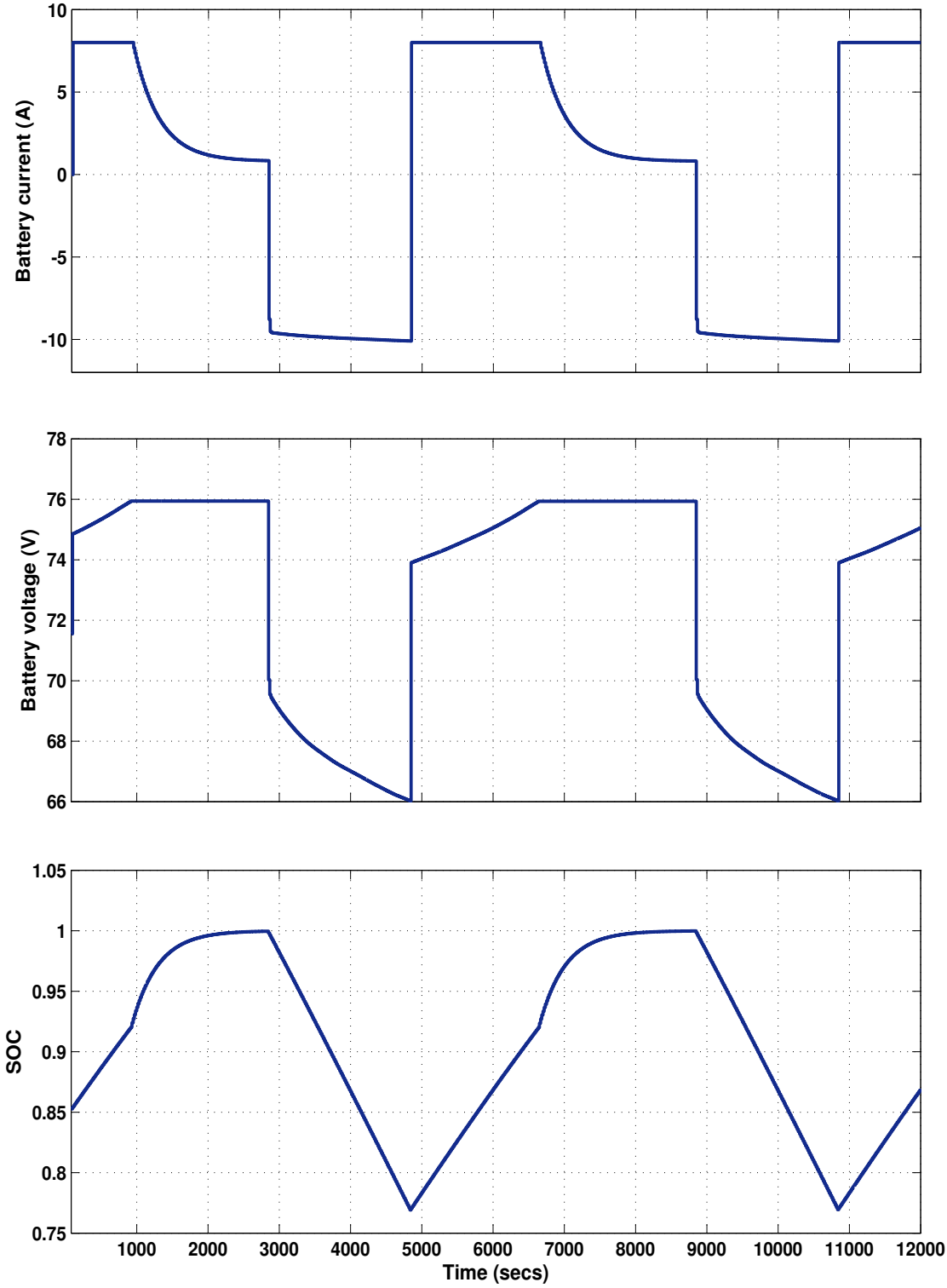


FIGURE 7.7: Battery behavior for selection-1 from IPI/Cost Pareto set

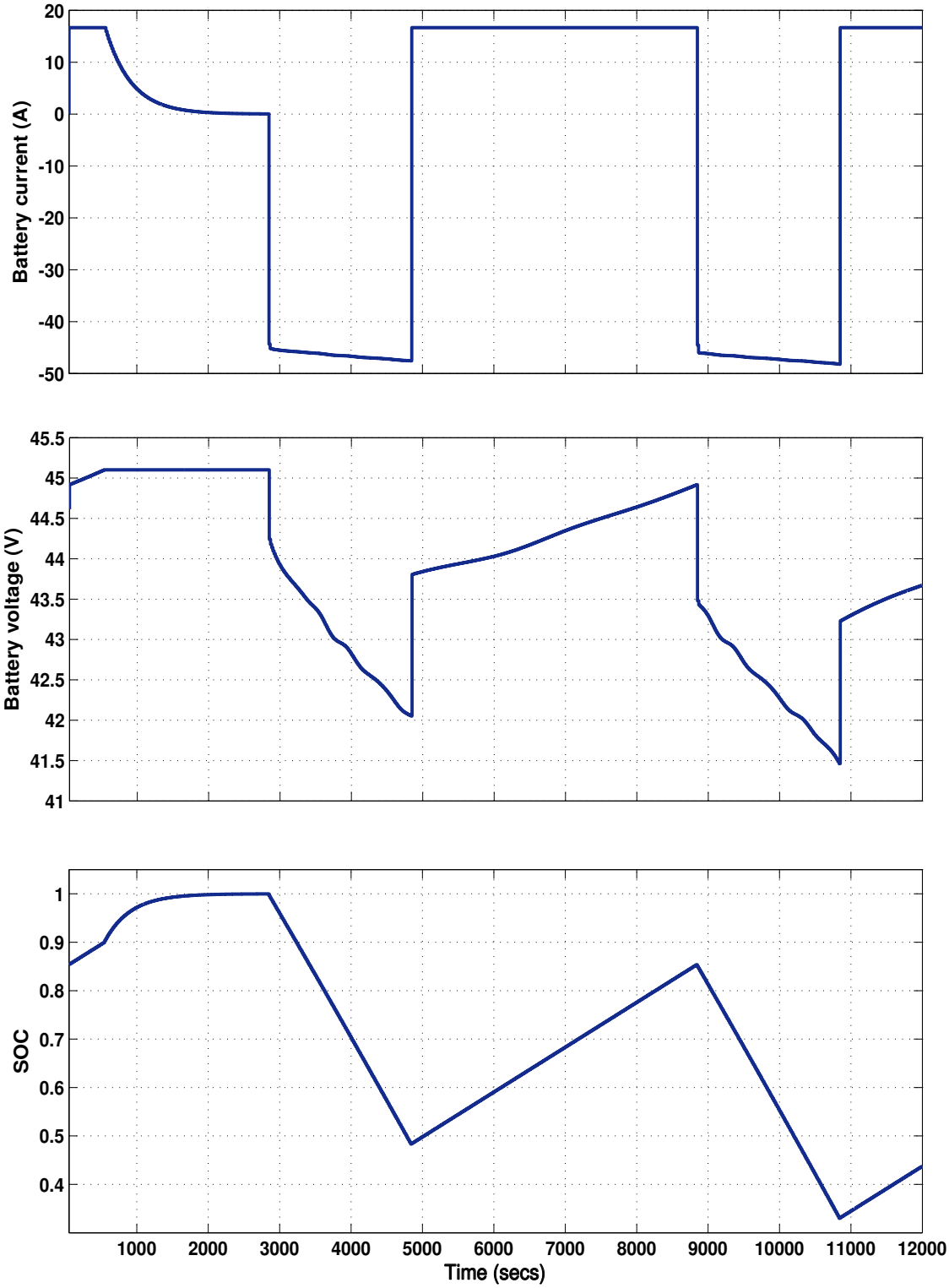


FIGURE 7.8: Battery behavior for selection-2 from IPI/Cost Pareto set

#### 7.2.1.2 Tri-Objective Optimization

In bi-objective case studies presented in the previous section, two objectives were traded off while neglecting the third. Here we shall move one step ahead, and shall analyze the problem in its full perspective. The study is made taking all three objectives under consideration. The optimization is run for 50 generations with a population size of 110. Figure 7.9 shows the Pareto front. In a 3D representation, it is hard to visualize how the trade-offs are taking place. So the Tradeoffs are projected on two-objective planes in Figures 7.10, 7.11 and 7.12 The pattern of how the objectives change over the generations is shown in Figure 7.13.

Two solutions are selected in this case and the comparison is given in Table 7.4. The comparison of the results shows that solution-1 has best compromise between mass and cost but slightly higher IPI, whereas solution-2 has very low IPI but poor mass and cost compromise.

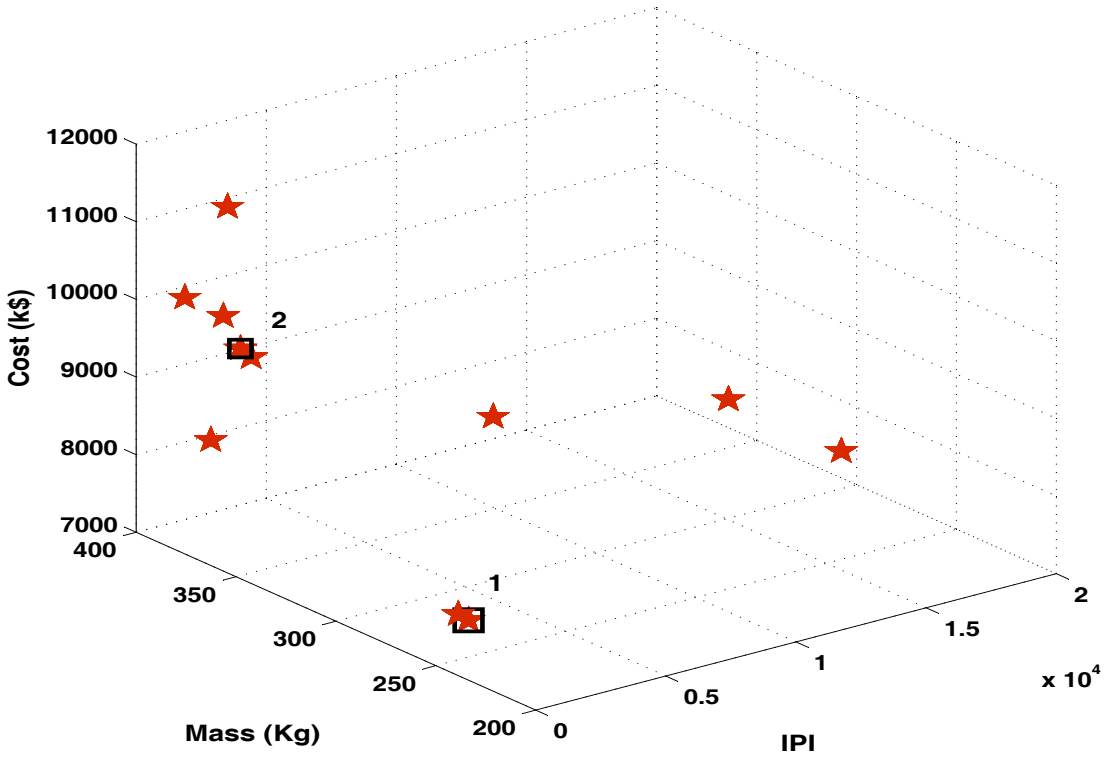


FIGURE 7.9: Approximate Pareto front for tri-objective optimization for the design of SEPS for LEO satellite

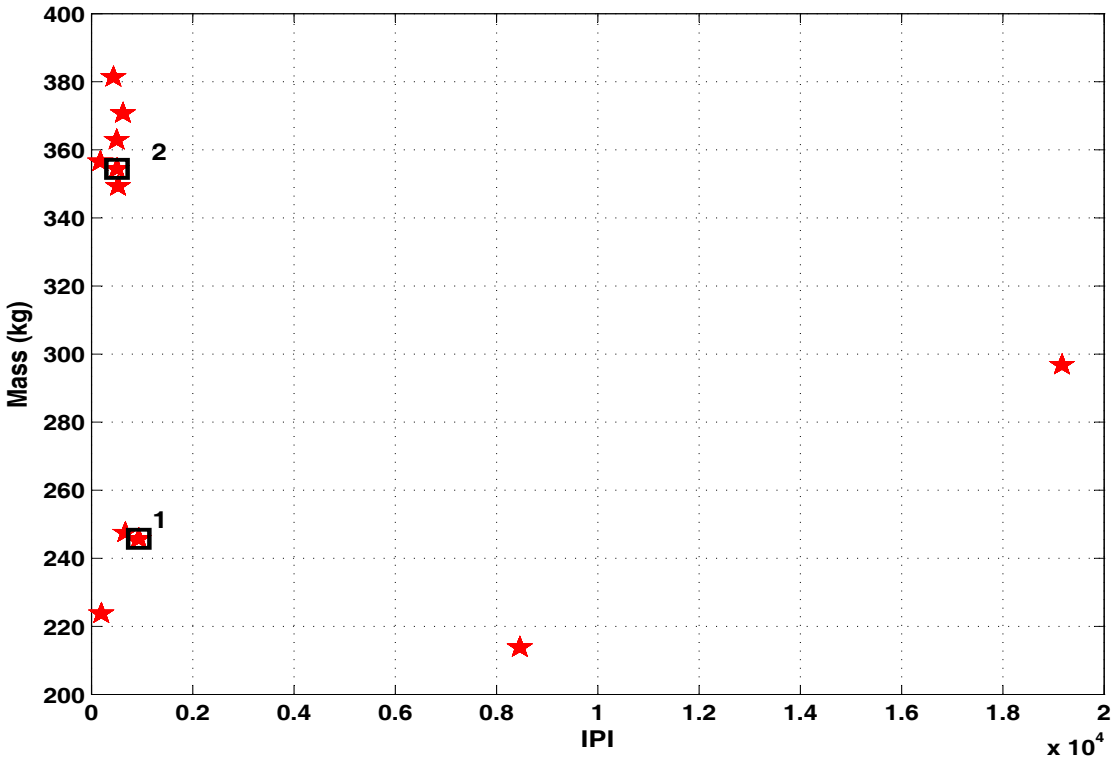


FIGURE 7.10: Projected view of Figure 7.9 on IPI-mass plane

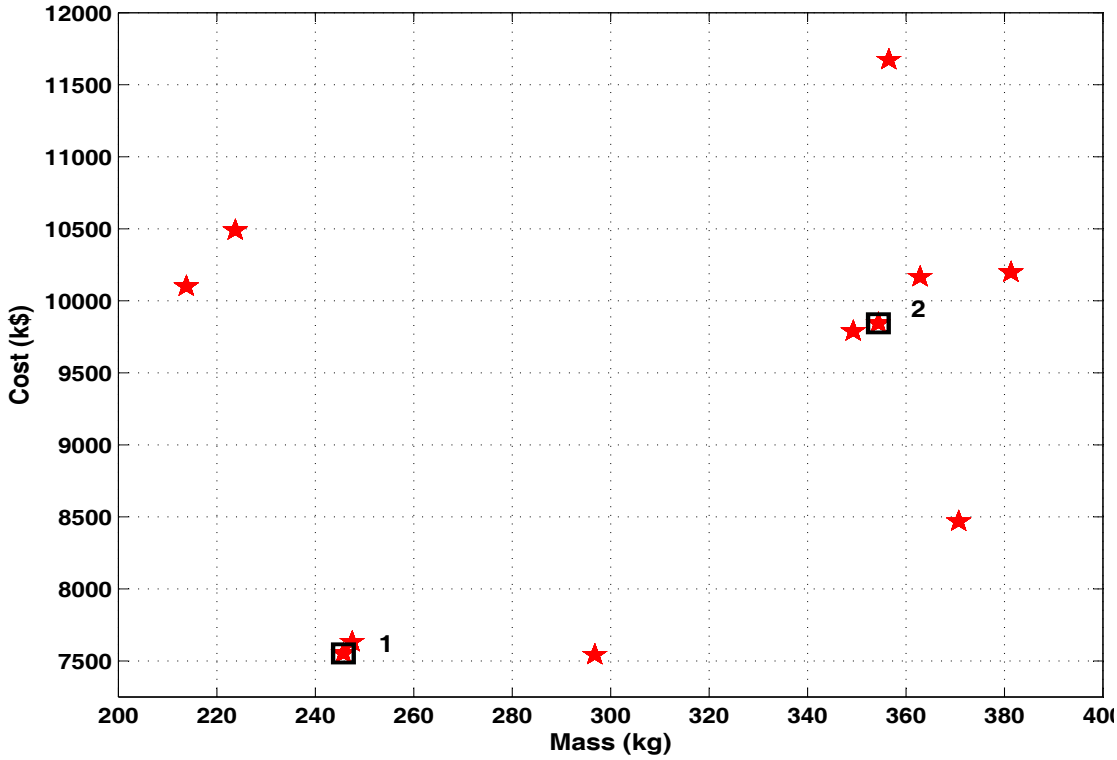


FIGURE 7.11: Projected view of Figure 7.9 on IPI-cost plane

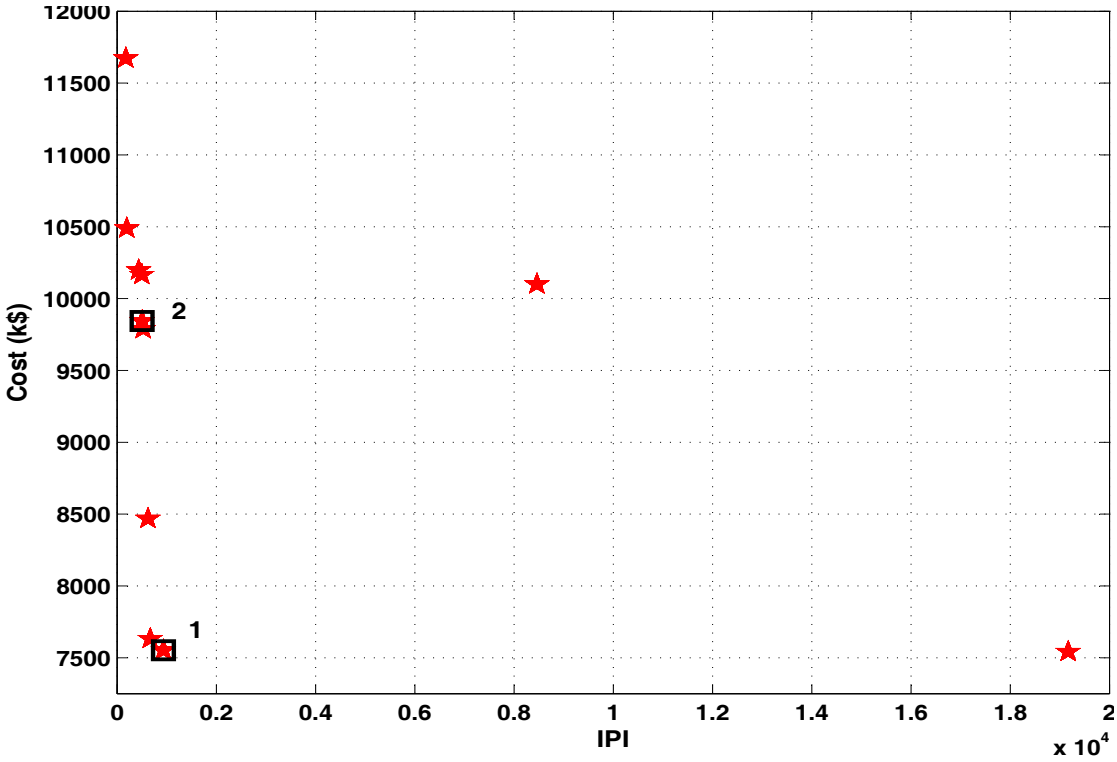


FIGURE 7.12: Projected view of Figure 7.9 on mass-cost plane

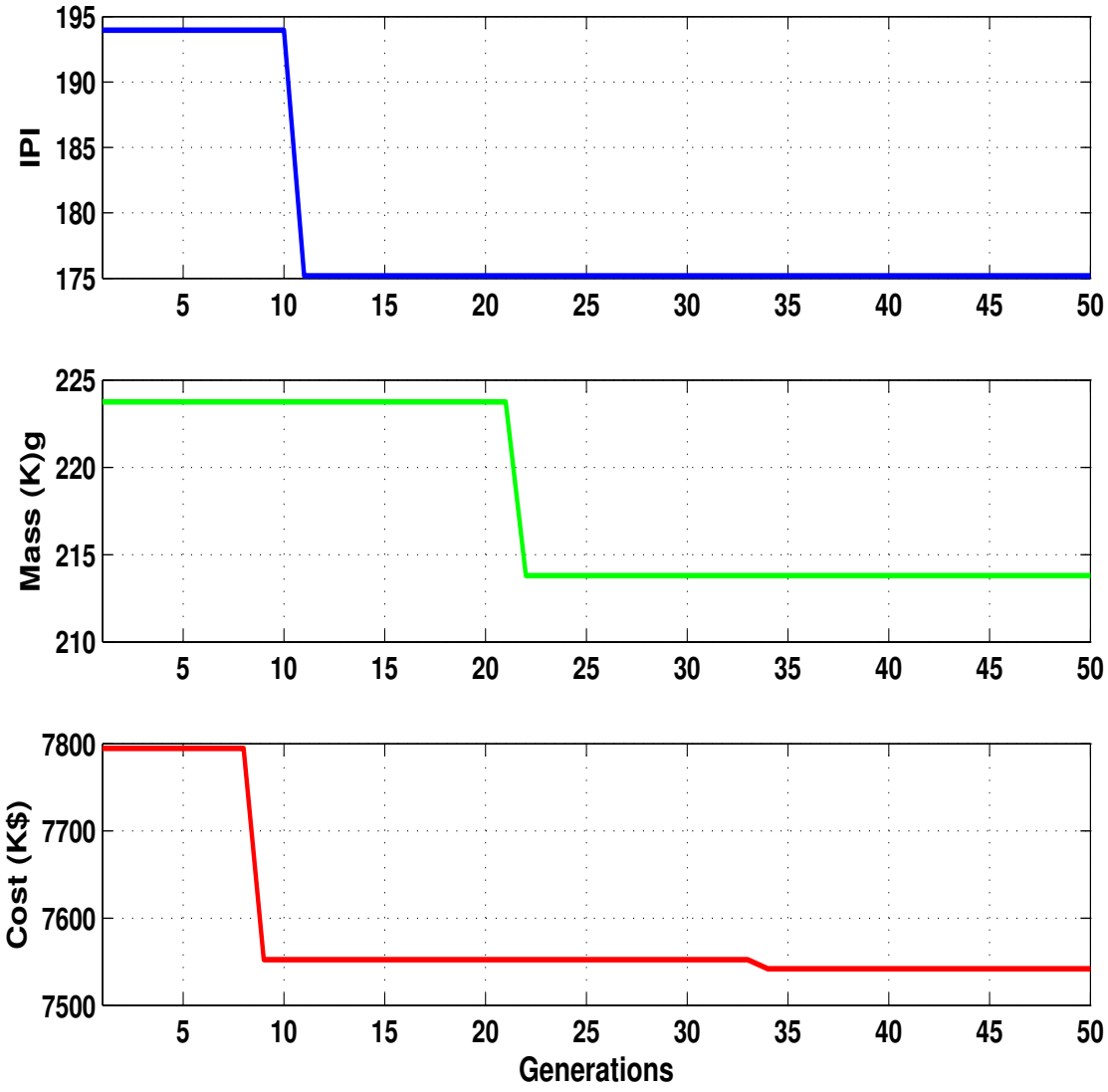


FIGURE 7.13: The minimum of each objective over the no. of generations

The comparison of the results shows that every trade gets improved at the cost of some other, and the design can be selected based on the preferences of the designer, for a given specific mission. By comparing the results obtained by treating the problem as single objective in chapter 6, then as bi-objective (section. 7.2.1.1) and finally as tri-objective, it is very clear that during optimization using WS approach the designer has to give the weighting to the objectives before optimization, hence limiting the solution to that particular set of weighted objectives. In addition, the designer may have to run a number of optimization runs with different weight combinations to get a set of Pareto optimal points. Even then, the results can be misleading in the case of combination of convex-concave Pareto front.

| Selection | Solution 1 | Solution 2 |
|---|---|---|
| Mass (kg) | 245.71 | 354.39 |
| Cost (k$) | 7552.43 | 9844.31 |
| Inverse performance index | 932.97 | 504.58 |
| Solar cell technology | High-$\eta$Si | Hybrid-1 |
| Battery technology | $Li-ion$ | $NiCd$ |
| Array Type | Rigid | Rigid |
| Bus voltage (V) | 50 | 100 |
| No. of batteries | 2 | 2 |
| No. of cells per battery | 11 | 54 |
| Maximum discharge rate ($\times$C) | 0.581 | 0.621 |

TABLE 7.4: Comparison of two compromised solution for tri-objective problem

In the previous section, where system design optimization was performed as three sets of bi-objective problem, we can see that Pareto front can predict the trade-off between two objectives very clearly and objectives have converging behavior. Observing this we can say that this approach can be very effective. The issue here is that while making acceptable trade-off between the objectives, the third objective may be getting worse. This problem can be solved using the third as a constraint. But such an approach has the disadvantage that, by predefining the limits on one objective we may sacrificing some solutions where other objectives can perform a lot better by just exceeding the constrained variable.

Multi-objective optimization with all design objectives taken into account gives the designer a complete overview. Analysis of projected views of the Pareto fronts, give a very clear picture of the objectives trade-off, helping the designer to choose the design best matching his requirements.

The GA is able to generate several good designs across the span of Pareto front in as low as 50 generations with 5250 function evaluations. On the other hand to obtain 20 points on the Pareto front using weighted sum approach the GA would require 20 different objective functions. Assuming a single objective GA converges in about 20 generations, the estimated computational cost in this case can be taken as 28000 function evaluations. The comparison of computational costs demonstrates that the NSGA-II is very effective multi-objective approach for SEPS design, and its effectiveness will increase as more design variable are taken into account.

| Parameter name | Value |
|---|---|
| Orbit | Geo synchronous orbit (GSO) |
| Orbit altitude | 35,786 km |
| Mission life | 15 Yrs. |
| Day light power requirements | 5800 W |
| Eclipse power requirements | 4700 W |

TABLE 7.5: List of mission parameters for communication satellite.

### 7.2.2 Case-2

In this case, the problem is solved for power system for a medium powered communication satellite. The mission parameters are given in Table 7.5.

The problem is solved using tri-objective methodology and results of these are compared with what is the chosen design. The approximate Pareto front for GSO satellite mission is shown in Figure 7.14. The progress of minimum of each objective vs. generations is shown in Figure 7.18. The objective values for baseline design are shown by solid squares in the figure for comparison. Here, three sets of solutions are selected for analysis among themselves and with the baseline design for the power system of the mentioned communication satellite. Selection-1 is highlighted by a circle, selection-2 by a square and selection-3 by a diamond shape. The parameters for all these are summarized in Table 7.6. From the comparison of results, it can be seen that selection-1 has best performance index but has highest mass and cost among all the selected solutions and baseline. Selection-2 has better mass and performance but higher cost figure. Selection-3 has performance lower than selection-1 and 2, while the mass and cost figures are much better than all others.

The trade-off study clearly shows that one objective is attained at the expense of other. Thus, while selecting design, the basic rule is to define clearly the priorities for design selection. The power system of communication satellite is designed keeping performance index as the highest priority. We have seen in previous discussion that selection-1 has much better performance than baseline design but at the same time, higher mass and cost. In case of selection-2, again performance is much better than baseline but still higher cost. Selection-3 has much better trade-off in terms of mass and cost, and the performance of this design is slightly lower than baseline, even if not much better.

| Parameter | Selection 1 | Selection 2 | Selection 3 | Baseline design |
|---|---|---|---|---|
| Mass (kg) | 556.04 | 401.62 | 350.35 | 474.70 |
| Cost (k$ ) | $2.64\times10^4$ | $2.358\times10^4$ | $1.992\times10^4$ | $2.221\times10^4$ |
| Inverse performance index | 102.30 | 113.73 | 1152.98 | 743.8 |
| Solar cell technology | GaAs | UTJ | UTJ | — |
| Battery technology | $NiH_2$ | $Li-ion$ | $Li-ion$ | — |
| Array Type | Rigid | Flexible | Rigid | — |
| Bus voltage (V) | 100 | 50 | 100 | — |
| No. of batteries | 1 | 1 | 2 | — |
| No. of cells per battery | 60 | 10 | 22 | — |
| Maximum discharge rate($\times$ C) | 0.605 | 0.553 | 0.654 | — |
| Battery capacity (Ah) | 104 | 50 | 50 | — |
| Solar array area ($m^2$) | 92 | 68.4 | 62.1 | — |

TABLE 7.6: Comparison of baseline and compromised solutions GEO satellite power system problem

Analyzing the dynamic simulation results shown in Figure 7.19, we can see that the battery is approaching maximum allowable SOC 45% very well, and it is very likely that it will not exceed this limit over any number of orbit cycles. So it is clear that the design selection-3 is the better solution. In the solution, the mass and cost of the system are lower and even the performance is well within acceptable limits. Therefore, this design is selected as the optimal.

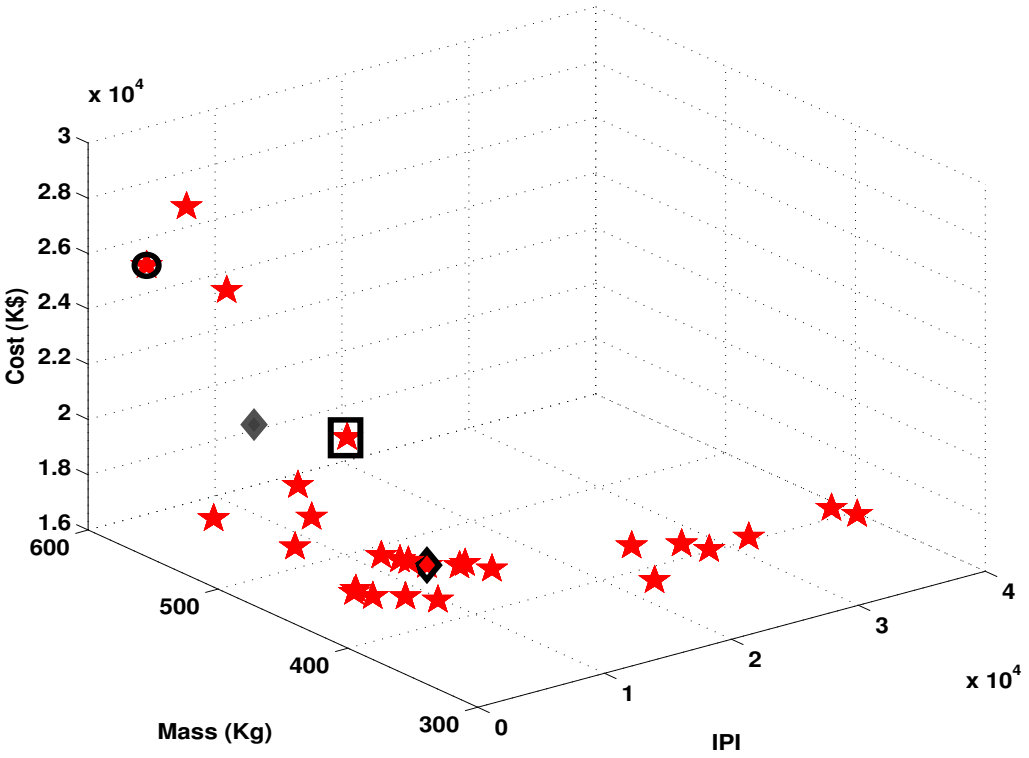


FIGURE 7.14: Approximate Pareto front for tri-objective optimization for the design of SEPS for GSO communication satellite

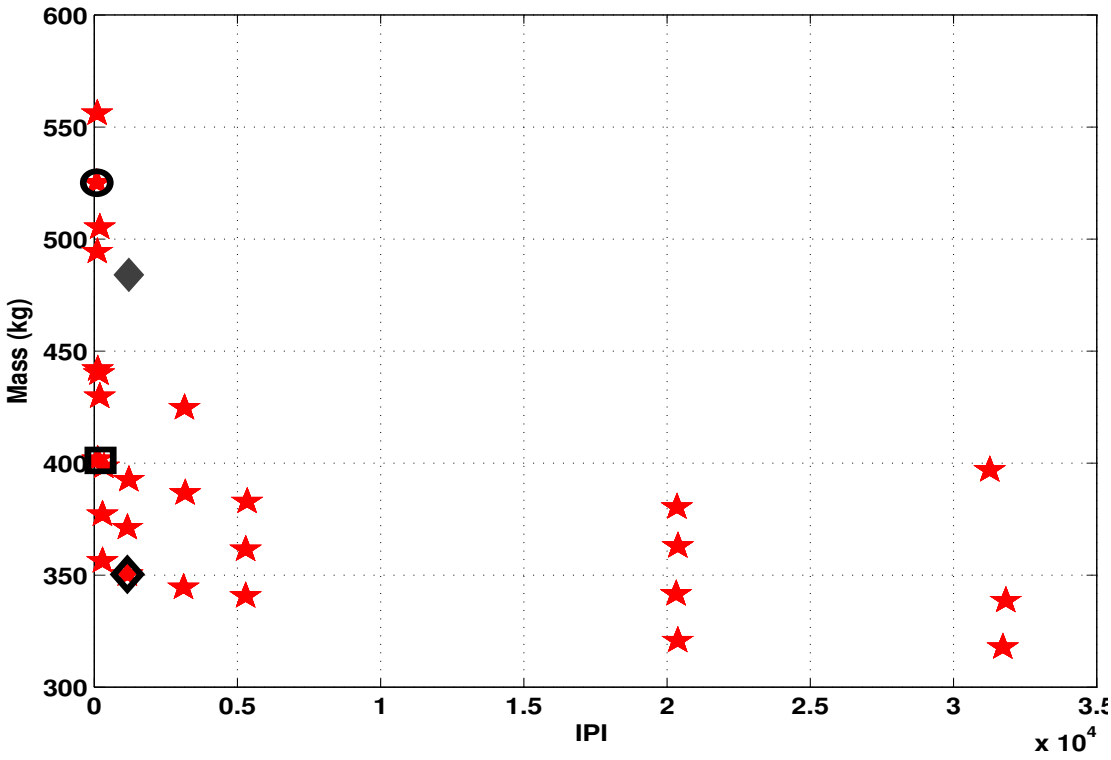


FIGURE 7.15: Projected view of Figure 7.14 on IPI-mass plane

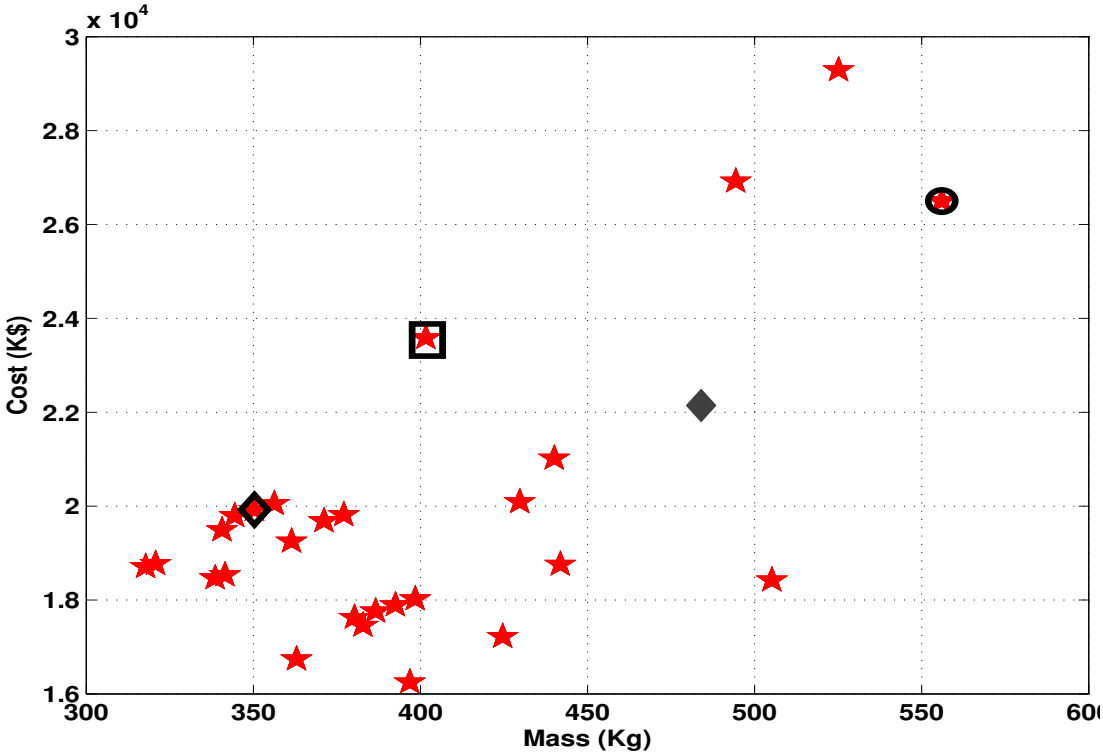


FIGURE 7.16: Projected view of Figure 7.14 on IPI-cost plane

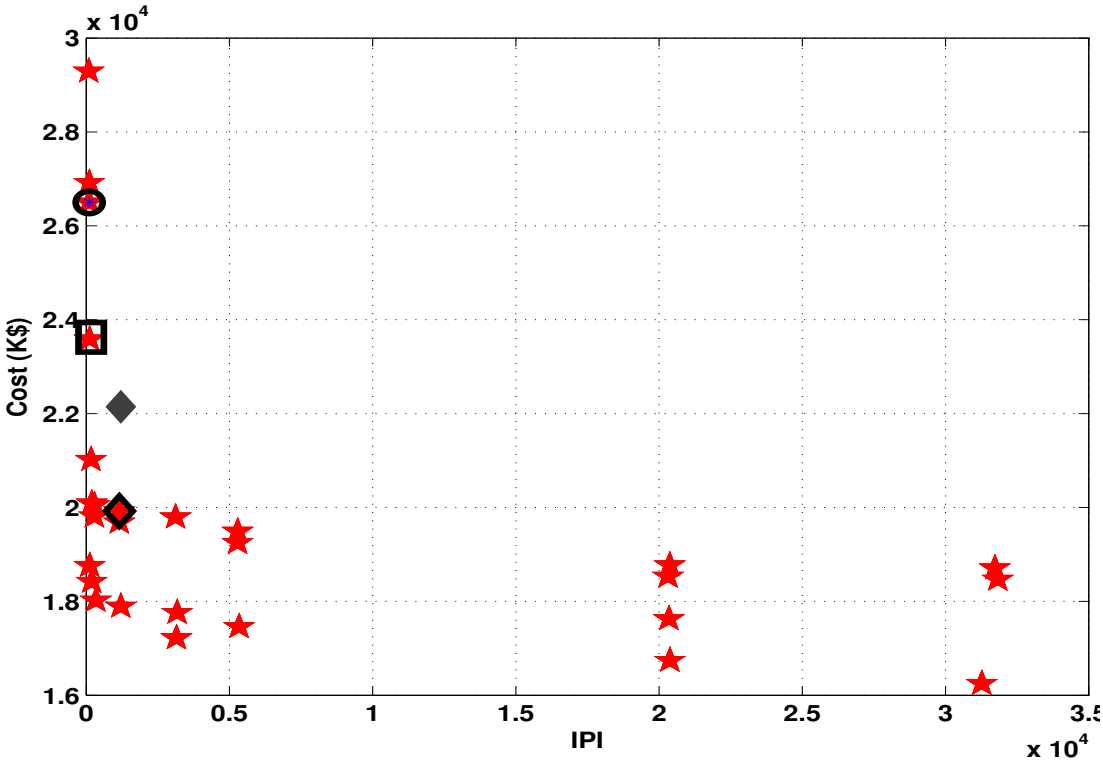


FIGURE 7.17: Projected view of Figure 7.14 on mass-cost plane

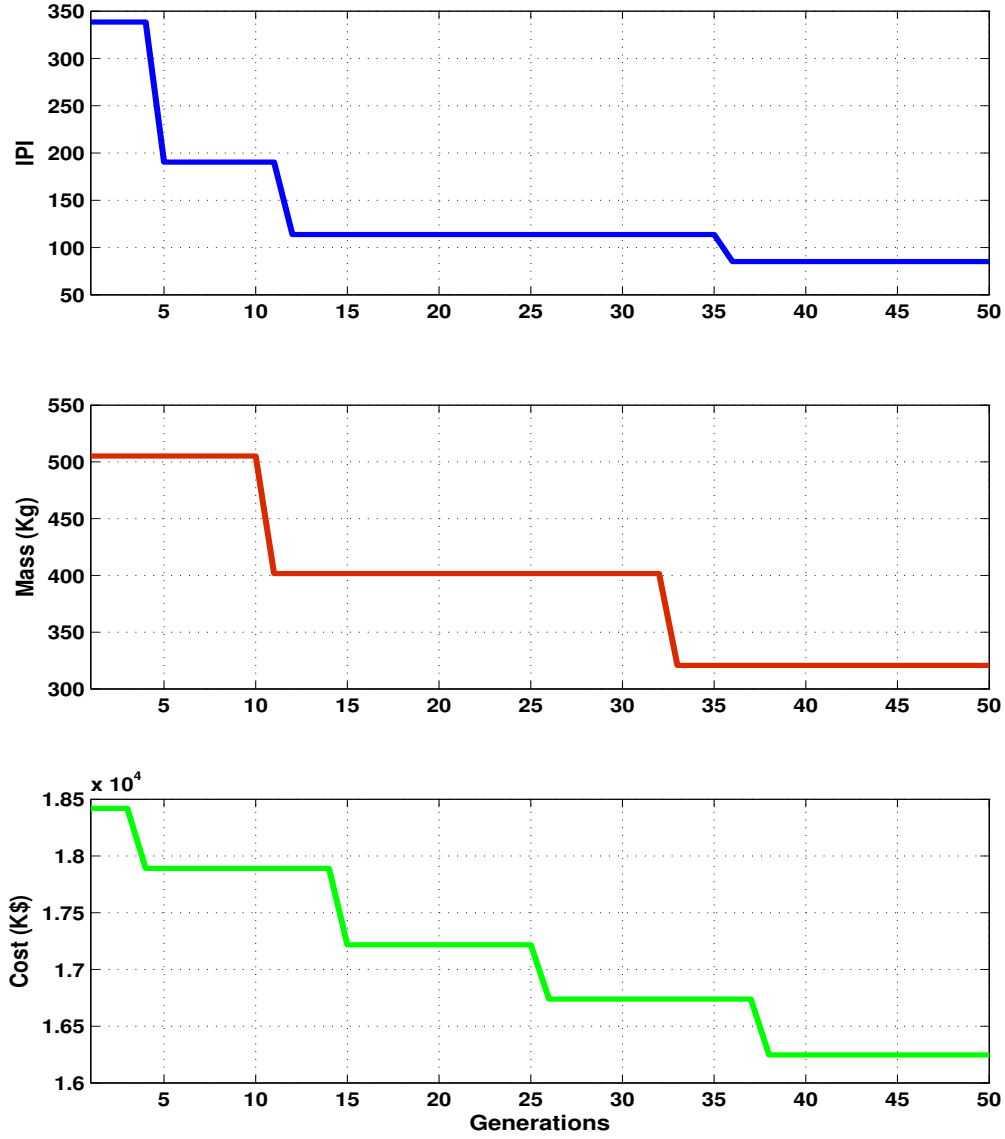


FIGURE 7.18: The minimum of each objective over the generations

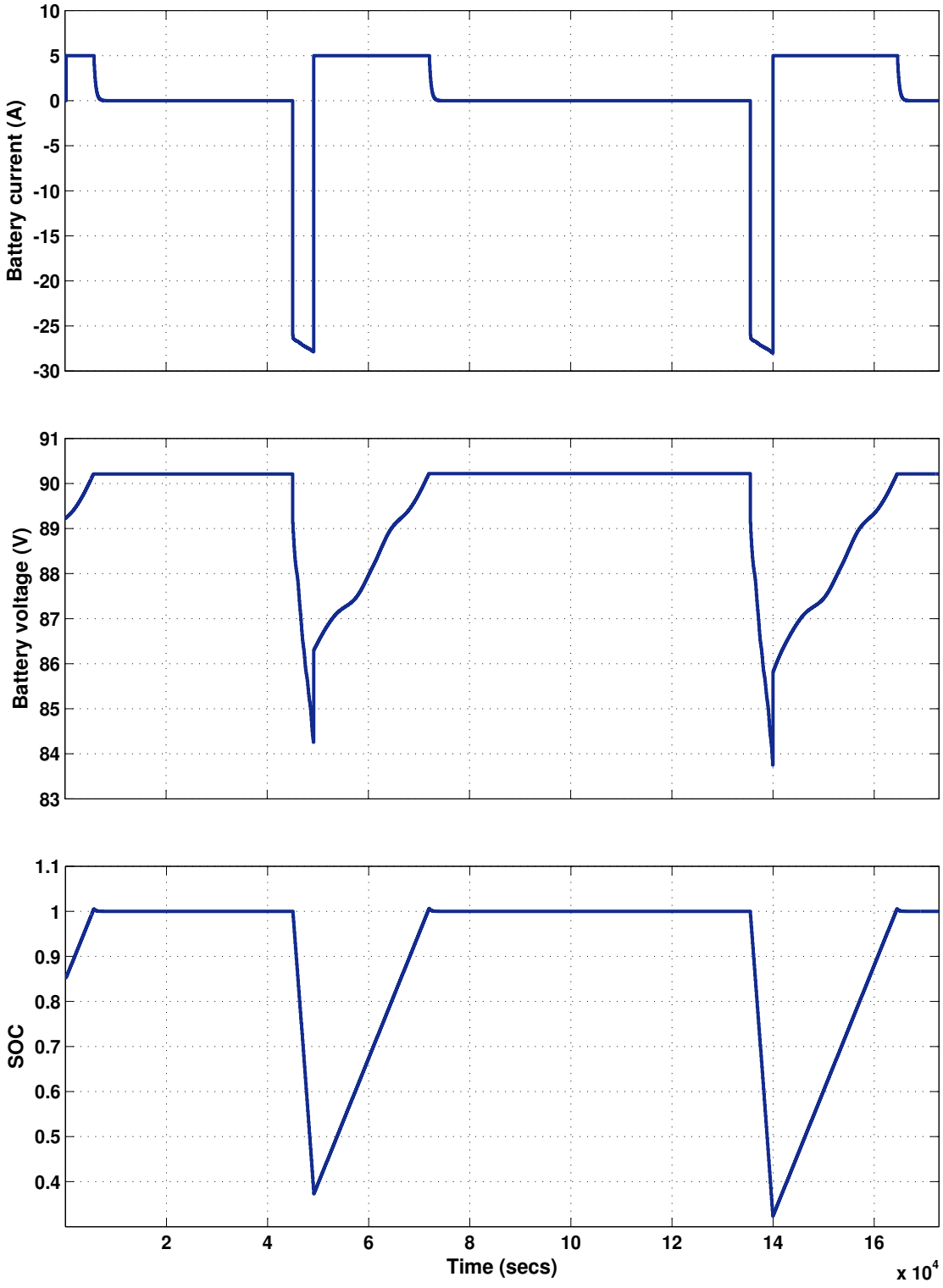


FIGURE 7.19: Battery behavior for selection-3 design

# Chapter 8

# Conclusions and Future Work

## 8.1 Summary

The research reported in this thesis has been focused on the design and development of an optimization framework for computer-automated design of spacecraft power subsystems, providing a means for evaluating the performance along with the mass and the cost factors. The performance index takes into account the solar array figure of merit, operational constraints of battery and also the reliability of power system for selected technologies. The system design optimization approach accounts for design configurations available in industry, as well as reliability issues, and thus helps the system design engineer in making informed decisions that are based on quantitative and qualitative analysis. Two main objectives are identified for the research presented here.

The first objective achieved has been the development of a systematic framework for the spacecraft power system design, search and optimization problem, which takes the subsystem level trade-offs into account, in a way that all major issues of concerns to a design engineer are addressed. Existing work done on this topic as reported in the literature is limited either to technology selection only or to enumerative search over a range of solar array and battery designs. In some cases, this results in a design which is not readily available in market. The approach developed in this thesis can make use of the data sets of design options available with each technology selection; hence the designs selected do not have any development issues.

The second objective has been to develop a complete spacecraft power system simulation model based on a platform which is practical and widely in use in engineering which requires minimal test data from the space industry. In achieving this objective, a model for solar cell/array based on solar cell data available in a given cell's data sheet has been successfully developed. Unfortunately, this is not the case for a battery model. The main hurdle in achieving the same goal was the unavailability of any kind of data sheets for battery cells used in space applications. The author tried her best in getting such information which may be used for designing an efficient battery model, but to no avail. However, this did not stop us to generate a model, based on experimental and simulation test data available in the research literature. The results of this approach are well within the accuracy required for this work.

Evolutionary computational techniques are employed in this work to solar cell parameter optimization. This thesis has demonstrated a very useful application of EC in solving engineering modeling and design problems.

The research has also shown that genetic algorithms can be very effective in solving hybrid design problems consisting of discrete and continuous design variables. Following design optimization objectives, our main focus has been on solving design problems as a multi-objective optimization problem. To achieve this, a sizing- and an analysis-tool have been developed, in order to evaluate the performance of earth orbiting satellites in terms of mass, cost and performance.

The results in chapter 6, provide an insight into the performance of GAs, using a weighted sum approach for spacecraft power system conceptual design. The problem here does not involve a very large search space, but the GA does show its effectiveness. The results from the weighted sum approach on spacecraft power system design optimization are presented there with pre-defined weights to the objectives of high performance, minimal cost and mass. Spacecraft power system trade-offs with reference to solar cell technology, solar array technology, battery technology and, bus voltages are also discussed. The mass, cost and performance benefits of these different power system technology choices are quantified by defining an objective function which takes into account the individual objectives given certain weights. Finally, this formulation is applied through the GA to automate the design process and to obtain optimized trade choices on the basis of defined objective function in time efficient manner. The results have demonstrated that this approach is able to generate optimal solutions for pre-defined set of preferences.

However, to get a complete picture of these tradeoffs, we need a large number of optimization runs.

In chapter 7, a multi-objective optimization approach, based on the NSGA-II has been implemented for the spacecraft power system design. In this research, we consider three design objectives: namely, i) minimization of the mass, ii) minimization of the cost, and iii) maximization of the performance. The problem of SEPS for LEO mission has been solved as bi- and tri-objectives and the designs have been compared in the metaphor of Pareto optimality. It is clear in the case of bi-objective applications that the non-dominated solutions obtained are well distributed and have a satisfactory diversity. Solutions to the tri-objective problem and the projected views of the results have been obtained, giving a very clear understanding of the trade space. The set of Pareto-optimal designs gives a very clear picture to the designer on how different design solutions affect competing objectives, and helps to evaluate major design trade-offs. The three dimensional version of NSGA-II has been able to generate 25 Pareto-optimal designs across the span of the Pareto front in one run of the algorithm. To the best of the author's knowledge, this is the first public attempt to investigate a multi-objective approach for design optimization of spacecraft power systems. In the last part, this research has demonstrated the application of multi-objective optimization to generate Pareto-optimal solutions for power system design of geo-synchronous communication satellites. For this SEPS design problem, it is shown that the current approach is able to give designers a better insight to the design trade-offs and helps them select the optimal solution. The implementation of multi-objective GA does not add significant computational burden more than what is required by single objective optimization. In fact, the computational cost of multi-objective GA is significantly lower than the most commonly used GA methods.

## 8.2 Areas of Future Research

The work presented in this thesis applies only to the DET type power systems. The analysis tool developed here is capable of working for sun regulated systems, although the design optimization problem is demonstrated only on the regulated bus topology. One desirable feature would be to incorporate different architectures, such as peak power tracking systems, etc. This can be achieved through

incorporating comparative analysis of physical parameters of these architectures in the sizing tool and by the addition of their models in the analysis tool.

The problem solved in this thesis has covered technology and configuration issues, and the design of a system for the state-of-the-art technology with different configurations has been considered. The spacecraft power system design presented can be extended to discover novel and structurally efficient designs. This formulation requires a larger trade space, and needs to incorporate the cost of manufacture for new design architectures. It can provide an extra feature to the designers in the scenarios where the cost and the time for development can be included in the new and efficient designs.

The reliability model implemented here assesses the system reliability based on component and subsystem technology choices. Other measures could be implemented in addition to this, so that reliable designs can be distinguished from unreliable ones. One common measure is *failure modes, effects and criticality analysis* (FMECA), which is implemented as fault tree analysis to find single point failures after system architecture design. Redundancy is added if the single point failures are detected to reduce the risk of mission failure[40].

Although the problem solved in this thesis is for conceptual designs and the design analysis is performed for steady state operation only, by incorporating features of transient analysis through detailed circuit design of various components, such as shunt regulators, battery regulators and dc-dc converters, it can be extended to detailed SEPS designs.

The proposed optimization methodology for spacecraft power system can be extended to other spacecraft subsystems with very little effort. Then, these subsystems can be integrated to solve a broader spacecraft design optimization problem.

# Bibliography


[1] Mosher, T., "Spacecraft Design Using a Genetic Algorithm Optimization Approach," *Proceedings of IEEE Aerospace Conference*, 1998.

[2] Moshre, T., "Conceptual Spacecraft Design Using a Genetic Algorithm Trade Selection Process," *Journal of Aircraft*, January 1999, pp. 200–208.

[3] Kordon, M., Klimeck, G., Hanks, D., and Hua, H., "Evolutionary Computing for the Design Search and Optimization of Space Vehicle Power Subsystems," *Proceedings of IEEE Aerospace Conference*, Big Sky, Montana, March 2004.

[4] A.Capel, e. a., "Power System Simulation of Low Orbit Spacecraft: The EBLOS Computer Program," *Proceedings of IEEE Power Electronics Specialist Conference*, 1982, pp. 272–285.

[5] Lee, J., Cho, B., Kim, S., and Lee, F., "Modelling and Simulation of Spacecraft Power System," *IEEE Transaction on Aerospace and Electronics System*, Vol. 24, May 1988, pp. 295–304.

[6] Colombo, G., Grasselli, U., Luca, A., and Spizzichino, A., "A Novel Modeling Method for Photovoltaic Cells," *Proc. of* $35^{th}$ *Annual IEEE Power Electronics Specialists Conference*, June 2000, pp. 1950–1956.

[7] Jiang, Z., Dougal, R., and Liu, S., "Design and Testing of Spacecraft power System using VTB," *IEEE Transaction on Aerospace and Electronics System*, Vol. 39, July 2003, pp. 976–989.

[8] Terrile, R. J., Adami, C., Aghazarian, H., Savio N. Chau, V. T. D., Ferguson, M. I., Fink, W., Huntsberger, T. L., Klimeck, G., Kordon, M. A., Lee, S., von Allmen, P., and Xu, J., "Evolutionary Computation Technologies for Space Systems," *IEEE Aerospace Conference*, Big Sky, MT, March 2005.

[9] A.Capel, Chapoulie, P., Zimmerman, S., and Sanchis, E., "Dynamic Performance Simulation of a Spacecraft Power System," *Proceedings of Sixth European Space Power Conference*, May 2001.

[10] George, J. and Peterson, J., "Multidisciplinary Design Assistant for spacecraft (MIDAS)," *AIAA paper 95-1372*, 1995.

[11] Riddle, E., "Use of Optimization Methods in Small Satellite System Analysis," *Proceedings of 12th AIAA/USC Conference on Small Satellite*, Logan, United States, August 1998.

[12] Riddle, E., "Evaluation of Multidisciplinary Design Optimization techniques as Applied to Spacecraft Design," *Proceedings of IEEE Aerospace Conference*, Big Sky Resort, MT, March 2000.

[13] Fukunaga1, A. S., Chien, S., Mutz, D., and Sherwood, R. L., "Automating the Process of Optimization in Spacecraft Design," *IEEE Aerospace Conference*, 1997.

[14] Lamarra, N. and Dunphy, J., "Interactive Shareable Design Environment for Collaborative Spacecraft Design," *Proceedings of IEEE Aerospace Applications Conference*, March 1998, pp. 487–496.

[15] Pullen, S. and Parkinson, B., "System Design under Uncertainty: Evolutionary Optimization of the Gravity Probe-B Spacecraft," *NASA-CR-20200*, August 1996.

[16] Hassan, R. and Crossley, W., "Conceptual Satellite Design with Uncertain Reliability Values Via Genetic Algorithms Using Population-Based Sampling," *43rd AIAA/ASME/ASCE/AHS/ASC Structures, Structural Dynamics, and Materials Conference*, April 2002.

[17] Terrile, R., Kordon, M., Mandutianu, D., Salcedo, J., and Wood, E. Hashemi, M., "Automated Design of Spacecraft Power Subsystems," *IEEE Aerospace Conference*, March 2006.

[18] Obayashi, S., Sasaki, D., Takeguchi, Y., and Hirose, N., "Multiobjective Evolutionary Computation for Supersonic Wing-Shape Optimization," *IEEE Transactions on Evolutionary Computations*, Vol. 4, July 2000, pp. 182–187.

[19] K., D. and S., G., "Design of truss-structures for minimum weight using genetic algorithms," *Finite element in analysis and design*, Vol. 37, 2001, pp. 447–465.

[20] Sivan, K., Joshi, A., and Suresh, B. N., "Reentry Trajectory Modeling and simulation: Application to Reusable Launch Vehicle Mission," *International Conference on Modeling, Simulation, Optimization for Design for Multi-Disciplinary Engineering Systems*, India, Sept. 2003.

[21] Jilla, C. and Miller, D., "A multiobjective, multidisciplinary design optimization methodolgy for the conceptual design of distributed satellte systems," *9th AIAA/ISMMO Symposium on Multi-Disciplinary Analysis and Optimization*, Atlanta, Georgia, Sept. 2002.

[22] Coello, C. A. C., "A Short tutorial on Evolutionary Multiobjective Optimization," *Proceedings of First International Conference on Evolutionary Multi-Criterion Optimization*, 2001, pp. 21–40.

[23] J., A., "A survey of Multiobjective Optimization in Engineering Design," Technical report LiTH-IKP-R-1097, Linkping University, Linkping, Sweden, 2000.

[24] Coello, C. A., "List of Publication," http://www.mathworks.com/matlabcentral/fileexchange/.

[25] K., D., *Multi-Objective Optimization using Evolutionary Algorithms*, Jhon Willey and Sons, Inc, 2001.

[26] Chipperfield, A. and Fleming, P., "Evolutionary design of Gas Turbine Aero-Engine Controllers," *Proceedings of IEEE International Conference on System, Man and Cybernetics*, Oct. 1998, pp. 2401–2406.

[27] Cvetkovic, D., Parmee, I., and Webb, E., "Multi-objective Optimization and Preliminary Airframe Design," *43rd AIAA/ASME/ASCE/AHS/ASC Structures, Structural Dynamics, and Materials Conference*, Denver, Colorado, April 2002.

[28] Patel, M. R., *Spacecraft power systems*, CRC Press, 2005.

[29] R., R. M., "Space solar cell-tradeoff analysis," *Solar energy materials and solar cells*, May 2003, pp. 175–208.

[30] Spectrolab, "Spectrolab Products - Space - Cells," http://www.spectrolab.com/prd/space/cell-main.asp, 2008.

[31] Dudley, G., "EUROPEAN SPACE TECHNOLOGY HARMONISATION TECHNICAL DOSSIER ON MAPPING Batteries + Fuel Cells," Technical Note, TEC-EPB/05.BTD/GD, 2006.

[32] Andresson, J., "Application of a Multiobjective GA to Engineering Design Problems," *Lecture Notes in Computer Science*, 2003.

[33] D.E., G., *Genetic Algorithm in Search Optimization and Machine Learning*, Addison Wasley Longman, Inc, 1989.

[34] Atiquzzaman, M., Liong, S.-Y., , and Yu, X., "Alternative Decision Making in Water Distribution Network with NSGA-II," *Journal of Water Resource Planing and Management.*, Vol. 132, March/April 2006, pp. 122–126.

[35] Kishor, A., Yadav, S. P., and Kumar, S., "Application of a Multi-objective Genetic Algorithm to Solve Reliability Optimization Problem," *In proceedings of International Conference on Computational Intelligence and Multimedia Applications, 2007.*, 2007, pp. 458–462.

[36] Deb, K., Pratap, A., Agarwal, S., and Meyarivan, T., "A Fast Elitist Multi-Objective Genetic Algorithm: NSGA-II," *IEEE Transaction on Evolutionary Computation*, 2002, pp. 182–197.

[37] Srinivas, N. and Deb, K., "Multi-Objective Optimization using Nondominating sorting in Genetic Algorithms," *Evolutionary Computation*, Vol. 2, No. 3, 1994, pp. 221–248.

[38] Michalewicz, Z., Dasgupta, D., and Riche, R. L., "Evolutionary algorithms for constrained engineering problems," *Computers & Industrial Engineering Journal*, 1999.

[39] Coello, C., "Theoretical and Numerical Constraint Handling Techniques used with Evolutionary Algorithms: A Survey of the State of the Art," *Computer Methods in Applied Mechanics and Engineering*, Vol. 191, January 2002.

[40] Larson, W. J. and (eds), J. R. W., *Space Mission Analysis and Design*, Microcosm Press, Torrance, CA, 1999.

[41] R.L., M., "Electrical power subsystem initial sizing," *IEEE Aerospace and Electronic Systems*, Vol. 5, Dec 1990, pp. 29–34.

[42] Broussely, M. and Pistoia, G., editors, *Industrial Applications of Batteries: From Cars to Aerospace and Energy Storage*, Elsevier Science, Mar 2007.

[43] Milano, P. D., "SISTEMI SPAZIALI: Sottosistema di Potenza (EPS)," www.aero.polimi.it/ lavagna/bacheca/Power.pdf, 1999.

[44] Hansen, F., "Satellite Technology Course Electrical Power Subsystem," http://www.dsri.dk/roemer/pub/sat_tech/FH_Electrical_Power_Subsystem _July_2004.pdf, 2004.

[45] Fellner, J. P., Loebera, G. J., Vuksona, S. P., and Riepenhoffb, C. A., "Lithium-ion testing for spacecraft applications," *Journal of Power Sources*, Vol. 119-121, June 2004, pp. 911–913.

[46] Habraken, S., Defise, J.-M., Collette, J.-P., Rochus, P., D'Odemont, P.-A., and M., H., "Space solar arrays and concentrators," *Acta Astronautica*, Vol. 48, No. 5, Mar 2001, pp. 421–429.

[47] Kelso, T., "Visually Observing Earth Satellites," *Satellite Times*, September/October 1996.

[48] Rauschenbach, H. S., *Solar cell array design handbook*, Van Nostrand Reinhold, 1980.

[49] Hough, W. W. and Elrod, B. D. ., "Solar array performance as a function of orbital parameters and Spacecraft Attitude," *Journal of Engineering for Industry*, Vol. 91, No. 1, February 1969, pp. 13–20.

[50] Leisgang, T., Johnson, A., and Hafen, D., "Dynamic performance battery model," *Proceedings of 23rd IECEC 889465*, 1988, pp. 439–441.

[51] Rogers, H. H., Stadnick, S. J., and Pemberton, T. M., "An empirical nickel-hydrogen battery model," *In proceedings of 29th AIAA Intersociety Energy Conversion Engineering Conference*, Monterey, CA, Aug 1994, pp. 81–85.

[52] Hafen, D. and Armantrout, J., "Nickel-hydrogen voltage-efficiency model," *In proceedings of 31st AIAA Intersociety Energy Conversion Engineering Conference (IECEC)*, Vol. 1, Aug 1996, pp. 369–373.

[53] Capel, A., "Mathematical model for the representation of the electricalbehaviour of a lithium cell," *In proceedings of IEEE 32nd Annual Power Electronics Specialists Conference, PESC.*, 2001, pp. 1976–1981.

[54] Gomadam, P. M., Weidner, J. W., Dougal, R. A., and White, R. E., "Mathematical modeling of lithium-ion and nickel battery systems," *Journal of Power Sources*, Vol. 110, No. 2, August 2002.

[55] Gao, L., Liu, S., and Dougal, R., "Dynamic lithium-ion battery model for system simulation," *IEEE Transaction on Components and Packaging Technologies*, Vol. 25, No. 3, September 2002.

[56] Chen, M. and Rincon-Mora, G., "Accurate electrical battery model capable of predicting runtime and I-V performance," *IEEE Transaction on Energy Conversion*, Vol. 21, No. 2, June 2006.

[57] Pop, V., Bergveld, H., Notten, P., and Regtien, P., "State-of-the-art of battery state-of-charge determination," *Measurement Science and Technology*, Vol. 16, No. 12, December 2005.

[58] Ratnakumar, B., Timmerman, P., Sanchez, C., and Di Stefano, S. ; Halpert, G., "Predictions from the macrohomogeneous model of an aerospace Ni-Cd battery," *Journal of the Electrochemical Soceity*, Vol. 143, Mar 1996, pp. 803–812.

[59] Patil, A., Cho, S., and Lee, F., "Design Considerations for a Solar Array Switching Unit," *In proceedings of 25th Intersociety Energy Conversion Engineering Conference (IECEC)*, 1990, pp. 373–379.

[60] Lee, D., Cho, B., Patil, A., and Lee, F., "Design of a single PWM section shunt switching unit for high powerspace system," *In proceedings of IEEE 26th Annual Power Electronics Specialists Conference (PESC).*, 1995, pp. 1145 – 1491.

[61] Seshadri, A., "Multiobjective Optimization using evolutionary algoritms(MOEA)," http://www.mathworks.com/matlabcentral/fileexchange/, 2006.

[62] Reuschenbach, H. S., *Solar cell array design handbook*, chap. Array Design, EuNew York, NY: Van NostrandSolar, 1980.

[63] Walker, G., "Evaluating MPPT Converter Topologies Using a MATLAB PV model," *Journal of Electrical and Electronics Engineering, Australia*, Vol. 21, 2000, pp. 49–56.

[64] Sharma, S. K., D., P., N., S., and B.L., A., "Determination of solar cell parameters: an analytical approach," *Journal of Physics D: Appllied Physics*, Vol. 26, No. 7, 1993, pp. 1130–1133.

[65] Jervase, J. A., Bourdoucen, H., and Al-Lawati, A., "Solar cell parameters extraction using genetic algorithm," *Journal of Measurement Science and Technology*, Vol. 12, 2001, pp. 1922–1925.

[66] aand C. D. Gelatt, S. K. and Jr., M. V., "Optimization by Simulated Annealing," *Science*, Vol. 4598, 13 May 1983, pp. 671–680.

[67] van Den Berg, E. and M.Karoon, "Algorithm and performance of a space dedicated solar array modelling tool," *In Proceeding of 6th European Space Power Conference*, European Space Agency,ESA, May 2000.

[68] Kirkpatrick, S., Gelatt, C., and Vecchi, M., "Optimization by simulated annealing," *Science*, Vol. 220, 1983, pp. 671–680.

[69] Balling, R. J., "Optimal steel frame design by simulated annealing," *Journal of Structure Engineering, ASCE*, Vol. 117, 1991, pp. 1780–1795.

[70] Xiao, W., Dunford, W. G., and Cape, A., "A Novel modeling method for PV cells," *In Proceeding of Power electronics specialists conference No.35*, June 2004, pp. 1950–1956.

[71] YEnsign Benson W. Lo, U., Phelps, M. R., and Michael, D. S., "Evaluation and Testing of the Solar Cell Measurement System Onboard the Naval Postgraduate School Satellite NPSAT1," *In Proceedings of the 22nd AIAA International Communications Satellite Systems Conference and Exhibit*, May 2004.

[72] Wang, Y. and Maier, M., "SEDSAT solar array output power analysis," *In Proceedings of the Thirtieth Southeastern Symposium on System Theory*, Mar 1998, pp. 345–349.

[73] Fifer, T. L., "Radiation Effects on Multi-Junction Solar Cells," Master's Thesis, Naval Postgraduate School Monterey CA, 2001.

[74] Michalewicz, Z., *Genetic Algorithms + Data Structures = Evolution Programs*, Springer; Third Ed., 1998.

[75] Sivan, K., Joshi, A., and Suresh, B. N., "Reentry Trajectory Modeling and simulation: Application to Reusable Launch Vehicle Mission," *Proceedings of International Conference on Modeling, Simulation, Optimization for Design for Multi-Disciplinary Engineering Systems, India*, Sept. 2003.

[76] Crosslev, W., "Optimization for Aerospace Conceptual Design Through the use of Genetic Algorithms," *First NASA/DoD Workshop on Evolvable Hardware*, July 1999.

[77] GKerslake, T., Haraburda, F., and Riehl, J., "Solar Power System Options for the Radiation and Technology Demonstration Spacecraft," *Proceeding of 35th Intersociety Energy Conversion Engineering Conference and Exhibit,(IECEC)*, 2000, pp. 47–57.

[78] Ratnakumar, B., Timmerman, P., Perrone, D., and Di Stefano, S., "Performance characteristics of an aerospace nickel hydrogen cell-experimental data and theoretical predictions," *In proceedings of 31st Intersociety Energy Conversion Engineering Conference (IECEC)*, 1996, pp. 374 – 379.

[79] Pop, V., Bergveld, H. J., Op het Veld, J. H. G., Regtien, P. P. L., Danilov, D., and Notten, P. H. L., "Modeling Battery Behavior for Accurate State-of-Charge Indication," *Journal of the Electrochemical Soceity*, Vol. 153, No. 11, Sept 2006, pp. A2013–A2022.

[80] Matsushima, T., Takagi, S., Muroyama, S., and Horie, T., "Fundamental characteristics of stationary lithium-ion secondary cells and a cell-voltage-management system," *In proceedings of 26th Annual International Telecommunications Energy Conference*, Sept 2004, pp. 149 – 154.

[81] Dong, S. and Delleur, A. M., "International Space Station Nickel-Hydrogen Extended Battery Discharge Model Analysis," *In proceedings of 26th Annual International Telecommunications Energy Conference*, August 2004.

[82] Di Stefano, S., Timmerman, P., and Ratnakumar, B., "Application of First Principle Nickel System Battery Models to Aerospace Situations," *In Proceedings of the 30th Intersociety Energy Conversion Engineering Conference, IECEC*, August 1995, p. 101104.

[83] Hafen, D. and Wallace, R., "Battery Model and Computer Simulation of a Multi-Battery/Solar-Array Spacecraft Electrical Power System," *In Proceedings of the 15th Intersociety Energy Conversion Engineering Conference (IECEC)*, August 1980, p. 100105.

[84] Fatemi, N., Pollard, H., Hou, H., and Sharps, P., "Solar array trades between very high-efficiency multi-junction and Si space solar cells," *In proceedings of 28th IEEE Photovoltaic Specialists Conference*, Sept 2000, pp. 1083–1086.

[85] Hoffman, D., "A systems model for power technology assessment," *In proceedings of 37th Intersociety Energy Conversion Engineering Conference, (IECEC),2002*, July 2004, pp. 21– 26.

[86] Vollerthun, A., "Design-to-cost applied within an integrated system model," *Journal of Reducing Space Mission Cost*, Vol. 1, 1998, pp. 225–242.

[87] Ralph, E., "High efficiency solar cell arrays system trade-offs," *In proceedings of 24th IEEE Photovoltaic Specialist conference*, 1994, pp. 1998–2001.

[88] Jiang, Z., Dougal, R., and Liu, S., "Application of VTB in Design and Testing of Satellite Electrical Power Systems," *Journal of Power Sources,*, Vol. 122, July 2003, pp. 95–108.

[89] Kim, S. and Cho, B., "Analysis of Spacecraft Battery Charger Systems," *In proceedings of 25th Intersociety Energy Conversion Engineering Conference (IECEC)*, Aug 1990, pp. 365 – 372.